

AD-A037 196

DOUGLAS AIRCRAFT CO LONG BEACH CALIF  
EFFECTS OF LABORATORY SIMULATED PRECIPITATION STATIC ELECTRICIT--ETC(U)  
JUL 76 R C TWOMEY F33615-75-C-3105  
MDC-J6952 AFFDL-TR-76-75 NL

UNCLASSIFIED

1 OF 2  
AD  
A037196



ADA 037196

AFFDL-TR-76-75

*[Handwritten signature]*  
*[Handwritten circled number 12]*

# EFFECTS OF LABORATORY SIMULATED PRECIPITATION STATIC ELECTRICITY AND SWEEP STROKE LIGHTNING ON AIRCRAFT WINDSHIELD SUBSYSTEMS

DOUGLAS AIRCRAFT DIVISION  
MCDONNELL DOUGLAS CORPORATION  
3855 LAKEWOOD BOULEVARD  
LONG BEACH, CALIFORNIA 90846

JULY 1976

TECHNICAL REPORT AFFDL-TR-76-75  
FINAL REPORT FOR PERIOD NOVEMBER 1975 - MAY 1976

*[Handwritten signature]*  
DDDC  
RECEIVED  
MAR 22 1977  
AUGUST 1977

Approved for public release; distribution unlimited

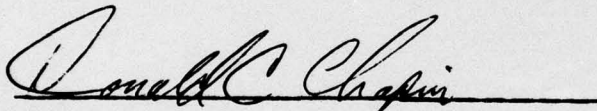
AIR FORCE FLIGHT DYNAMICS LABORATORY  
AIR FORCE WRIGHT AERONAUTICAL LABORATORIES  
AIR FORCE SYSTEMS COMMAND  
WRIGHT-PATTERSON AIR FORCE BASE, OHIO 45433

NOTICE

When Government drawings, specifications, or other data are used for any purpose other than in connection with a definitely related Government procurement operation, the United States Government thereby incurs no responsibility nor any obligation whatsoever; and the fact that the government may have formulated, furnished, or in any way supplied the said drawings, specifications, or other data, is not to be regarded by implication or otherwise as in any manner licensing the holder or any other person or corporation, or conveying any rights or permission to manufacture, use, or sell any patented invention that may in any way be related thereto.

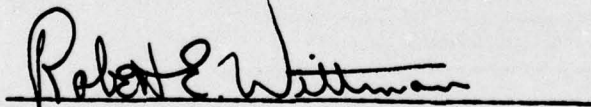
This report has been reviewed and cleared for open publication and/or public release by the appropriate Office of Information (OI) in accordance with AFR 190-170 and DODD 5230.9. There is no objection to unlimited distribution of this report to the public large or by DDC to the National Technical Information Service (NTIS).

This technical report has been reviewed and is approved for publication.



DONALD C. CHAPIN, Project Manager  
Improved Windshield Protection ADPO  
Vehicle Equipment Division

FOR THE COMMANDER:



ROBERT E. WITTMAN, Program Manager  
Improved Windshield Protection ADPO  
Vehicle Equipment Division

Copies of this report should not be returned unless return is required by security considerations, Contractual obligations, or notice on a specific document.

REPORT DOCUMENTATION PAGE		READ INSTRUCTIONS BEFORE COMPLETING FORM
1. REPORT NUMBER AFFDL-TR-76-75	2. GOVT ACCESSION NO.	3. RECIPIENT'S CATALOG NUMBER
4. TITLE (and Subtitle) EFFECTS OF LABORATORY SIMULATED PRECIPITATION STATIC ELECTRICITY AND SWEEP STROKE LIGHTNING ON AIRCRAFT WINDSHIELD SUBSYSTEMS.		5. TYPE OF REPORT & PERIOD COVERED TESTING & FINAL REPORT November 1975 - May 1976
7. AUTHOR(s) R. C. Twomey	9. PERFORMING ORGANIZATION NAME AND ADDRESS Douglas Aircraft Company McDonnell Douglas Corporation Long Beach, California 90846	6. PERFORMING ORG. REPORT NUMBER MDC-J6952
11. CONTROLLING OFFICE NAME AND ADDRESS Air Force Flight Dynamics Laboratory (AFFDL/FEW) Air Force Wright Aeronautical Laboratories Air Force Systems Command Wright-Patterson Air Force Base, Ohio 45433	10. PROGRAM ELEMENT, PROJECT, TASK AREA & WORK UNIT NUMBERS Project: 2202 Task: 02 Work Unit: 01	8. CONTRACT OR GRANT NUMBER(s) F33615-75-C-3105 <i>new</i>
14. MONITORING AGENCY NAME & ADDRESS (if different from Controlling Office)	12. 162p.	11. REPORT DATE Jul, 1976
16. DISTRIBUTION STATEMENT (of this Report) Approved for Public Release, Distribution Unlimited 16 2202   17 02	13. NUMBER OF PAGES 150	15. SECURITY CLASS. (of this report)
17. DISTRIBUTION STATEMENT (of the abstract entered in Block 20, if different from Report)	18a. DECLASSIFICATION/DOWNGRADING SCHEDULE	
18. SUPPLEMENTARY NOTES		
19. KEY WORDS (Continue on reverse side if necessary and identify by block number) Static Electricity                      Electromagnetic Interference Swept Stroke Lightning              Electrostatic Charging Transparent Window Material        Radar Cross Section Control Aircraft Windshield                  Anti-Static Coatings Electrical Transients                Electromagnetic Pulse (EMP)		
20. ABSTRACT (Continue on reverse side if necessary and identify by block number) Candidate outer ply materials for aircraft windshields subjected to laboratory simulated static electric charging and swept stroke lightning tests are evaluated. Very high values of static charge can accumulate on the outer insulating surface of a windshield. Electrical discharging can occur, usually in the form of surface flashing. The discharge generates electrical transients which might cause electromagnetic		

116400

*RB*

20. ABSTRACT (Continued)

interference and damage to electrical components, depending on the system and component design. Methods of generating the electrostatic charge for test purposes and the control and evaluation of the discharges are covered. Potential damage to aircraft windshields from swept stroke lightning is evaluated by subjecting test specimens to man-made lightning. Recommendations are included which should enable the design of windshield systems that are more immune to the effects of precipitation static charging and swept stroke lightning.

A study of the effects of nuclear electromagnetic pulse (EMP) in windshield design was added to the contract, with the results included in an appendix to this report.

ADDITIONAL INFO	
NTIS	White Section <input checked="" type="checkbox"/>
DDC	Buff Section <input type="checkbox"/>
UNANNOUNCED	<input type="checkbox"/>
JUSTIFICATION	
BY	
DISTRIBUTION/AVAILABILITY CODES	
Dist.	AVAIL. AND/OR SPECIAL
A	

## FOREWORD

This report is one of a series of reports that describes work being performed by Douglas Aircraft Company, McDonnell Douglas Corporation, 3855 Lakewood Blvd., Long Beach, California 90846, under the Windshield Technology Demonstrator Program. This work was sponsored by the U.S. Air Force Flight Dynamics Laboratory, Wright-Patterson Air Force Base, under Contract F33615-75-C-3105, Project 2202/0201.

Captain D. C. Chapin (AFFDL/FEW) was the Air Force Project Manager who monitored the program and provided reference material on a timely basis.

Mr. J. H. Lawrence, Jr. was Program Director for the Douglas Aircraft Company.

The work described in this specific report was accomplished by Mssrs. R. C. Twomey and J. T. Kung who were Principal Investigators. Mr. Twomey was the author of the report. Since part of the work used the facilities of the Lightning and Transients Research Institute, Miami, Florida, Mr. J. R. Stahmann, Vice-President and Associate Director, was a principal contributor to the lightning testing. Invaluable technical support was also contributed to Douglas, Long Beach testing, by Mr. H. Polner, and to the Miami testing, by Mssrs. J. Herring and J. Soman.

Program and technical guidance was most helpfully provided by Mr. M. P. Amason of the Douglas Aircraft Company, Avionics Engineering Subdivision.

The author wishes to thank the many unnamed individuals in the commercial and military aircraft manufacturing industry, the glass and windshield manufacturers and the commercial airlines for their excellent cooperation in sharing their experiences during the conduct of this work.

The author is grateful to Mrs. Kathy Van Abkoude for the layout and typing the report in a timely manner.

The initial report was submitted by the author on 10 June 1976.

## TABLE OF CONTENTS

SECTION		PAGE
I	INTRODUCTION . . . . .	1
	Background . . . . .	1
	Static Electricity . . . . .	1
	Swept Stroke Lightning . . . . .	1
II	TEST PLANS . . . . .	5
	Test Objectives . . . . .	5
	Static Electric Tests . . . . .	5
	Swept Stroke Lightning Tests . . . . .	5
	Test Specimen Description . . . . .	6
	<u>Test Setup</u> . . . . .	8
	Static Electric Tests . . . . .	8
	Swept Stroke Lightning Tests . . . . .	10
	Test Procedure . . . . .	10
	Static Electric Tests . . . . .	10
	Swept Stroke Lightning Tests . . . . .	15
III	CONDUCT OF TESTS AND TEST RESULTS . . . . .	17
	Final Test Specimen Details . . . . .	17
	Surface Resistivity & Volume Conductivity Measurements	19
	Surface Resistivity . . . . .	19
	Anti-Static Coating Discoloration . . . . .	27
	Effects on Light Transmission Due to the Anti-	
	Static Coating . . . . .	28
	Volume Conductivity . . . . .	28
	Description of Charge Spray Test Technique . . . . .	31
	Background . . . . .	31
	The Charge Spray Head Design . . . . .	34
	Charge Distribution . . . . .	37
	Charge Polarity Effects . . . . .	39
	Charging Anomalies . . . . .	42
	Edge Effects and Edge Geometry . . . . .	49

TABLE OF CONTENTS (Continued)

SECTION		PAGE
	Electrical Responses From Static Electric Discharges	56
	Background . . . . .	56
	High Impedance Responses . . . . .	58
	Low Impedance Responses . . . . .	60
	Other Transient Suppression Methods . . . . .	61
	Surface Discharge Current . . . . .	68
	Surface Markings . . . . .	70
	Swept-Stroke Lightning Tests . . . . .	72
	Test Site Description . . . . .	72
	Swept Stroke Generation . . . . .	74
	Instrumentation . . . . .	76
	Facility Calibration . . . . .	78
	Environmental Effects on Operations . . . . .	80
	Specimen Mounting Considerations . . . . .	81
	Changes to Specimen Configuration . . . . .	81
	Changes to Original Test Planning . . . . .	82
	Testing Overview . . . . .	82
	Tests on -515 Acrylic Specimen . . . . .	89
	Tests on -501 Soda Lime Glass Specimen . . . . .	89
	Tests on -505 Soda Lime Glass Specimen . . . . .	92
	Tests on -1 Herculite Glass Specimen . . . . .	94
	Tests on -503 Herculite II Glass Specimen . . . . .	94
	Tests on -509 Chemcor Glass Specimen . . . . .	96
	Tests on -507 Chemcor Glass Specimen . . . . .	97
	Special Test on -511 Chemcor Glass Specimen . . . . .	98
IV	CONCLUSIONS . . . . .	99
V	SUMMARY AND RECOMMENDATIONS . . . . .	105
	Overall Design Approach . . . . .	105
	Control of Electrostatic Charging . . . . .	105

TABLE OF CONTENTS (Continued)

SECTION	PAGE
Swept Stroke Lightning . . . . .	112
Control of Electrical Transients . . . . .	113
Radar Cross Section Control . . . . .	115
Electromagnetic Pulse (EMP) Effects in Windshield Design . . . . .	116
Electric Shock Hazards . . . . .	118
Design Verification Tests . . . . .	122
Areas Requiring Further Study . . . . .	122
REFERENCES . . . . .	128
APPENDICES	
A TEST SPECIMEN DETAILS . . . . .	129
B ELECTROMAGNETIC PULSE (EMP) EFFECTS IN WINDSHIELD DESIGN . . . . .	133

## LIST OF FIGURES

Figure	Title	Page
1	Static electric, transient response, and suppression test setup . . . . .	9
2	Swept-stroke and restrike lightning test schematic diagram . . . . .	11
3	Surface resistivity test setup . . . . .	12
4	Volume conductivity test setup . . . . .	14
5	Typical specimen mount . . . . .	18
6	Volume conductivity probe (left) and surface resistivity probe - front views . . . . .	20
7	Volume conductivity probe and surface resistivity probe - back views . . . . .	21
8	Test locations associated with Table II. (for specimens Z5942632-503 and -505) . . . . .	24
9	Test locations associated with Table III. (for specimens Z5942632-509 and -513) . . . . .	25
10	Point electrode surface charging configuration . . . . .	33
11	Multi-electrode charge spray head . . . . .	35
12	Charge spray test setup . . . . .	36
13	5/8-inch-thick acrylic sheet with positive spray head polarity - 125 kilovolts . . . . .	40
14	5/8-inch-thick acrylic sheet with negative spray head polarity - 125 kilovolts . . . . .	41
15	-515 acrylic test specimen with divided surface area for preliminary tests . . . . .	43
16	Mylar sheet in corner of -1 Herculite II specimen . . . . .	46
17	Mylar sheet and peripheral conducting ring on -1 Herculite II specimen . . . . .	47

LIST OF FIGURES (Continued)

Figure	Title	Page
18	-511 Chemcor specimen on metal grid board . . . . .	51
19	Edge conductor on -511 Chemcor specimen . . . . .	51
20	Surface discharge pattern for edge treatment of Figure 19 . . . . .	52
21	Chemcor specimen with 1/4-inch peripheral surface border . . . . .	53
22	Final electrical edge geometry for static charge tests .	54
23	Surface flashover on -515 acrylic specimen using edge geometry of Figure 18 . . . . .	55
24	Schematic of high impedance voltage measurement test setup . . . . .	58
25	Schematic of low impedance termination test setup . . .	60
26	Multi-flash back foil response in 16 ohm load on -1 Herculite II specimen . . . . .	61
27	<i>Composite of transient suppression test circuitry . . .</i>	62
28	Spark gap suppressed transients . . . . .	63
29	Response traces for circuit of Figure 27 . . . . .	63
30	Suppressed responses, -501 soda lime specimen . . . . .	65
31	Suppressed responses, -511 Chemcor specimen . . . . .	66
32	Circuit for measuring surface flash current . . . . .	69
33	Surface current response in a $30 \times 10^{-3}$ -ohm shunt . . .	69
34	Surface tracking on -501 soda lime specimen . . . . .	71
35	LTRI swept stroke lightning test setup view toward air exit of wind tunnel . . . . .	72

LIST OF FIGURES (Continued)

Figure	Title	Page
36	LTRI facility showing restrike generator, etc. . . . .	73
37	Calibration of swept stroke generator - no wind . . . .	79
38	Calibration of swept stroke generator - with wind . . .	79
39	Calibration of restrike generator . . . . .	80
40	-515 acrylic test specimen with restrike at 17 milli- seconds . . . . .	90
41	Restrike attachment to -501 soda lime glass specimen . .	91
42	Restrike markings on -501 soda lime glass specimen . . .	92
43	Restrike attachment to -505 soda lime glass specimen . .	93
44	Restrike markings on -505 soda lime glass specimen . . .	93
45	Restrike markings on -1 Herculite glass specimen . . . .	94
46	Restrike markings on -503 Herculite II glass specimen . .	95
47	Signal waveforms for -503 Herculite II glass specimen . .	96
48	Restrike to -509 Chemcor glass specimen . . . . .	97
49	Restrike markings on -507 Chemcor glass specimen . . . .	98
50	Outer surface edge grounding method . . . . .	110
51	Methods for reducing electrostatic charging area . . . .	111
52	Method for grounding RCS coating . . . . .	117
53	Schematic diagram of potential electric shock circuit. .	120

## LIST OF TABLES

Table	Title	Page
I	TEST SPECIMENS . . . . .	8
II	SURFACE RESISTIVITY OF PPG INDUSTRIES TEST SPECIMENS AT VARIOUS SURFACE LOCATIONS . . . . .	22
III	SURFACE RESISTIVITY OF CORNING GLASS WORKS TEST SPECIMENS AT VARIOUS SURFACE LOCATIONS . . . . .	23
IV	LIGHT TRANSMISSION LOSS DUE TO ANTI-STATIC COATING . .	29
V	VOLUME CONDUCTIVITY DATA . . . . .	30
VI	CURRENT DISTRIBUTION FROM CHARGE SPRAY HEAD . . . . .	39
VII	BACK FOIL CURRENT & OFF-SURFACE CO-PLANER RING CURRENT . . . . .	48
VIII	BACK FOIL CURRENT & ON-SURFACE PERIPHERAL RING CURRENT . . . . .	48
IX	SUMMARY OF THE LIGHTNING SWEPT STROKE TESTS . . . . .	84

## LIST OF ABBREVIATIONS AND SYMBOLS

AC	Alternating Current
~	Alternating Voltage Source
ASTM	American Society for Testing and Materials
AWG	American Wire Gauge
A	Ampere
A/V	Amperes per Volt
E	Applied Voltage
≈	Approximately equal to
a	Area
f/( )	Camera Aperture Setting
CM	Centimeter
CM <sup>2</sup>	Centimeters squared
Corning	Corning Glass Works
I	Current in Amperes
DIA	Diameter
DC	Direct Current
DIV	Division
Douglas, DAC	Douglas Aircraft Company, McDonnell Douglas Corporation
EMP	Electromagnetic Pulse
HCL	Hydrochloric Acid
IRAD	Independent Research and Development
KA	Kiloamperes (1,000 Amperes)
KV	Kilovolt (1,000 volts)
K	Kilo (1,000)

LIST OF ABBREVIATIONS AND SYMBOLS (CONCLUDED)

LTRI	Lightning and Transients Research Institute
T	Light Transmission
MTL	Material
Meg	Megohm (one million ohms)
MOV	Metal Oxide Varistor
$\mu$ A	Microamperes (one millionth of an ampere)
$\mu$ F, MFD	Microfarad (one millionth of a Farad of capacitance)
$\mu$ H	Microhenry (one millionth of a Henry of inductance)
MPH	Miles Per Hour
m	Milli (one thousandth)
mA	Milliamperes (one thousandth of an ampere)
MM	Millimeter
MIN	Minimum
#	Number
%	Percent
PF	Picofarad ( $10^{-9}$ Farad of Capacitance)
PPG	PPG Industries
NESA	PPG Trade Name for Stannous Oxide Conductive Coatings
RCS	Radar Cross Section
RMS	Root Mean Square
SEC	Seconds of time
$R_S$	Surface Resistivity
t	Thickness
T	Time in milliseconds
TYP	Typical
V	Volt

## SECTION I INTRODUCTION

This report presents the plans and results of a series of tests to evaluate candidate outer-ply materials for aircraft windshields when subjected to the effects of static electricity and swept stroke lightning.

The report is structured in four parts. Section II contains the test plans, while Section III discusses the testing and the test results. Section IV presents the conclusions drawn from the test program. Section V summarizes the test results and other related work conducted during this program and presents windshield system design recommendations.

The contract for this work was ammended later in the program to add a study of the interaction of nuclear electromagnetic pulse and windshield anti-icing conductive coatings. The results are presented in Appendix B.

### Background

#### Static Electricity

Triboelectric charging of the aircraft and the influence of charged clouds will cause a significant static electric charge to be distributed on the external surfaces of an aircraft. Charge which forms on insulating surfaces can build in intensity until it reaches a potential sufficient to flash over to an adjacent conductive surface. When the insulating surface is an electrically heated windshield, potentially troublesome problems may occur: namely, mechanical damage due to the electrical discharge, electromagnetic interference due to the discharge, and transitory distraction of sight of the flight crew due to the brilliant electrical discharge flash.

The electric charge buildup on the insulating outer surface of the windshield has two possible discharge paths. First, it can discharge to the metal windshield frame as a surface discharge. Second, it can

penetrate the outer face ply of the windshield to the electrically conductive heating layer on the inner surface of the outer ply. Penetration of the outer ply in the extremes can be in the form of a dielectric breakdown, or as the result of a high resistance conductive path through the outer ply material. The exact nature of the conduction through the outer ply is very complex and may involve both breakdown and conduction. This discharge through the material is a potential problem because it may degrade the outer ply material and lead to more serious mechanical or electro-mechanical problems.

Discharge across the outer surface may generate electrical noise which is coupled to the windshield heating circuitry and to other circuits. This electromagnetic interference may be detrimental to proper circuit operation. Discharge through the outer ply material may also cause electromagnetic interference.

#### Swept Stroke Lightning

During a lightning strike to the nose of an airplane in flight, the ionized lightning channel is swept back over other portions of the aircraft by the forward motion of the aircraft. The channel remains attached to the initial point until the combination of the voltage drop in the channel and the conductivity of the aircraft material under the swept channel offers a more attractive electrical path for the continuing and restrike current in the channel. When this occurs, a new attach point is established and the process repeats itself until the total flash is over or the aircraft flies out of the channel.

The tendency to establish new attach points bears a direct relationship to the dielectric strength or electrical conductivity of the aircraft surface material over which the flash is swept. When this material is the windshield of an airplane, the size of the windshield and therefore the path length between conducting metal structure has a large influence on the probability of lightning attachment to the windshield. Thus, large windshields are potentially more vulnerable to lightning than are small windshields.

The purpose of these tests was to evaluate certain candidate outer face ply windshield materials for their ability to prevent dielectric puncture or material damage in the presence of the lightning environment.

The basic windshield materials are normally good electrical insulators and offer little incentive for attachment of the swept stroke. However, the application of electrically conductive material to the outer surface for precipitation static control and to the inner surface of the outer ply for electrical heating may alter the normal insulating qualities of the basic windshield material and present a potential problem.

## SECTION II

### TEST PLANS

The following plan was prepared at the beginning of the program to guide the testing to be conducted in Section III.

#### Test Objectives

The objectives of these tests are to evaluate the candidate windshield outer face ply materials to ascertain their suitability in highly electrified environments.

#### Static Electric Tests

The objectives of these tests are as follows:

1. To evaluate the surface resistivity and volume conductivity of the windshield outer ply test specimens.
2. To evaluate the dielectric breakdown characteristics of the test specimens when subjected to simulated precipitation static (p-static) charging. Leakage currents due to both surface flashover and volume conductivity or punch through will be investigated to identify potential failure modes.
3. To evaluate the amplitude and waveshape of transient currents induced in simulated anti-icing circuitry, and to evaluate transient suppression techniques.

#### Swept Stroke Lightning Tests

The specific objectives of these tests are as follows:

1. To evaluate the effect of external anti-static conductive coatings with respect to their possible tendency to create attach points for the swept stroke lightning.
2. To evaluate the dielectric characteristics of the outer face ply materials (both bulk material characteristics and thickness) as they may influence lightning attachments.

3. To evaluate the windshield dimension in the path of the swept stroke as it affects swept stroke attachment to the windshield.
4. To evaluate the effects of prior exposure of the test specimens to precipitation static charging and discharging.

#### Test Specimen Description

The test specimens are flat sheet samples of candidate windshield outer face ply materials. The chemical composition and ply thickness are highly influenced by non-electrical factors, but are representative of materials that would be used in a real windshield. Appendix A defines the specimens.

The static electric test specimens, as delivered from their manufacturers, will not have electrical anti-icing coatings or anti-static coatings. Some of the specimens used in the swept stroke lightning tests, however, will have a high resistance anti-static coating of stannous oxide on what would be the exposed, outer surface in an actual windshield. The anti-static coating will be applied by the glass manufacturer.

All specimens will have aluminum foil attached to the inside surface to simulate the highly conductive resistive coating used to heat the windshield during anti-icing activity. Transparent stannous oxide, indium oxide, or proprietary gold coatings are normally used for this anti-icing function; however, a cost trade-off was made which allowed more specimens if the anti-icing coating could be simulated. For the purpose of these tests inexpensive aluminum foil is used. The aluminum foil has a higher conductivity than the normal anti-icing coating but that will not affect the static charge redistribution characteristics to be studied in this program.

It is recognized that if lightning puncture were to occur, the test specimen damage effect could be different using aluminum foil to simulate the heater element. The damage to the actual heater element might be worse due to its higher resistance value and resulting energy dissipation

level. However, it should be noted that this test will use only the outer face ply material, and not the fully laminated windshield assemblies. Therefore, the test criteria will be to determine whether a lightning strike will puncture the outer ply surface rather than to determine the degree of damage to a windshield. A puncture on the outer ply surface by a lightning strike will be considered unacceptable since the ensuing environmental effects might rapidly degrade the structural integrity of the outer ply.

Test specimens incorporating anti-static coatings will be selected to evaluate the effect of anti-static coatings on the swept-stroke and re-strike characteristics of the windshield surface. The coating deterioration characteristics under swept-stroke/restrike conditions will be evaluated.

The test specimens listed in Table I are detailed on drawing Z5942632 (attached as Appendix A). Since the potential problems caused by static electricity and swept stroke lightning increase with the size of the windshield, it is desirable to concentrate the evaluations on the largest size that might reasonably be used. The B-1 aircraft is a good model as it has one of the largest exposed areas with maximum dimensions of approximately 48 inches by 72 inches. Therefore, sample sizes as close as practicable to the size of the B-1 windshield will be ordered from the material manufacturers.

The anti-static coating of stannous oxide is specified to have a maximum resistance of one megohm per square. This value is a compromise between electrically acceptable higher values and more producible lower values.

The uncoated specimens will be used in the static electric tests. All specimens will be used in the swept stroke lightning tests with the exceptions of the -511 and -513 which are stand-in replacements for the -507 and -509 in the event of their destruction during either series of tests.

TABLE I. TEST SPECIMENS

SPECIMEN (Z5942632)	MATERIALS*	SIZE (INCHES)	THICKNESS (INCHES)	COATING*
-1	Herculite II	48 X 62	0.110	None
-501	Soda Lime	48 X 62	0.187	None
-503	Herculite II	48 X 62	0.110	Anti-Static
-505	Soda Lime	48 X 62	0.187	Anti-Static
-507	Chemcor	37 X 53	0.085	None
-509	Chemcor	37 X 53	0.085	Anti-Static
-511	Chemcor	37 X 53	0.105	None
-513	Chemcor	37 X 53	0.105	Anti-Static
-515	Acrylic	48 X 62	0.125	None

\*See Appendix A.

### Test Setup

#### Static Electric Tests

The static electric tests will be conducted within a microwave anechoic chamber. This location has been chosen to permit isolating the test activity from the surrounding electromagnetic and physical environment. The chamber is air conditioned and dust controlled, and can be completely darkened for corona and flashover observation and still photography. The chamber temperature and relative humidity will be recorded for each test. The test setup is shown in Figure 1.

The charge spray electrode housing will be suspended above the horizontally mounted test specimen. Provisions are made to adjust the distance between the charge spray electrodes and the test specimen.

The high-voltage control console will be located within the test chamber and contains the voltage amplitude control, on-off control, over-voltage and overcurrent cut-off circuits, as well as the output voltage and current meters. Microammeters will be used to measure the total current, as well as the current through the various paths of interest.

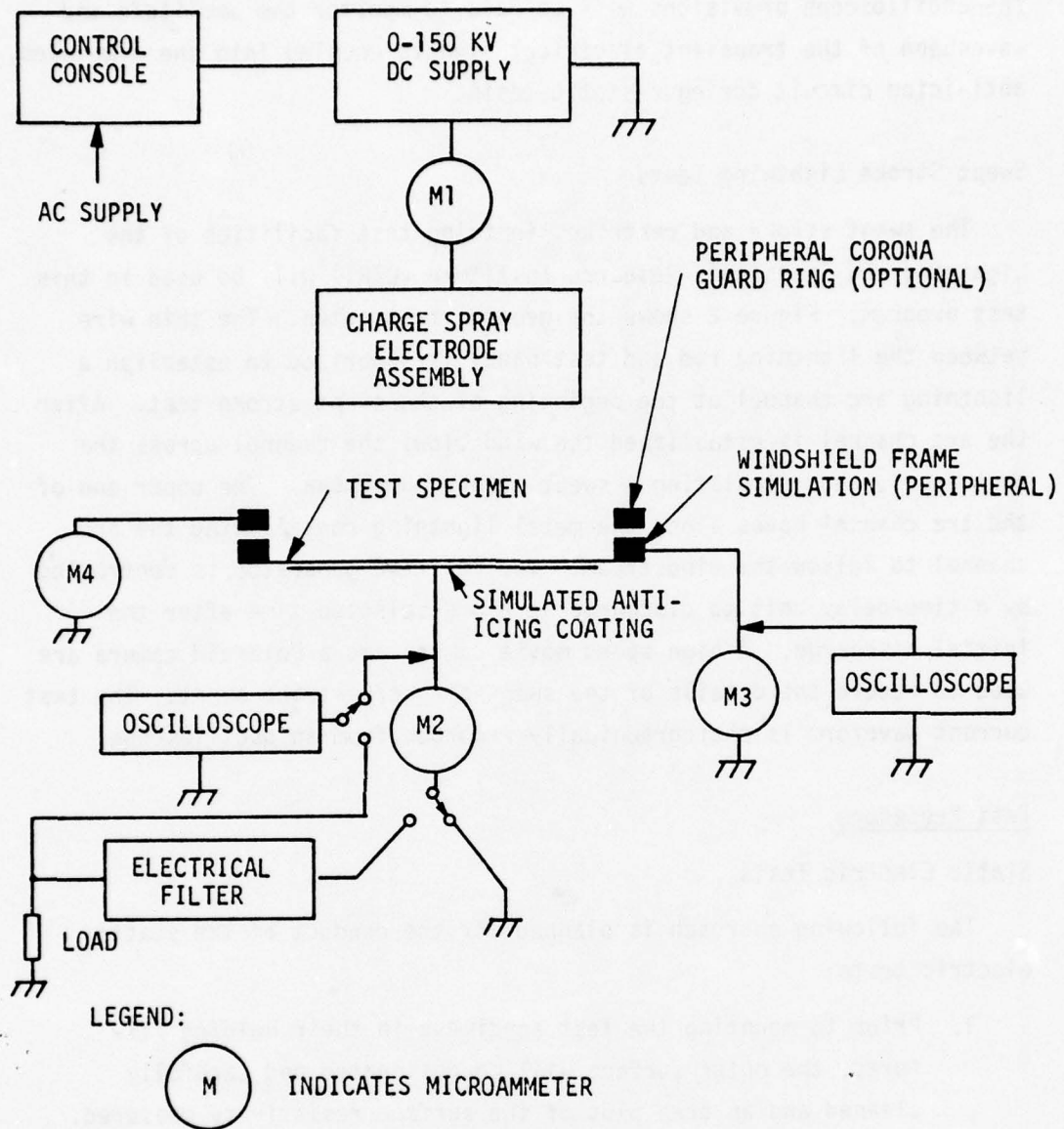


Figure 1. Static electric, transient response, and suppression test setup.

The oscilloscope provisions will be used to monitor the amplitude and waveshape of the transient electrical signals coupled into the simulated anti-icing circuit during p-static tests.

#### Swept Stroke Lightning Tests

The swept stroke and restrike lightning test facilities of the Lightning and Transients Research Institute (LTRI) will be used in this test program. Figure 2 shows the general test setup. The thin wire between the lightning rod and test panel is vaporized to establish a lightning arc channel at the beginning of the swept stroke test. After the arc channel is established the wind blows the channel across the test panel, thus simulating a swept stroke phenomena. The upper end of the arc channel moves along the metal lightning rod allowing the arc channel to follow the windstream. The restrike generator is controlled by a time-delay unit to discharge at a pre-selected time after the initial discharge. A high speed movie camera and a Polaroid camera are used to record the details of the swept-stroke/restrike event. The test current waveform is photographically recorded from an oscilloscope.

#### Test Procedure

##### Static Electric Tests

The following approach is planned for the conduct of the static electric tests:

1. Prior to mounting the test specimens in their holding fixtures, the outer surface will be designated and carefully cleaned and an area plot of the surface resistivity measured. The measuring method and test probe are those recommended by the American Society for Testing and Materials (ASTM) F7.08 committee for surface resistivity. Figure 3 shows the test equipment.

These measurements are to be made on the test specimen prior to applying the aluminum foil simulated anti-icing coating

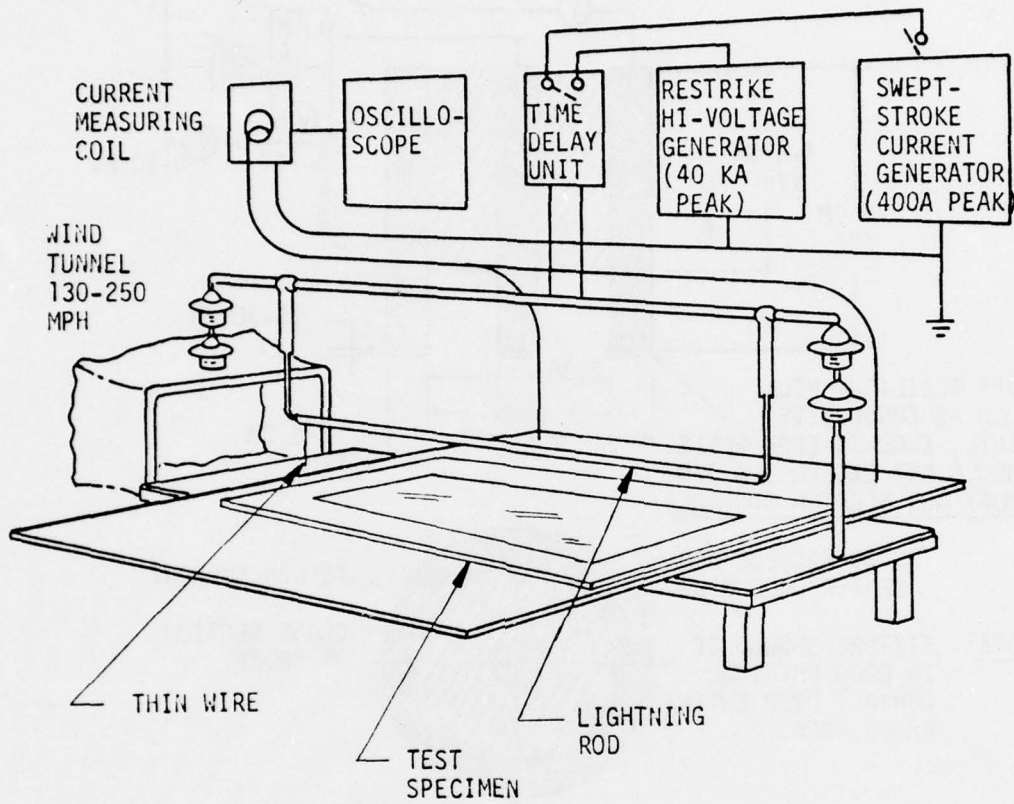
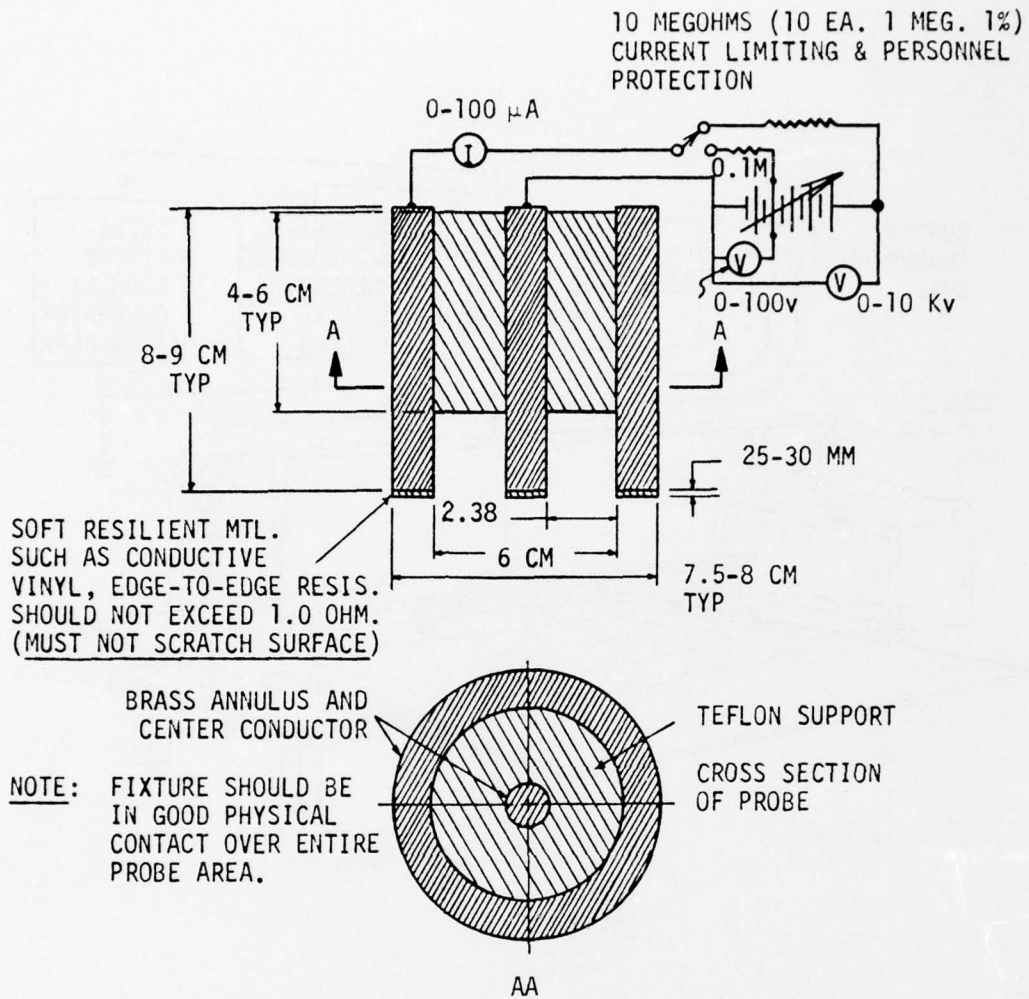


Figure 2. Swept-stroke and restrike lightning test schematic diagram.



- TEST: 1. PLACE FIXTURE ON SURFACE TO BE MEASURED.
2. INCREASE VOLTAGE FROM ZERO OR LOW VALUE TO OBTAIN 40  $\mu$ A CURRENT (TYP).
3. SURFACE RESISTIVITY WILL BE 4 TIMES THE RESISTIVITY READING OF THE FIXTURE. THIS WILL BE OHMS/SQUARE.

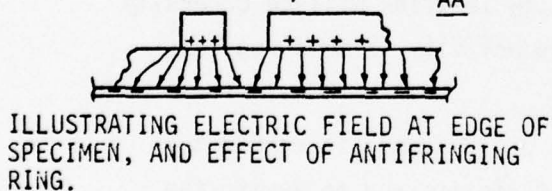
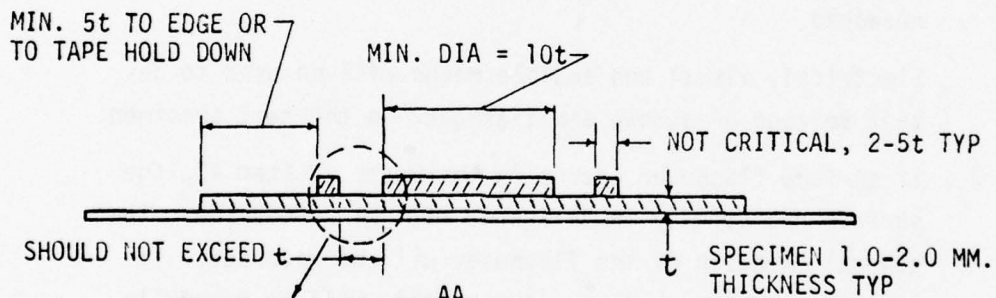
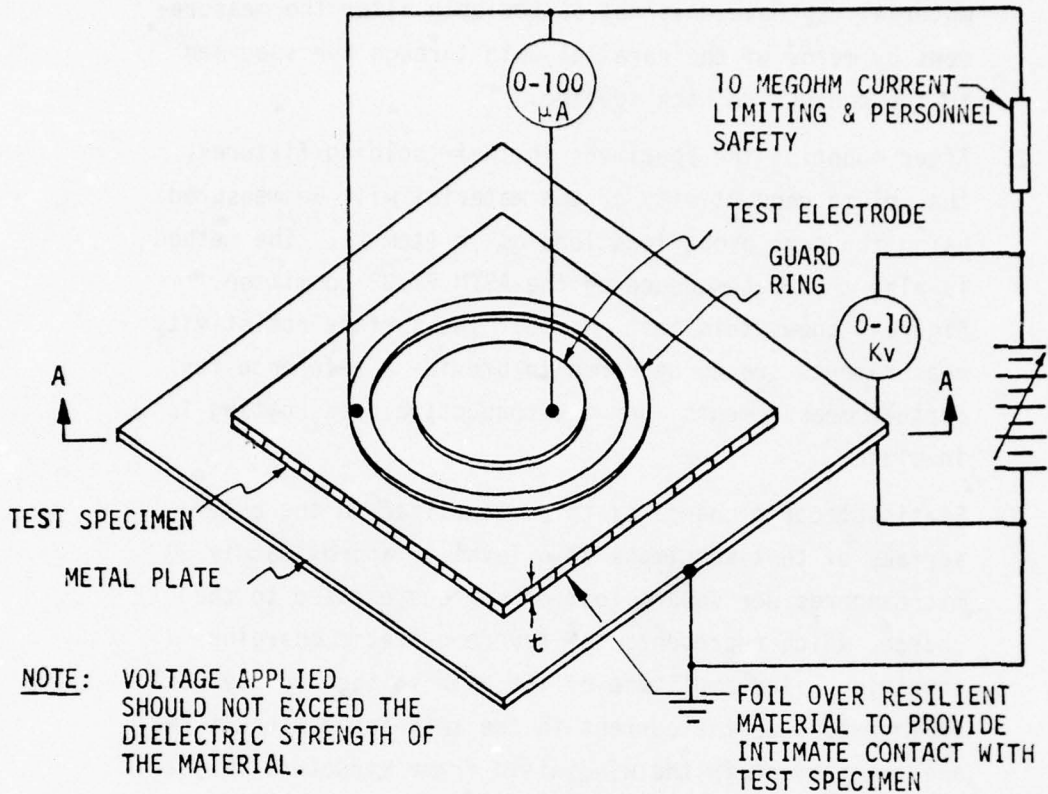
Figure 3. Surface resistivity test setup.

to assure that any volume conductivity the windshield material may have does not appreciably alter the measurement by means of the parallel path through the specimen to the conductive back coating.

2. After mounting the specimens in their holding fixtures, the volume conductivity of the material will be measured using the same probe locations as in Item #1. The method is also that recommended by the ASTM F7.08 committee. Figure 4 shows this test method. The surface resistivity measurements are to be rerun to provide a reference for further measurements when the conductive back coating is in place.
3. Static electric charge is to be deposited on the outer surface of test specimens at a level of approximately 30 microamperes per square foot of surface exposed to the charge, which represents the severe p-static charging condition. The amplitude of the high voltage supply will be increased as the current in the anti-icing circuit (M2) and the current in the windshield frame structure (M3) are measured. The total generator current (M1) is also measured.

Electrical, visual and audible means will be used to detect voltage breakdown and flashover on the test specimen.

4. If surface flashover occurs in the tests of Item #3, the surface resistivity in this area will be remeasured. The general location of the flashover will be recorded. If specimen puncture occurs, the location will be carefully recorded and the volume conductivity in this region remeasured.
5. Interference control tests will be made to record the interference signal characteristics and to verify the



TEST: INCREASE APPLIED VOLTAGE FROM ZERO OR LOW VALUE AND ADJUST FOR  $40 \mu\text{A./1000 CM}^2$  + 20% OF AREA UNDER TEST ELECTRODE. WAIT UNTIL READING STABILIZES.

Figure 4. Volume conductivity test setup.

effectiveness of various candidate filter techniques to be used to suppress electrical transients induced in the anti-icing circuit. These tests will be conducted in conjunction with the static charge testing of Item #3.

6. Data are to be recorded to fully define the details of the test setup, the test instruments, and the test results. The test specimens will be fully defined as to their source of manufacture, type of material, manufacturing data pertinent to the tests, and test and handling history.

#### Swept Stroke Lightning Tests

The following procedure is planned for the conduct of the swept-stroke lightning tests:

1. Perform a surface resistivity and volume conductivity test on each of the specimens prior to swept-stroke lightning tests.
2. Perform swept-stroke/restrike lightning tests on the windshield test specimens. The restrike time will be set to simulate the most critical test condition. A high speed movie camera and a Polaroid camera will be used to record the swept-stroke/restrike event. Photographs will record the test current waveform. The aluminum foil tape simulating the anti-icing heater element will be instrumented to monitor the lightning strike current flow, if any. The environmental conditions will also be recorded.

Aluminum foil tapes will be applied over the specimen surface to adjust the windshield dimension to be tested. Tests will be conducted repeatedly, each time increasing the dimension until a puncture occurs in the test specimen or the maximum windshield dimension is reached.

SECTION III  
CONDUCT OF TESTS AND TEST RESULTS

Section III of this report describes the conduct of the actual testing and interprets the data. The tests dealing with static electric charging were conducted first, followed by the swept stroke lightning tests.

Final Test Specimen Details

Section II of this report listed the nine test specimens. Due to unexpected delays in the receipt of some of the specimens from the manufacturers, the test sequence for the static electric tests were not exactly as planned. In fact, the availability of some specimens with anti-static coatings, before all of the uncoated specimens were available, provided the incentive to conduct short evaluations of their anti-static characteristics, even though these tests were not originally planned.

Handling the nine large glass and acrylic samples (over 23,000 square inches total) presented a challenge since it was necessary to provide for their safe storage when not actually being tested, as well as to provide for their rapid installation in the test fixtures. The constraints of both the static electric test fixture at the Douglas Aircraft Plant in Long Beach, California, and the outdoor swept-stroke lightning test fixture at the Lightning and Transients Research Institute in Miami, Florida, with its 220-mile-per-hour wind velocity, were considered in arriving at a feasible, yet economical means of supporting the specimens. The need to safely ship the specimens from coast-to-coast was also an important constraint.

An effective, low cost specimen mounting was devised which placed each specimen on individual cushioned wood pallets. The mounting method is shown in the sketch of Figure 5.

The test specimens were first coated with aluminum foil to simulate the anti-icing heater element. The aluminum back foil was laid on the

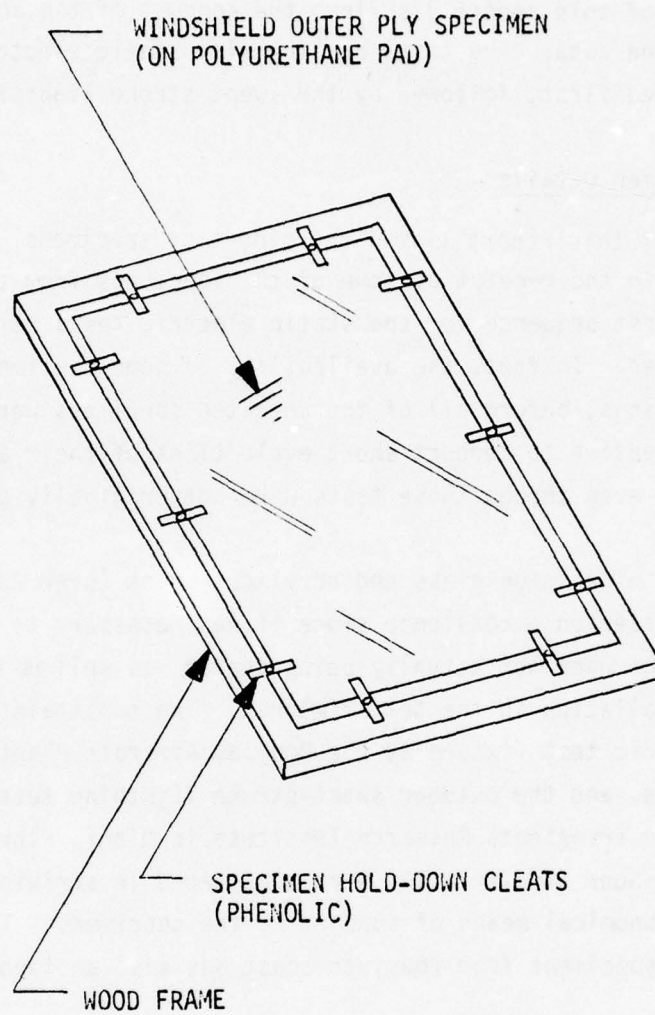


Figure 5. Typical specimen mount.

specimens with a half-inch circumferential non-conducting border at each edge of the specimen to permit various edge configurations, as discussed later. The 48-inch wide specimens were back coated with two 2-foot-wide sheets of 0.001-inch-thick foil, trimmed to proper size at the edges. The two sheets were laid out side by side on the specimen after a light application of sprayed-on adhesive. The two sheets were electrically connected by a 1/4-inch-wide band of aluminum foil tape, which had a conductive adhesive. All foil surfaces were carefully rolled to provide a smooth surface. The 37-inch-wide Chemcor specimens were similarly coated with aluminum foil, except that one 2-foot-wide by 0.001-inch-thick sheet, and one 1-foot-wide by 0.0007-inch-thick sheet were used. Therefore, for these specimens the back foil joint was off center.

All of the wood mounting pallets were similar in that they provided a large sheet of 1/2-inch-thick polyurethane foam to cushion the specimen, and a nominal 4-inch-wide wood border to protect the specimen edge and to provide a surface on which to mount various simulated edge structures. Electrical contact to the back foil of each specimen was made by non-permanent pressure contact between the back foil and a 3-inch-square pad of aluminum foil affixed to the polyurethane foam. A length of stranded wire interconnected the foil pad and the external measuring circuits.

Each specimen was held to the wood pallet by a number of small phenolic cleats located around the specimen periphery. These hold-down cleats served the dual purpose of holding the specimens on the test pallets during laboratory handling and shipping, and restraining the specimen when the 220-mile-per-hour wind was passed over it during the swept-stroke lightning tests.

#### Surface Resistivity & Volume Conductivity Measurements

##### Surface Resistivity

The ASTM test method discussed in Section II of this report was used to

measure the surface resistivity. The test probe used had the same "foot-print" dimensions as that shown in Figure 3, Section II; however, the probe design was simplified. Figures 6 and 7 show photographs of the surface resistivity probe (smaller of the two) and the volume conductivity probe.

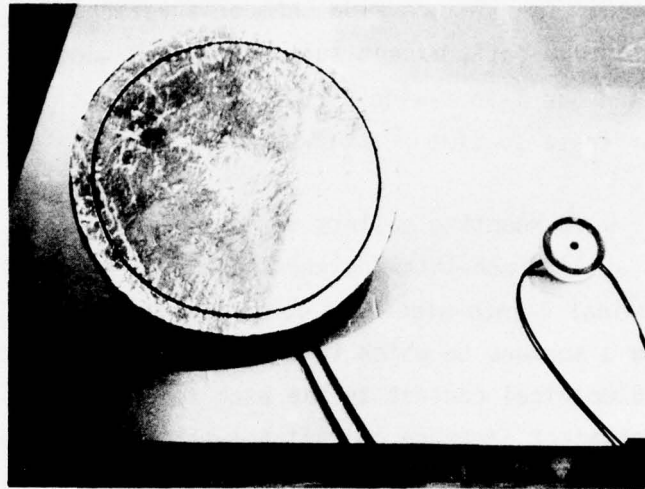


Figure 6. Volume conductivity probe (left) and surface resistivity probe - front views.

The surface resistivity of each test specimen was measured. Those specimens which did not have an anti-static coating measured infinite surface resistivity, within the capabilities of the instrumentation. (No current was detected at voltages up to 15 kilovolts.) Coating the back side with the aluminum foil did not alter the infinite resistivity reading on the other side.

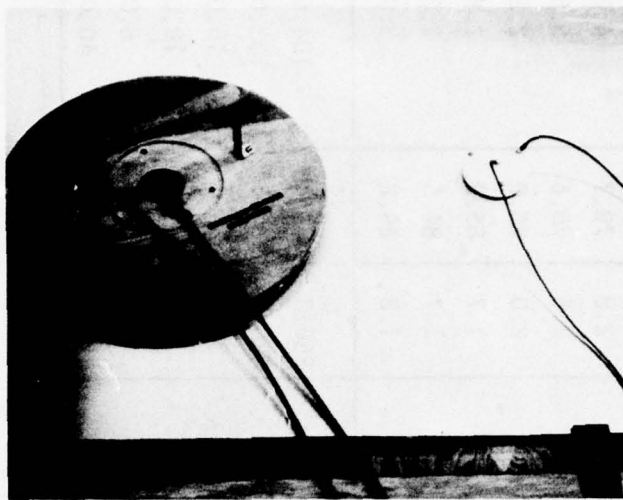


Figure 7. Volume conductivity probe and surface resistivity probe - back views.

The surface resistivity of the anti-static coated specimens was measured at various surface locations on each specimen and compared with the values obtained by the glass manufacturers. Data for the two PPG Industries specimens are shown in Table II. Similar data for the two Corning Glass specimens are shown in Table III. The Douglas readings were made with the probe pictured in Figures 6 and 7 and a Simpson 260 volt-ohm meter. The specific test equipment employed by PPG and Corning is not known. The variations in the data do raise questions regarding the methods and techniques and reinforce the need for the standardization efforts of the ASTM in this field.

Note that the readings for the Z5942632-503 Herculite II specimen made by PPG and by Douglas are fairly close, with the Douglas readings generally - but not always - higher than those made by PPG. The measurements for the Z5942632-505 Soda Lime specimen do not follow the same

TABLE II. SURFACE RESISTIVITY OF PPG INDUSTRIES TEST SPECIMENS AT VARIOUS SURFACE LOCATIONS

SAMPLE	LOCATION*	PPG READINGS		DAC READINGS $R_S$	LOCATION*	PPG READINGS		DAC READINGS $R_S$
		$R_S$	$\tau$			$R_S$	$\tau$	
Z5942632  -503 HERCULITE II 0.110 INCH THICK	a	2.0	81.0	2.2	g	2.8	70.7	4.2
	b	1.8	80.8	2.2	h	2.6	70.6	5.6
	c	1.9	80.0	2.6	i	2.0	85.0	2.8
	d	1.9	80.0	3.0	j	1.7	85.3	2.8
	e	4.0	72.5	3.8	k	1.7	84.5	2.8
	f	3.1	71.7	3.6	l	1.8	84.2	3.0
-505 SODA LIME 0.187 INCH THICK	a	20.0	84.5	14.0	g	250.0	87.4	104.0
	b	30.0	87.9	14.8	h	220.0	90.6	132.0
	c	28.0	88.4	20.0	i	33.0	86.4	16.0
	d	47.0	88.0	40.0	j	9.0	86.2	10.0
	e	45.0	87.0	19.2	k	7.0	86.8	8.0
	f	55.0	88.2	28.0	l	50.0	89.3	40.0

\*See Figure 8.

SURFACE RESISTIVITY ( $R_S$ ) (Kilo Ohms/Square)

LIGHT TRANSMISSION ( $\tau$ ) (Percentage)

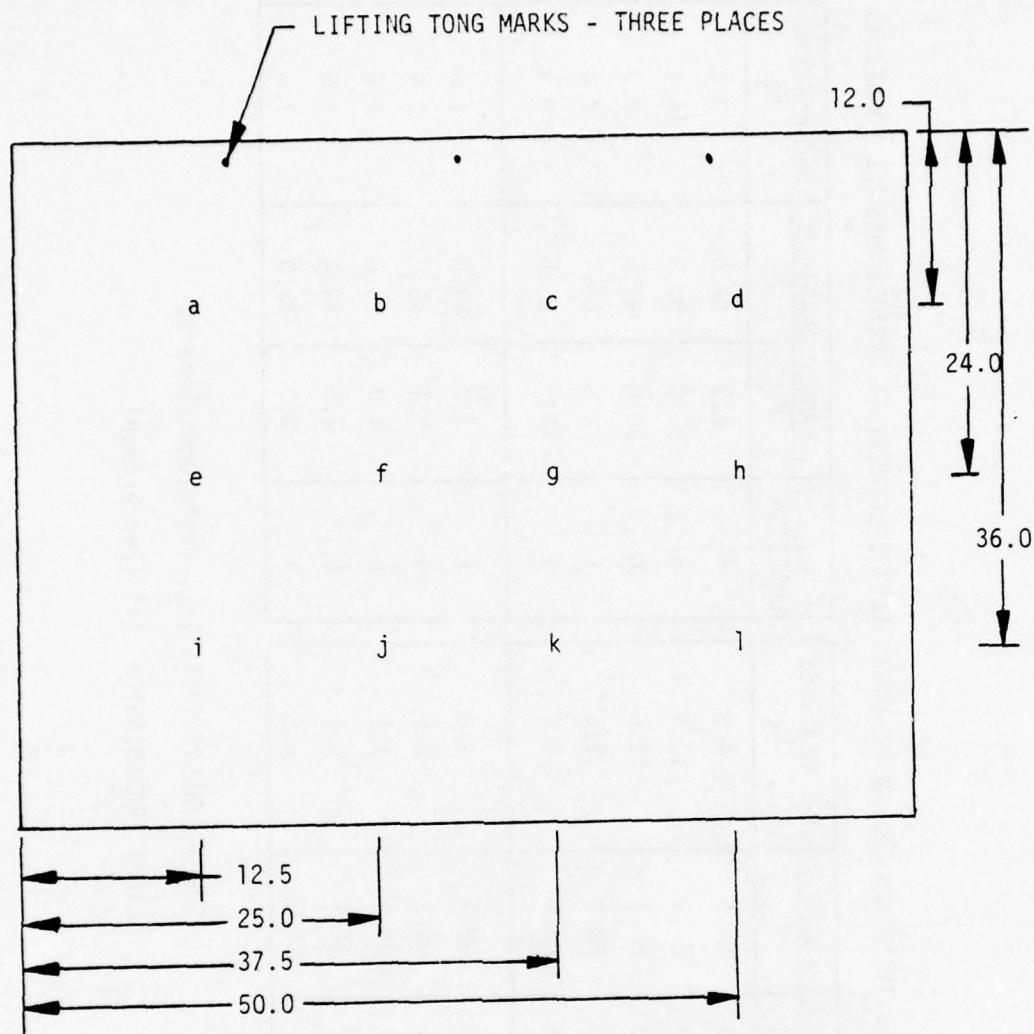
TABLE III. SURFACE RESISTIVITY OF CORNING GLASS WORKS TEST SPECIMENS AT VARIOUS SURFACE LOCATIONS

SAMPLE	LOCATION	CORNING READINGS		DAC READINGS	* LOCATION	CORNING READINGS		DAC READINGS
		$R_S$	$\tau$			$R_S$	$\tau$	
Z5942632	a	7.0	85.5	4.8	f	6.2	86.9	3.4
	b	23.0	87.0	10.4	g	30.0	87.5	14.2
	c	26.0	87.7	11.6	h	20.0	87.6	7.0
	d	10.0	86.9	5.6	i	8.5	86.1	4.4
	e	6.6	86.6	3.2	j	14.0	85.6	8.8
-509 CHEMCOR 0.085 INCH THICK	a	6.0	88.1	4.8	f	2.2	84.8	1.6
	b	4.6	85.2	2.6	g	3.1	85.0	2.4
	c	2.7	84.8	1.6	h	4.0	85.0	2.6
	d	2.4	84.7	1.4	i	7.5	88.4	5.6
	e	2.5	84.6	1.8	j	9.0	89.0	7.4
-513 CHEMCOR 0.105 INCH THICK	a	6.0	88.1	4.8	f	2.2	84.8	1.6
	b	4.6	85.2	2.6	g	3.1	85.0	2.4
	c	2.7	84.8	1.6	h	4.0	85.0	2.6
	d	2.4	84.7	1.4	i	7.5	88.4	5.6
	e	2.5	84.6	1.8	j	9.0	89.0	7.4

\*See Figure 9.

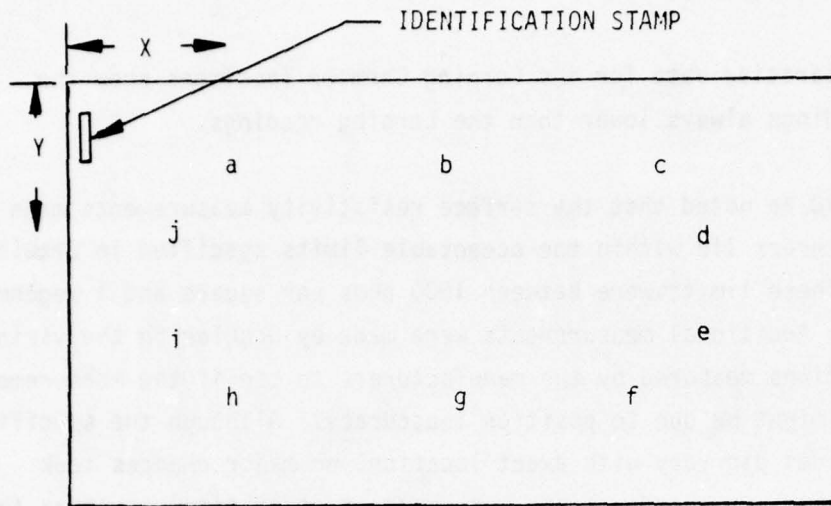
SURFACE RESISTIVITY ( $R_S$ ) (Kilo Ohms/Square)

LIGHT TRANSMISSION ( $\tau$ ) (Percentage)



NOTE: All dimentions given in inches.

Figure 8. Test locations associated with Table II.  
(For specimens Z5942632-503 and -505.)



Location	Z5942632-509		Z5942632-513	
	X (inches)	Y (inches)	X (inches)	Y (inches)
a	16	6.25	8.75	6.5
b	26	7.25	19.25	6.5
c	35	7	29.5	7
c	48	11.75	46.5	11.5
e	49.25	26	47.5	23
f	43	27	38.5	30
g	31.5	27.5	27.75	29.25
h	22.75	27.5	20	28.25
i	8	26	8.75	26.5
j	6	13.5	8.75	16.5

Figure 9. Test locations associated with Table III.  
(For specimens Z5942632-509 and -513.)

trend. Here the Douglas measurements were sometimes substantially lower than those made by PPG.

The comparative data for the Corning Chemcor specimens show the Douglas readings always lower than the Corning readings.

It should be noted that the surface resistivity measurements made by the manufacturers lie within the acceptable limits specified in Drawing Z5942632. These limits were between 1000 ohms per square and 1 megohm per square. Additional measurements were made by Douglas in the vicinity of the locations measured by the manufacturers to see if the measurement differences might be due to position inaccuracy. Although the specific measured values did vary with exact location, no major changes took place. Further, unrecorded tests were made at other times to check the ageing stability of the surface coatings and measurement reliability. Nothing was noted that changes the previous observation that the methods of measurement must have been different at the three facilities (PPG, Douglas, and Corning).

Since the manufacturing methods used to apply the anti-static coatings appear to be quite unprecise at best, further measurements of the surface resistivity were made on some of the panels at other locations on the panels. Two corners of the -505 soda lime specimen were found to have no resistive coating, while the other two corners showed a resistivity which was generally lower than the central area of the panel. The periphery of the -503 Herculite II panel surface showed resistivity values in the region of two to four times the general value of the central area. The -509 Chemcor specimen was measured on the surface corners and found to have values similar to those in the central area.

Drawing Note 1.3 on the specimen drawing, Z5942632, states that any conductive coating overspray on the back and edges of the test specimen shall be removed. Apparently this was not achieved for the edges, although no resistive coating was detected on the back side of the panels.

The lack of conductivity at some surface periphery areas and the presence of conductivity on some edges could pose a significant user problem relating to grounding the anti-static coating and electrically isolating this coating from the anti-icing coating and its circuitry. It is also significant that these electrical flaws went undetected by the inspectors at all three companies. The edge conductive material was removed after engineering inspection in the Douglas Lightning Test Laboratory.

#### Anti-Static Coating Discoloration

Stannous oxide anti-static coatings have been reported to be relatively trouble free by commercial airline users. However, there is no regular check of their resistivity. Isolated reports of coating removal or severe discoloration have been heard but documented data are difficult to find.

One specific incidence of removal and discoloration did occur when the stannous oxide was being removed from the specimen edges during the Douglas tests. The coating was removed by a multi-step operation as follows: First, apply a slurry of zinc powder mixed in water to the area to be removed. Next, after the zinc mixture has dried, a strong solution of HCL is carefully applied to the zinc. This is followed by several washings with clear water. The water, too, must be carefully applied to confine all activity to only the specific area where stannous oxide removal is desired.

Although great caution was used, a drop or two of the wash water got on the face of the panel. The result was a small, brown, non-conducting spot that could not be washed away.

It is not expected that aircraft maintenance crews will use zinc powder and HCL as they work on or in the vicinity of an aircraft windshield. However, cleaning materials that are used around aircraft can and have contained mixtures of chemicals which react with aircraft metals to produce a compound that can stain the stannous oxide.

A specific instance of chemical staining to an anti-static stannous oxide coating occurred to a Jet Commander aircraft formerly owned by the Douglas Aircraft Company. This aircraft was being repainted by an outside contractor and sustained irreversible damage, in the form of large colored splotches, to the windshield from some of the chemicals used during the repainting operation.

#### Effects on Light Transmission Due to the Anti-Static Coating

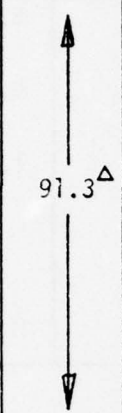
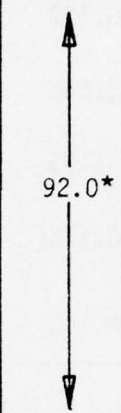
Tables II and III also show the measured light transmission through the specimens at the same locations where the surface resistivity was measured. Data were not available to Douglas on the light transmission prior to applying the anti-static coating, but data were available on the light transmission measured on other Corning Chemcor specimens of the same type and thickness material. These data are shown in Table IV. Comparison of these clear pane data with the data of Tables II and III indicates a light transmission reduction of approximately 6 percent for the -513 Chemcor specimen where the surface resistivity averages 3180 ohms per square and 4.6 percent for the -509 Chemcor specimen where the surface resistivity averaged 7340 ohms per square - based on the Douglas resistance measurements.

#### Volume Conductivity

The volume conductivity tests were conducted using essentially the test setup described for the ASTM method of Figure 3, Section II of this report. The test probe consisted of a circular central electrode of one square foot area. A 50 microampere meter movement and a 13 kilovolt supply were used in lieu of the values shown. The photographs of Figures 6 and 7 also show the volume conductivity probe. The volume conductivity was calculated as follows:

$$\text{CONDUCTIVITY (MHOS/INCH)} = \frac{I t}{E a}$$

TABLE IV. LIGHT TRANSMISSION LOSS DUE TO ANTI-STATIC COATING

Z5942632-509 CHEMCOR 0.085" THICK % LIGHT TRANSMISSION				Z5942632-513 CHEMCOR 0.105" THICK % LIGHT TRANSMISSION			
LOCATION	CLEAR	COATED	LOSS	LOCATION	CLEAR	COATED	LOSS
a		85.5	-5.8	a		88.1	-3.9
b		87.0	-4.3	b		85.2	-6.8
c		87.7	-3.6	c		84.8	-7.2
d		86.9	-4.4	d		84.7	-7.3
e		86.6	-4.7	e		84.6	-7.4
f		86.9	-4.4	f		84.8	-7.2
g		87.5	-3.8	g		85.0	-7.0
h		87.6	-3.7	h		85.0	-7.0
i		86.1	-5.2	i		88.4	-3.6
j		85.6	-5.7	j		89.0	-3.0

NOTES: LOCATIONS CORRESPOND WITH THOSE OF TABLE III  
 Δ MEASURED BY CORNING ON -507 SPECIMEN  
 \* MEASURED BY CORNING ON -511 SPECIMEN

where:

I = leakage current in Amperes

t = sample thickness in inches

E = applied voltage

a = area of active test probe = 144 square inches

Table V shows the leakage current, specimen thickness, and calculated value of volume conductivity for the four uncoated glass specimens. The leakage current for the -515 acrylic test sheet was so low that it could not be measured with the available equipment. Therefore, its volume conductivity is considerably lower than that of the glass specimens.

TABLE V. VOLUME CONDUCTIVITY DATA

TEST SPECIMEN (Z5942632)	THICKNESS (INCHES)	LEAKAGE CURRENT (MICROAMPERES)	TEST VOLTAGE (KILOVOLTS)	VOLUME CONDUCTIVITY (MHOS/INCH)
-1 Herculite II	0.110	5	13	$2.44 \times 10^{-13}$
-501 Soda Lime	0.187	9	13	$8.99 \times 10^{-13}$
-507 Chemcor	0.085	2	13	$9.08 \times 10^{-14}$
-509 Chemcor	0.105	2	13	$1.12 \times 10^{-13}$
-515 Acrylic	0.125	0	13	--
DC-10 Soda Lime (Plate Glass)	0.193	8	13	$8.25 \times 10^{-13}$

An additional specimen of soda lime glass was available in the form of an outer ply for a DC-10 airplane windshield. This 0.193 inch thick test part was made from plate glass and had a NESAs anti-icing resistive coating applied to one side. The NESAs coating was used as the back conductor. This specimen is of interest because the plate glass process is different from the float glass process used to produce the Z5942632-501 specimen. There has been some speculation that the molten tin, upon which the float glass is floated during the cooling process, might migrate slightly into the glass and alter its conductivity. The slight difference in the readings for the float glass -501 specimen and the plate glass DC-10 specimen does not appear significant in light of the precision of this measurement. Therefore, no conclusion can be drawn from this experiment regarding differences between float and plate glass.

Similarly, the two values of volume conductivity obtained for the Chemcor specimens are open to question since the same leakage current was recorded for the two different specimen thicknesses. A much more sensitive current detector would be required to resolve this question. Merely

substituting a more sensitive meter movement could lead to meter damage because the high initial charging current noted on normal specimens when the probe was moved to a new location was sufficient to drive the meter needle off scale. A logarithmic meter response would appear to be ideal for this application.

The volume conductivity measurements do appear mutually consistent for the specimen types. This conclusion is based on the rough observations of charge retention time noted for the various materials during the simulated precipitation static charging tests reported later in this report. For a given ambient relative humidity, the acrylic panel held a charge the longest period of time, followed by the Chemcor, Herculite II, and Soda Lime specimens in that order.

### Description of Charge Spray Test Technique

#### Background

To study the effects of static electric charge desposition on windshield specimens, it would be ideal to deposit this charge just as it occurs by the natural triboelectric action of impinging particles on the windshield surface of an aircraft in flight. This approach has had limited success. Attempts using ice crystals injected into a high velocity windstream (Reference 1) have been used for small test samples. The auxiliary equipment complexity and operating cost of a setup large enough to deposit the charge evenly over a 4 X 5-foot sample were out of the question for the limited funding of the test series which are the subject of this report.

Another triboelectric charging approach using dry flour (Reference 2) had also demonstrated limited success for charge deposition on small samples. This approach was also discarded because of cost and equipment complexity as well as for the possibility of violent explosion due to the presence of a large volume of combustible dust and electrical arcing discharges.

Surface charging, while not triboelectric in origin, can be achieved by applying very high voltage to an electrode held over the surface of a dielectric sheet, such as a windshield. The dielectric must have another electrode of opposite polarity on the opposite side. This second electrode can be a point electrode, but it is most effective when it is a planer conductor, such as a sheet of metal or the deposited conductive coating of an electrical heating element. High voltage direct current is applied to the two electrodes in increasing amplitude until either puncture or surface breakdown occurs. Figure 9 depicts a point electrode configuration. This method of charging has several disadvantages as discussed below.

One of the main objectives of any simulation of triboelectric charging is to achieve a charge distribution similar to that caused by particle impingement charging on a real windshield. Since the wind flow over a real windshield is distributed over the whole area, the particle impingement caused by this wind flow will also be distributed. Normally, the distribution will not be uniform, but for this windshield technology study, a uniform charge distribution appeared to be the best compromise among the near infinite variations that could take place. A uniform distribution also appears much more realistic than the highly non-uniform distribution created by one electrode over the center of a large sheet of dielectric, as represented by Figure 9.

Another reason for avoiding the single point electrode setup for use over large area dielectric specimens was that the voltage gradient between the single point electrode and the planer conductor on the other side of the test specimen (representing an anti-icing conductor) could be unrealistically high. This condition could induce unrealistic discharge puncture of the test specimen rather than the more natural surface arcing, if the charge density had been more uniformly distributed. This possibility of puncture increases with the size of the test specimen, assuming the single point electrode is held over the center of the specimen.

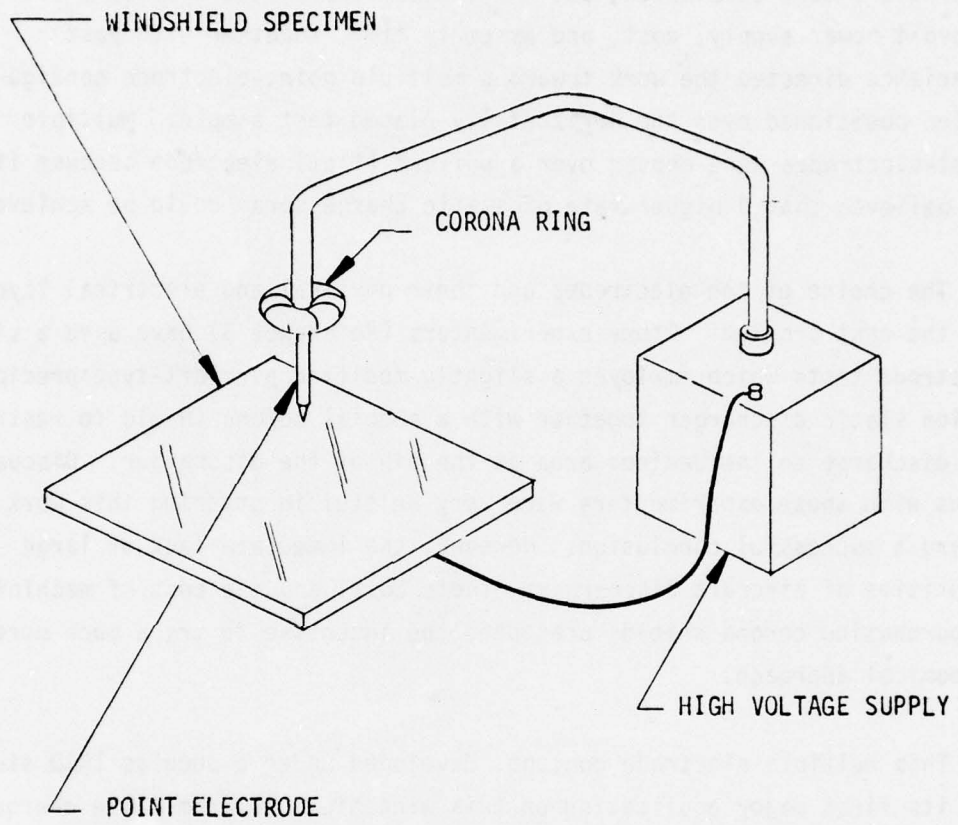


Figure 10. Point electrode surface charging configuration.

## The Charge Spray Head Design

Achieving a uniform charge distribution over more than twenty square feet of specimen surface presented a significant problem if costs were to be held to an acceptably low level. Several possible charge spray configurations were considered, but the limitations of the available 150-kilovolt power supply, cost, and assembly time, together with past experience directed the work toward a multiple point-electrode configuration positioned over the horizontally placed test sample. Multiple point-electrodes were chosen over a uniform (flat) electrode because it was believed that a higher rate of static charge spray could be achieved.

The choice of the electrodes and their physical and electrical layout was the next problem. Other experimenters (Reference 3) have used a single electrode tests which employed a slightly modified aircraft-type precipitation static discharger together with a special corona shield to restrict the discharge to the desired area at the tip of the discharger. Discussions with these experimenters were very helpful in steering this work toward a successful conclusion. However, the immediate lack of large quantities of aircraft dischargers, their cost, and the cost of machining or purchasing corona shields presented the *incentive to try a much more economical approach.*

This multiple electrode concept, developed under a Douglas IRAD study, had its first major application on this windshield program. The charge spray head design criteria required a large number of discharge points positioned over the test specimen and with respect to each other so that an even charge density appeared at the test sample surface, while still avoiding too much mutual interaction among adjacent discharge points.

Decoupling of the individual discharge points from each other and from the voltage source was thought to be desirable in order to create, as nearly as practicable, a multitude of individual, non-interacting, ionizing sources. Uninhibited imagination and raids on the microwave laboratory "junk box" and the office supply room produced the charge

spray head design shown in the photographs of Figures 9 and 10. The point electrodes were made from ordinary lead pencils which were sharpened at both ends. The lead pencil seemed ideal for this use. It was inexpensive, (the cheapest available offered the greatest end-to-end electrical resistance), it was reasonably well insulated except at the sharpened points, the discharge point was easily formed in a pencil sharpener, and spares were readily available.

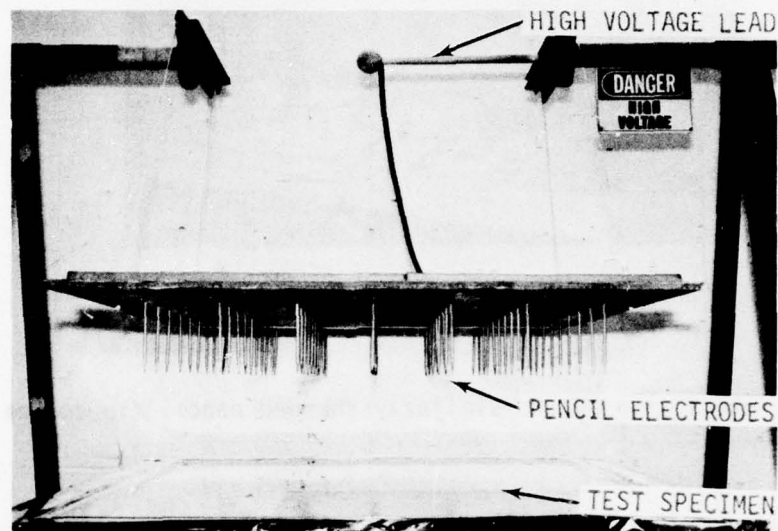


Figure 11. Multi-electrode charge spray head.

The charge spray head support board (Figures 11 and 12) was made from a surplus 73" x 44" x 1/2" sheet of fiberglass honeycomb material which had seen previous duty as a radome material sample. It was chosen because of its rigidity and light-weight - and its availability.

Holes were drilled in the fiberglass panel on 6-inch centers. The spacing was somewhat arbitrary but it appeared to be a good compromise between pencil length and pencil spacing - all aimed at reducing the

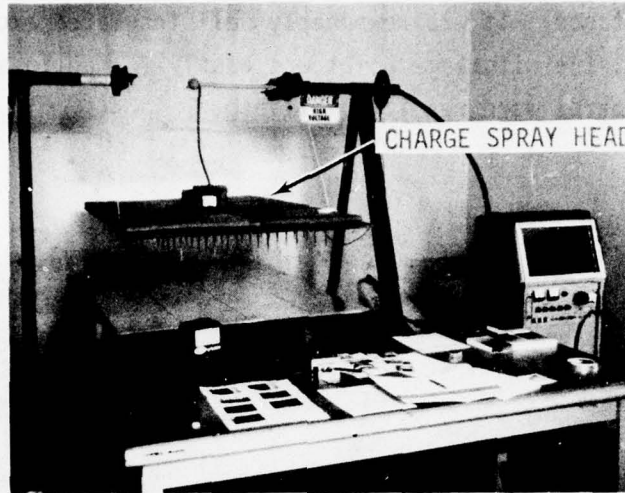


Figure 12. Charge spray test setup.

destructive interaction of the similarly charged pencil tip corona points.

Electrical interconnection of the pencils was achieved by allowing each pencil to protrude through the fiberglass panel where the exposed lead at this end - sharpened in a "draftsman's" pencil sharpener to expose more lead - entered conductive plastic foam consisting of one inch thick sheets of surplus radar reflective material. This back foam was Emerson and Cumings ECCOSORB ANW-75 which comes in two-foot square by one-inch thick sheets. Adjacent sheets of this material were interconnected with metal staples made from short lengths of copper wire.

The resistance of the foam sheets provided resistive isolation between the individual pencils. A total of seven dozen pencils was mounted on the board. Corona from all but the exposed pencil tips was eliminated, or

controlled, by the use of field geometry. The flat sheets of foam and their interconnecting wire staples provided a very low voltage gradient. The edges and corners of the foam sheets did show some tendency toward corona at extreme voltages. However, most of this corona was eliminated by cutting the sharp exposed square corners of the foam to reduce the voltage gradient to a level below the corona point.

Figure 12 shows the charge spray head suspended by ropes. The console on the right contains the controls for the Sorenson Model 1151 high voltage supply. The high voltage supply was located outside of the room in which the tests were conducted and a high voltage insulated cable was routed into the room, through a hollow phenolic tube (from which the high voltage sign is hanging), to the point where a water resistor drops vertically to the surface of the charge spray head.

The water resistor was made from a section of flexible plastic tubing filled with a water and salt solution. The need for the electrical isolation provided by this resistor was debatable in this application, but it served as a convenient and very flexible lead from the stiff high voltage wire to the charge spray head total-current meter shown sitting on top of the foam sheets.

Annoying corona at the right angle junction between the water resistor and the high voltage cable was eliminated by the corona shield shown in Figure 11. This corona shield was made from a well used tennis ball that had its ruffled nap soaked in salt brine. A few drops of water once in while provided very effective corona protection. (Rolling the ball in the graphite waste from the pencil sharpener would be an effective and more permanent alternative to salt water.)

#### Charge Distribution

Prior work by the Stanford Research Institute (Reference 4) had established a charging rate of 30 microamperes per square foot of the effective frontal area as a realistic value for heavy precipitation

static charging on a large transport airplane. Therefore, if all of the current delivered to the charge spray head were to be captured by the 24 square foot windshield, a total high voltage source current of 720 microamperes would be adequate. Actually, the supply had to be capable of more than this amount to account for extraneous corona loss and current flow to the metal structure surrounding the windshield.

The charge distribution characteristics of this test method were determined by mounting the charge spray head parallel to and from eight to eleven inches above a grid of metal squares. The grid consisted of a 4 X 6 foot pattern of one-foot square aluminum foil plates mounted to a sheet of plywood, as seen in Figure 12. The metal squares were connected to a twenty-four-point tap switch which allowed connection of a microammeter between a selected square and ground. The twenty-three remaining squares were returned to ground. In this way, the average charge current in each square foot of the area under the spray head could be measured.

From the start, with eleven-inch pencil tip-to-grid spacing, the charge spray distribution was remarkably uniform. Early trials produced variations of less than 10 percent among most of the squares, and a maximum deviation at one point of only 18 percent. As might be expected, the current to the peripheral squares was generally higher than the current to the interior squares. Adjustments were made to the charge distribution by removing some of the peripheral pencils and by shortening other pencils - a process that required a few quick turns in the pencil sharpener.

Table VI is an example of the uniformity of charge distribution that is possible with this technique. These data are for a pencil tip-to-grid spacing of eight inches. It appeared quite possible to achieve even greater uniformity; however, other factors, such as the exact sample size and edge geometry would negate the practical need for more uniformity.

Eleven inch tip-to-board electrode spacing was used for most of the tests to eliminate a tendency for direct flashover from the peripheral electrodes to the ground foil on the specimen under high voltage test conditions.

TABLE VI. CURRENT DISTRIBUTION FROM CHARGE SPRAY HEAD

GRID NO.*	GRID CURRENT ( $\mu$ A)	% DEVIATION FROM MEAN	GRID NO.	GRID CURRENT ( $\mu$ A)	% DEVIATION FROM MEAN
1	38.0	-4.3	13	38.0	-4.3
2	34.5	-13.3	14	39.5	-0.5
3	41.5	+4.5	15	40.5	+2.0
4	41.0	+3.3	16	40.5	+2.0
5	42.5	+7.0	17	41.5	+4.5
6	33.5	-15.6	18	37.5	-5.6
7	35.0	-11.9	19	34.5	-13.1
8	40.5	+2.0	20	41.5	+4.5
9	40.0	+0.7	21	43.0	+8.3
10	41.5	+4.5	22	44.0	+10.8
11	42.5	+7.0	23	45.0	+13.3
12	40.5	+2.0	24	36.5	-8.1

\*Grid #1 is at LH rear, #6 is at LH front, #19 is at RH rear, #24 is at RH front in Figures 11 and 12.

#### Charge Polarity Effects

Initial exploratory use of the charge spray head had the pencils connected to positive polarity with respect to the grid board squares. This was a purely arbitrary polarity and happened to be that of the power supply as it was initially connected. Charge distributions were measured with this polarity and with the opposite polarity. The change in polarity caused very little change in the charge spray distribution; however, there was a significant difference in the required charge head voltage to produce a given current. As an example, with the pencils spaced 11-1/8 inches from the grid board and the pencils positive, 85 kilovolts were required to produce an average current of 34.2 micro-

amperes in each of the metal grids. Changing the polarity so that the pencils were negative required only 76 kilovolts to produce an average grid current of 35.6 microamperes. From this observation it would appear that the pencil tips are a more effective electron source than the flat grid board.

The effects of polarity are further demonstrated by the photographs of Figures 13 and 14. These are photographs of a 2 foot by 6 foot by 5/8-inch-thick sample of acrylic which was available before the planned test specimens of this program arrived.

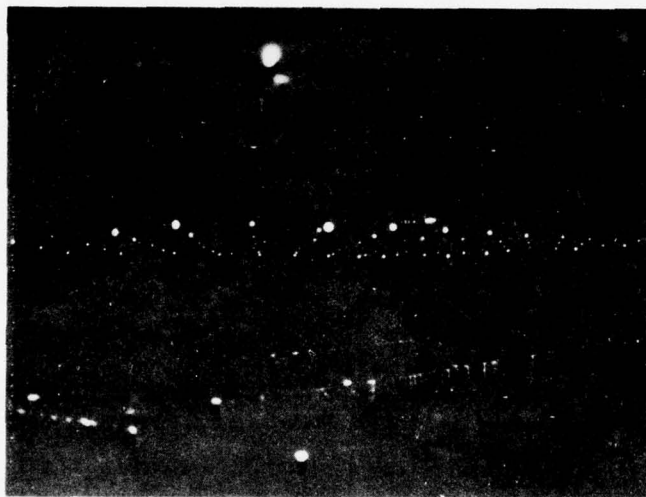


Figure 13. 5/8-inch-thick acrylic sheet with positive spray head polarity - 125 kilovolts.

Figure 11 is a multi-second time exposure of the corona activity for the condition of pencil electrodes positive with respect to the grid board on which the acrylic sheet was placed. Note the "city lights" effects of the corona at each pencil tip. The corona activity around the edge of the acrylic sheet was very low. The charge head potential was 125 kilovolts, with 2 milliamperes total current.

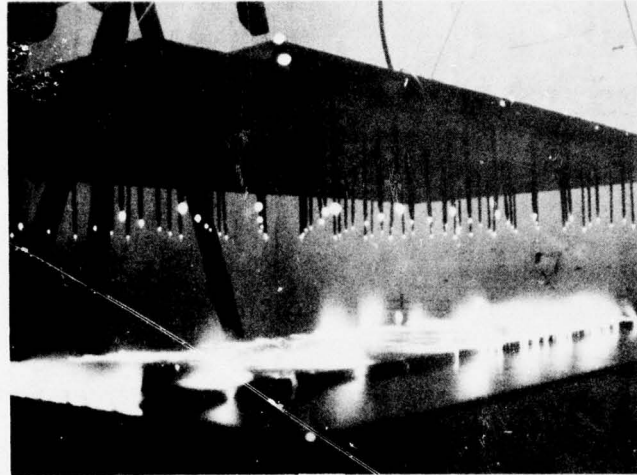


Figure 14. 5/8-inch-thick acrylic sheet with negative spray head polarity - 125 kilovolts.

Figure 14 shows the effect of changing the polarity. Figure 14 was still at 125 kilovolts but the charge head was then negative with respect to the grid board; otherwise the conditions were the same. Figures 13 and 14 were taken from the same viewing angle. Starting with Figure 14, a double exposure photographic technique was employed to enable some of the background hardware to be photographed. For Figure 14, the background was shot at  $f/22$  and  $1/125$  second. The corona exposure was shot at  $f/4.5$  and 12 seconds. The effects of multiple surface discharges and the grazing angle view caused significant overexposure. The total current in the charge spray head for Figure 14 was 2.1 milliamperes. Most of this current passed directly to the grid board and bypassed the acrylic sheet.

In an actual aircraft, ice crystals impinging on the windshield will generally acquire a positive charge, leaving the aircraft with a negative

charge (Reference 4). Therefore, for the remainder of these tests, the charge spray head was operated at negative potential to deposit negative charge on the specimen's upper (or outer) surface.

#### Charging Anomalies

The preliminary check out of the charge spray head had produced some very impressive surface discharges when using the available dielectric samples. (See Figure 14.) When the actual test specimens of this program became available, no problems were anticipated in generating the surface discharges necessary to the measurement of the electrical responses in the simulated anti-icing coating.

Because of the ease with which very large discharges were produced on the 5/8-inch-thick acrylic panel, there was concern for the possibility of puncturing the surface of the thinner test specimens which were the subject of these tests. Therefore, a cautious approach was followed. The most expendable and least expensive windshield candidate specimen was the Z5942632-515 acrylic panel. This 0.125-inch-thick sample, mounted on its test holder as described in Section III, was electrically divided into four equal surface areas by the application of 1/2-inch-wide aluminum tape laid on the upper surface. Figure 15 is a composite photograph of the test setup. The surface-dividing foil was grounded by a wire running to the right side end of the 1/2-inch foil. The back foil (simulating the anti-icing coating) was also grounded. The charge spray head board was spaced 13 inches from the specimen surface and the charge spray head was negative in polarity. The 1/2-inch surface tape was intended to reduce the surface distance over which an arc might take place, thereby reducing the surface potential and lowering the probability of surface puncture.

No surface arcing could be achieved with the test setup of Figure 15. This photo was made with 85 kilovolts applied to the charge spray head and 5 milliamperes total current. Since this was the maximum current capacity of the high voltage supply, no higher voltage could be applied.

For this condition, the current divided with approximately 2.8 milli-amperes in the back foil and 2.2 milliamperes in the 1/2-inch-wide surface foil. At 85 kilovolts, corona was observed around the edges of the acrylic sheet and at the edges of the surface tape. The additional corona dots appearing on the acrylic surface are actual reflections of the corona glow of the pencil electrode tips. For this specific test, the back foil on the -515 acrylic specimen was continued to the edge of the acrylic panel. Therefore, some, if not most, of the back foil current was due to corona at the edge of the foil.

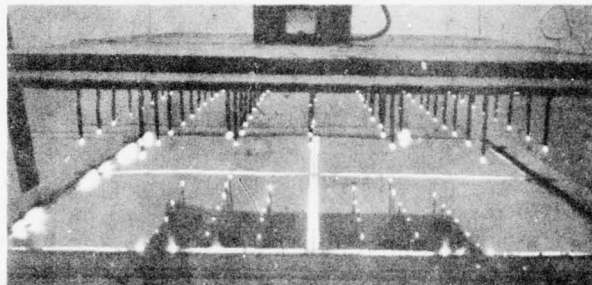


Figure 15. -515 acrylic test specimen with divided surface area for preliminary tests.

It was not evident why surface arcing was not taking place, but at least there appeared no danger of puncturing the surface of the acrylic specimen. Therefore, the 1/2-inch tape was removed from the surface. However, with this new configuration surface arcing still did not take place, regardless of the voltage applied. The edge corona still persisted, indicating a high voltage gradient and current flow around the edge to the back foil. For this setup, one milliamperes of charge head current at 55 kilovolts resulted in one milliamperes of current in the back foil circuit.

The lack of surface arcing still was not explainable. The relative humidity in the test room was at or around 40 percent during these measurements. The wet bulb-dry bulb thermometers had not been available during the previous exploratory tests during which surface arcing was readily achieved.

It was theorized that perhaps the edge corona noted on the periphery of the acrylic specimen was altering the surface charge; therefore, a series of tests was made during which grounded 1/2-inch wide aluminum tape was progressively placed on the four sides of the upper surface periphery. No surface arcing occurred during these tests. The edge corona just transferred from the acrylic edge to the edge of the surface mounted foil. During these tests, the total plasma current in the charge spray head progressively diverted from the back foil to the surface mounted edge foil until only about one tenth of the total current flowed in the back foil when surface foil covered all four edges of the specimen.

Next, the surface foil was removed from the -515 acrylic specimen and a new 1/2-inch conducting tape border was placed in the upper surface plane of the acrylic sheet but spaced 1/2-inch outboard of the periphery of this sheet. This change still produced no surface arcing. Current versus voltage measurements for both edge foil configurations showed nearly equal edge foil current up to about 70 kilovolts, at which time the back foil current began to rise disproportionately for the configuration where the edge foil was located away from the acrylic surface. This indicated that there was probably current flow around the edge of the specimen due to localized edge corona.

The acrylic testpanel had been expected to be rather easily charged to a flashover potential because of its very high surface resistivity and low volume conductivity. Since these tests did not produce the expected results, a different test specimen was tested.

The Z5942632-1 Herculite II, with back foil and mounting the same as the initial mounting for the acrylic panel, was mounted under the charge spray head. The voltage was raised to around 90 kilovolts, at which time two or three large "oak tree" shaped surface discharges took place in rapid order. The relative humidity was a very low 25 percent this day. Unfortunately, no photograph was obtained of this discharge. Subsequent attempts to cause a repeat of the phenomena were unsuccessful. The voltage was raised to 100 kilovolts where the back foil current reached the 5-milliampere limit of the power supply. At this high voltage level, there were periodic direct flashovers from the pencil electrodes on the periphery of the charge head to the back foil of the specimen. The flash path was along the side of the glass - not through it. To alleviate this condition, the charge spray head board was raised to 16 inches above the specimen surface. This greater spacing stopped the direct electrode to back foil flashover but apparently did nothing to induce surface arcing. Edge corona was produced at 120 kilovolts and 4.6 milliamperes back foil current.

To investigate what characteristics would induce surface arcing, a 15-inch square of 0.005-inch-thick Mylar was placed on top of the -1 Herculite II specimen corner. Two edges of the Mylar sheet coincided with the corner edges of the glass panel. Surface arcing on the Mylar sheet took place at charge spray head voltages around 100 kilovolts. This discharge activity was quite steady, with the vast majority of flashes going to the two edges of the Mylar sheet which were to the interior of the Herculite II panel. This suggested that something in the edge geometry of the glass specimen might be inhibiting the flash-over. Figure 16 is a photograph of this test setup. The photograph recorded one of the rare flashes to the outside edge of the Mylar as well as flashes to the inside edges.

The same Mylar sheet was moved a few inches toward the center of the -1 Herculite II specimen to remove the Mylar edges from the immediate proximity of the Herculite II edge. With this configuration, surface

arcing on the Mylar occurred to all four edges. The relative humidity was down to 23 percent at this time.

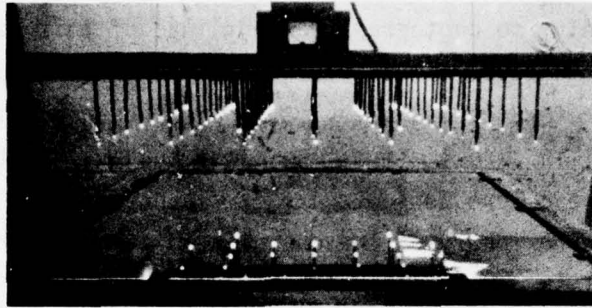


Figure 16. Mylar sheet in corner of -1 Herculite II specimen.

The surface discharges on the Mylar sheet were evidently due to the greater surface resistivity and lower volume conductivity of the Mylar as compared to similar qualities of the Herculite II. The surface flash current, leaving the Mylar surface edge, did not puncture the Herculite II, but was dissipated in the lower surface resistivity and higher volume conductivity of the Herculite II.

The same test previously conducted on the -515 acrylic sheet, wherein an off-surface, co-planer ring of aluminum foil was placed about 1/4-inch away from the glass edge, was conducted on this -1 Herculite II specimen with the Mylar insert. This grounded ring did not affect the surface arcing activity on the Mylar sheet. Figure 17 shows a photograph of this setup.

The current distribution between the back foil and the ring were measured for various spray head voltages. The setup was as shown in Figure 17 except that the Mylar sheet was removed. These data are shown

in Table VII. Table VIII is data for a test setup similar to that shown in Figure 17, except that the off-surface peripheral ring has been moved onto the edge surface of the -1 Herculite II glass. The data of Tables VII and VIII were taken to study the amount of charge current that goes through the glass due to volume conductivity versus that which goes to the edge conductor. The differences appeared more pronounced at the higher voltages, where once again (as with the acrylic panel), the off-surface ring did not block the current flow around the edge of the specimen as did the on-surface ring.

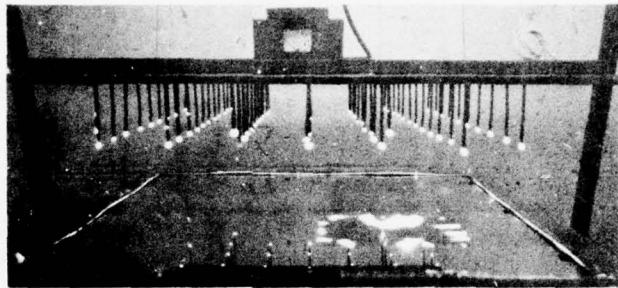


Figure 17. Mylar sheet and peripheral conducting ring on -1 Herculite II specimen.

Substantiation that a surface charge was actually being deposited on the glass was shown by the initial, high rate of change in current measured in the back foil circuit each time the voltage was changed. This was due to the charging current component as the capacitance of the circuit formed by the glass, back foil, and surface charge reached a state of equilibrium.

TABLE VII. BACK FOIL CURRENT & OFF-SURFACE CO-PLANER RING CURRENT

CHARGE SPRAY HEAD VOLTAGE (kv)	TOTAL SPRAY HEAD CURRENT (mA)	BACK FOIL CURRENT (mA)	CO-PLANER RING CURRENT (mA)
30	25 ( $\mu$ A)	19 ( $\mu$ A)	-
40	100 ( $\mu$ A)	62 ( $\mu$ A)	40 ( $\mu$ A)
47	195 ( $\mu$ A)	100 ( $\mu$ A)	100 ( $\mu$ A)
50	.27	.14	- (10 mA scale)
60	.5	.22	.2
70	.77	.27	.45
80	1.16	.34	.75
90	1.8	.41	1.9
100	2.5	.49	2.3
110	3.4	.57	2.9
120	4.4	.64	3.6

} meters  
} required  
} electro-static  
} shielding

TABLE VIII. BACK FOIL CURRENT & ON-SURFACE PERIPHERAL RING CURRENT

CHARGE SPRAY HEAD VOLTAGE (kv)	TOTAL SPRAY HEAD CURRENT (mA)	BACK FOIL CURRENT (mA)	ON-SURFACE PERIPHERAL RING CURRENT (mA)
30	30 ( $\mu$ A)	18 ( $\mu$ A) (100 $\mu$ A scale)	-
40	86 ( $\mu$ A)	50 ( $\mu$ A)	40 ( $\mu$ A) (on 1 mA scale)
47	155 ( $\mu$ A)	80 ( $\mu$ A)	80 ( $\mu$ A) (on 1 mA scale)
50	.26	.12	- (10 mA scale)
52*	.27	.12	-
60	.475	.155	.2
62*	.5	.16	.25
70	.74	.19	.45
72*	.77	.19	.5
80+*	1.16	.22	.85
90*	1.8	.275	1.5
100*	2.5	.32	2.15
110	3.35	.37	2.9
120	4.35	.43	3.7

} meters  
} required  
} electro-static  
} shielding

\*Voltage adjusted to give total head current same as for Table VII.

Another interesting and troublesome side effect was the electrostatic charge build up on the glass faces of the meters used to measure the back foil and ring current. These were Simpson Model 260 Multi-Meters that were placed on the table several feet from the charge spray head (see Figure 12.) The effect, which became quite pronounced at voltages in excess of 100 kilovolts, caused the meter needles to react in a jerky, non-uniform way. A grounded Faraday shield was improvised to shield the meters from the high voltage field. The shield solved the problem.

When testing at very high voltage levels, all objects in the room became charged to sparking level voltages. Dielectrics as well as ungrounded conductors took on a charge that could produce an annoying but harmless shock, if touched. Some of the corona spots shown in Figure 15 were the results of corona on extraneous objects. Even spots on the wall and the overhead fluorescent lights would flash and glow.

#### Edge Effects and Edge Geometry

The mystery of the non-flashing specimens caused many other experiments to be performed in order to explain and control the phenomena. Each successive test further reinforced the opinion that the specimen edge geometry was the governing factor; however, the possibility that the charge spray method of surface charge deposition might not be a valid way of simulating the actual triboelectric charging was constantly re-examined.

In an actual aircraft the windshield charge is caused by the impact of particles on the windshield, rather than by an electron flow, as was the case in this test setup. Metal objects on and around the windshield test specimen will have an influence on the electron flow before it strikes the windshield specimen. In the triboelectric case, the particles will not be appreciably influenced by the conductivity of, or the charge on, the surface of impending impact.

For the above reasons, some of the edge configuration studies which used metal tape employed strips of Mylar over the tape to reduce or eliminate direct electron flow to the conductor. The presence of un-insulated metal did have some influence on the local charge distribution, but this influence did not explain the continuing lack of success in obtaining surface arcing on the windshield test specimens.

Photos of the 5/8-inch-thick acrylic sheet used to obtain surface arcing during the early exploratory tests were restudied. The test specimen was also re-examined. At one point, an actual DC-10 aircraft windshield assembly with soda lime glass was placed under the charge spray head and surface arcing was easily obtained at 90 kilovolts and 1 milliamperere.

By this time the Chemcor test specimens had arrived, and being smaller in size (37" X 53") than the acrylic and PPG specimens, an un-mounted specimen was placed on top of the conducting foil of the grid board. The specimen chosen was the -511 which was 0.105 inches thick and had no anti-static coating. The glass was centered on the 4' X 6' grid board and the voltage was slowly increased. The results were spectacular. Huge "oak tree" surface discharges were easily attained at charge spray head voltages as low as 75 kilovolts. Figure 18 shows a 15 second exposure of the -511 Chemcor specimen on the grid board. The voltage was 75 kilovolts and the total current was 0.5 milliamperes. The relative humidity was 36 percent.

It should be noted that this Chemcor specimen would hold a strong surface charge for five minutes or more after the high voltage supply was turned off. This was in contrast to the short charge retention time for the Herculite II and soda lime specimens.

Once surface arcing had been achieved, the edge geometry was further studied. The test setup in Figure 18 was modified by the edge configuration shown in the sketch of Figure 19. The change in surface discharge pattern is shown in the photograph of Figure 20. Note that only

the left and right edges of the -511 specimen had the edge treatment shown in Figure 19 when the photo of Figure 20 was taken. The presence of the narrow metal foil on the edge of the glass appeared to have swept the charge from a path about six inches wide from both sides of the glass.

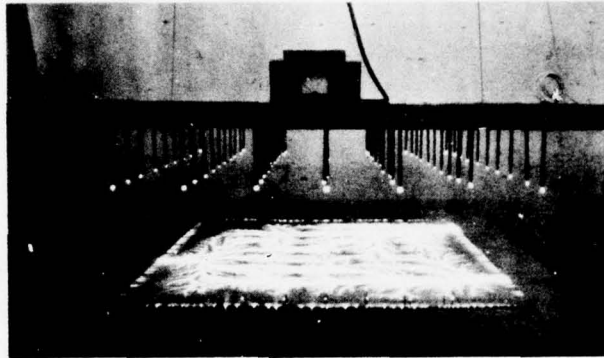


Figure 18. -511 Chemcor specimen on metal grid board.

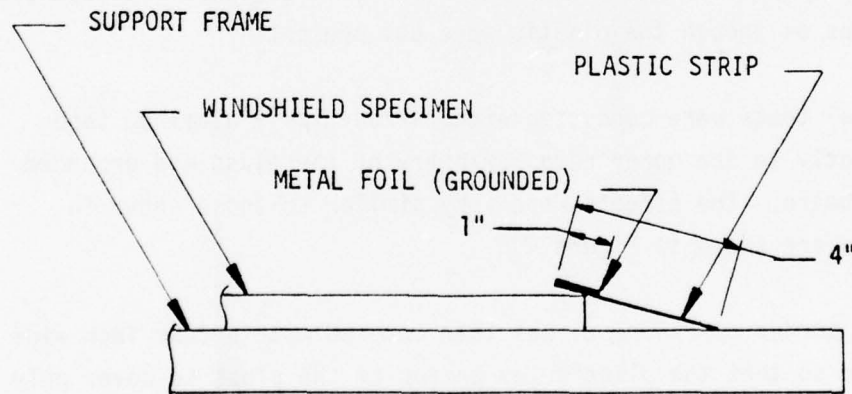


Figure 19. Edge conductor on -511 Chemcor specimen.

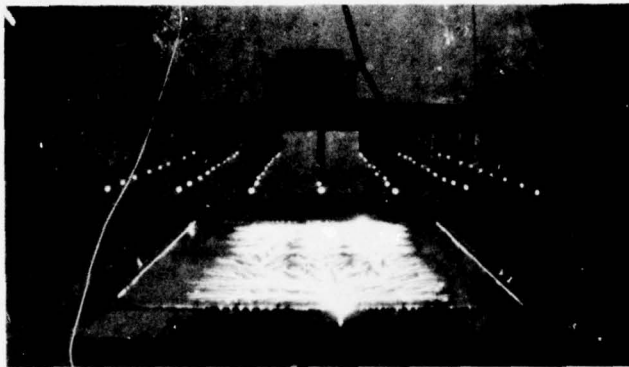


Figure 20. Surface discharge pattern for edge treatment of Figure 19.

The metal foil was placed on the four inch wide plastic strips (see Figure 19) to permit rapid changes in the configuration. However, the possibility of altering the local electron flow to the grid board due to the presence of the four inch wide plastic strips was considered. Therefore, the test was repeated with the plastic strips moved off of the glass surface and lying flat on the grid board and butted up against the edge of the glass. The aluminum foil on the plastic strips was still grounded and in the same relative position. Full surface flashovers returned and the effect was as though the plastic were not present.

Additional tests were conducted with narrow (1/4") aluminum tape applied directly to the upper edge periphery of the glass and grounded to the grid board. The effects were very similar to those shown in Figure 20 and are shown in Figure 21.

The foil border of Figure 21 was then covered with a four inch wide plastic strip so that the plastic lay on top of the glass to cover only the 1/4" wide aluminum tape. All surface flashing ceased with this configuration, although considerable edge corona was evident and the

total current increased from 1.5 milliamperes to 3.2 milliamperes for the same 100 kilovolts on the charge head. The increased current was probably due to the steady state edge corona. This corona may also have influenced the charge and charge distribution on the glass surface.

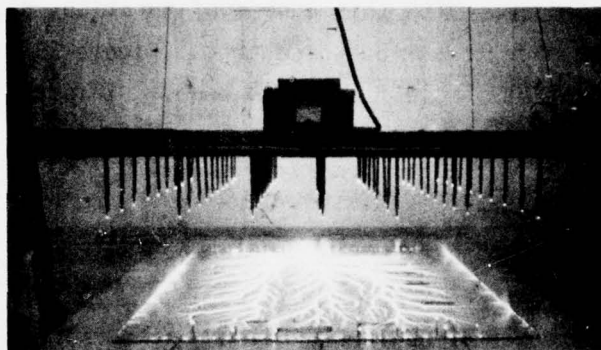


Figure 21. Chemcor specimen with 1/4-inch peripheral surface border.

During the testing process, the unmounted -513 Chemcor glass specimen with an anti-static coating was placed on the grid board with the anti-static coating facing the charge spray head. No surface arcing could be achieved. Full surface discharges were easily produced after turning the specimen over so that the uncoated surface faced the charge head.

While one objective of an actual windshield design could be the elimination of surface flashover, other design approaches may include the acceptance of surface flashover and, where necessary, incorporate other means to control the electrical transients resulting from the flashover. In order to do this, it was necessary to be able to produce surface flashover at will in the laboratory.

The success so far at finally achieving large surface flashover was still confined to specimens placed on the grid board. This was not the specimen configuration needed for the remainder of the tests. More edge configuration study was required to achieve a test setup that could produce surface discharges.

Finally, the specimen mounting technique was slightly modified per the sketch of Figure 22. With this edge configuration, all uncoated specimens could be made to surface-discharge. Figure 23 is a photograph of a typical single flash "oak tree." This photograph was taken on the -515 acrylic specimen.

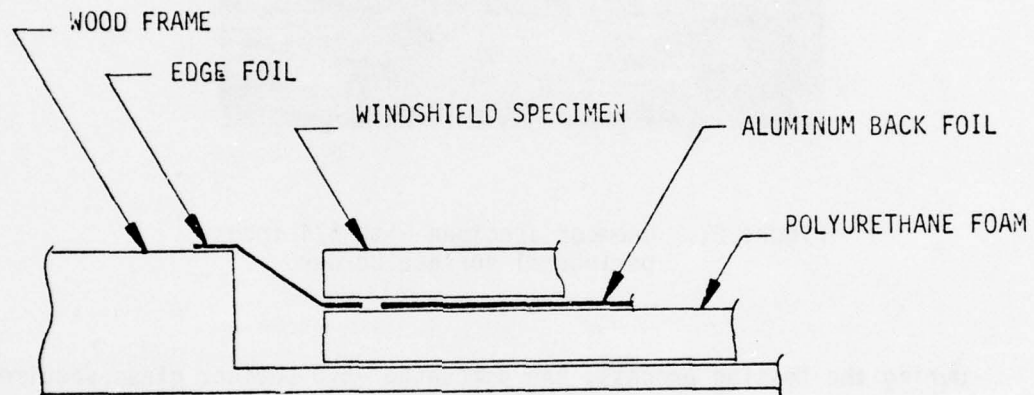


Figure 22. Final electrical edge geometry for static charge tests.

With the achievement of surface discharges "on demand," the test program was finally ready to progress to the measurement of the induced electrical effects. However, before describing the induced electrical effects, a brief review of what is happening during surface charging may clarify why attainment of a surface discharge was the important factor and why the specific charge spray voltage and current which achieved the discharge are of less importance.

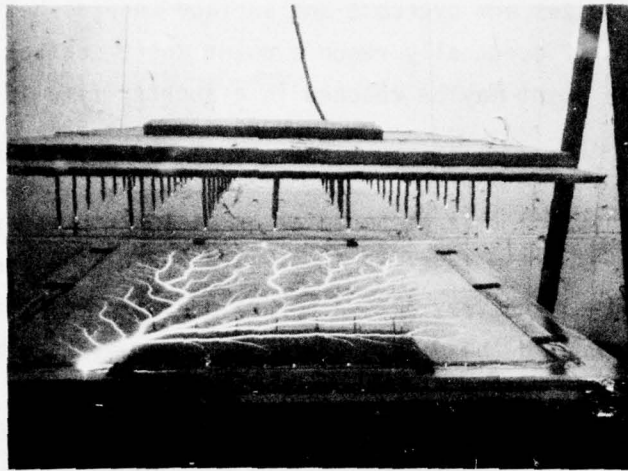


Figure 23. Surface flashover on -515 acrylic specimen using edge geometry of Figure 18.

The windshield test specimen may be thought of as an electrical capacitor with some of the charge stored in the specimen material and much of it stored on the outer surface. Low rates of charging caused by low charge spray voltage will deposit a charge on the upper surface of the specimen. Depending on the specimen surface resistivity, volume conductivity and edge geometry, some of this charge will drain off of the upper surface and from the windshield material itself. When the charge drain is faster than the charge application, surface discharging will not take place.

If the charge dissipation is reduced by such means as choosing a windshield outer ply material with lower volume conductivity or surface resistivity (as was the case with the Mylar experiments), a given rate of charge application will permit a surplus of charge to build to a level which will cause the air on the surface to ionize and lead to the

visible flash discharge. Conversely, as the charging rate for a given windshield material is increased, a point can be reached where the surface and volume losses are overcome and surface charges begin to accumulate, and will eventually reach a point where surface flashover will occur. This point may be reached in a shorter time if the charging rate is increased.

The tests indicated that where metal or dielectric material on or near the periphery of the test specimen caused very high local voltage gradients, localized and very active corona could form. The corona tended to stream upward toward the pencil electrodes and diverted a significant portion of the total charge current away from the specimen. Under these conditions, surface discharges on the specimen would not take place. For this reason, edge corona should be avoided if this test method is to be useful.

The amplitude of the surface discharge is more a function of the specimen electrical qualities and charged surface area than it is a function of the charge spray head voltage, because once the charge - charge dissipation equilibrium point is passed, the surface charge will continue to increase until surface flashover or specimen puncture occurs. (Surface puncture was never experienced during these tests.)

#### Electrical Responses From Static Electric Discharges

##### Background

It was the purpose of this phase of the testing to measure and evaluate the electrical signals induced in an anti-icing conductive coating when static electrical discharges occur on the windshield outer surface. The prior evaluation of surface charging did not reveal a tendency for electrical penetration or punch-through of the windshield outer ply candidate materials. The results of excessive charge were always surface and/or volumetric leakage or surface discharge. The discharges took place as brilliantly ionized channels which flashed to the simulated

surrounding aircraft structure. All of the test specimens which did not have an anti-static coating on the exposed surface were shown to be capable of accumulating a surface charge sufficient to cause surface discharge.

The external surface discharge can produce electrical transients in the circuitry represented by the anti-icing conductive film and any electrical wires or devices which are directly connected to or indirectly coupled to this film. The transients induced in directly connected circuits were measured during these tests. The data also provided a good estimate of the current that flowed in the conductive heating film during a discharge.

The test setups used to measure the transients and the suppression methods and hardware used were selected to provide general information and are not intended to establish design limits. In an actual aircraft system, the transient levels and suppression approach - if required - would be greatly influenced by the design of the windshield anti-icing coating and anti-icing control circuits.

There are several methods of supplying electrical heating power to the resistive coating on the windshield. These result in three generalized classes of electrical ground referencing for the resistive coating:

- ° Full electrical ground isolation when the power is off.
- ° High impedance ground connection when three phase line-to-line power is used and only one phase leg is opened to remove power.
- ° Low impedance ground connection when one bus of the electrical heater is always maintained at structure ground reference.

The charge spray technique of windshield charging used in these tests requires a ground return circuit, although it may be a high impedance circuit. Therefore, for practical reasons the first two of the above possible ground return situations were combined by providing a 10,000 ohm ground return for the test specimen back foil which simulated the anti-icing coating.

The low impedance condition was simulated by returning the back foil to ground through a 16-ohm resistor. This value was chosen because it represents the bus-to-bus anti-icing coating resistance of the most likely windshield configuration being studied on this program. For this low impedance condition, one bus would be connected to structure (and electrical system) ground while the other bus would be fed power that was intermittently open circuited to remove power. Thus, this power feed saw a worst case (for static electricity) impedance of approximately 16 ohms to ground.

#### High Impedance Responses

High impedance voltage response measurements were made using the test setup depicted in Figure 24.

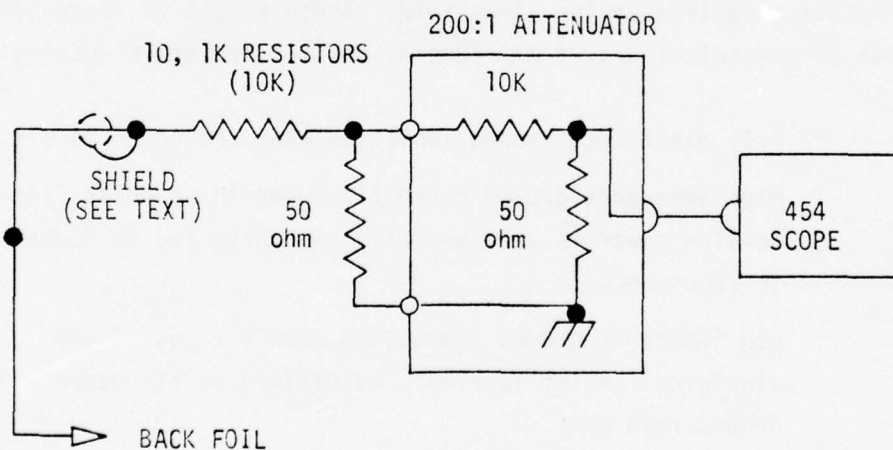


Figure 24. Schematic of high impedance voltage measurement test setup.

The shield on the wire connecting to the back foil of Figure 24 had to be connected to the wire since the transient voltage would cause arcing between the wire and its shield when the shield was grounded. The first 10,000-ohm resistor in the voltage divider chain actually consisted of ten 1,000-ohm, 1-watt resistors in series. This was necessary to prevent impulse breakdown in the resistor, and a false, high reading on the oscilloscope.

The Z5942632-1 Herculite II specimen with 110 kilovolts on the charge spray head produced oscillatory transients in the 10,000-ohm load resistor of as much as 80 kilovolts peak-to-peak during some surface discharges. The discharge voltage is not a direct function of the charge spray head voltage but is a function of the energy discharged and the circuit constants. Therefore, flashes that discharged a large portion of the glass surface produced the greatest discharge current and the greatest voltage across the 10,000-ohm load resistor. Many flashes exceeded 40 kilovolts peak-to-peak. The initial surface discharge would cause circuit ringing with a rise time of approximately 0.01 microseconds. Well defined oscilloscope trace photographs were not obtained for these high voltage, high frequency transients; therefore, none is included in this report.

Suppression of these high frequency, high voltage transients is possible with the use of special spark gap arresters. The specific method to use would require detailed knowledge of the windshield and wiring layout as well as the characteristics of the associated control circuitry.

A more effective method of high voltage transient control would be based on consideration of the complete windshield system. With this approach, it is quite likely that full electrical isolation (an open circuit, infinite resistance) could be avoided and that a reasonably low impedance could be achieved at all times between the anti-icing coating and the airplane structure.

### Low Impedance Responses

Because a low impedance path between the anti-icing coating and aircraft structure represents a realistic and more desirable case, the test-circuit of Figure 25 was used to evaluate the type of signals that might be encountered.

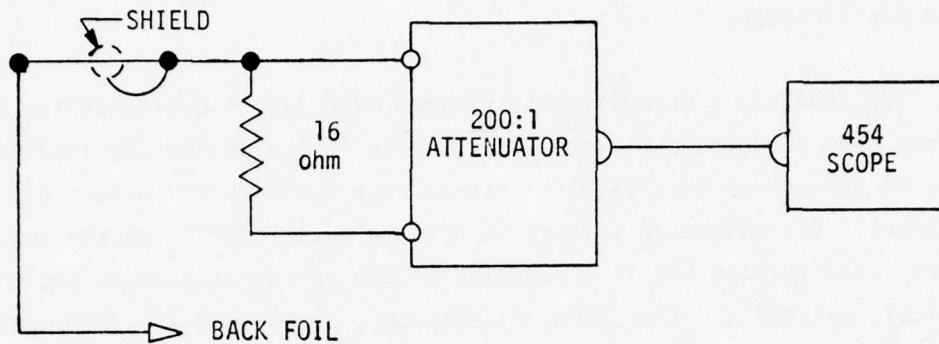
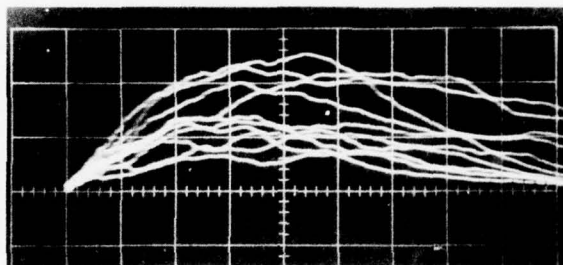


Figure 25. Schematic of low impedance termination test setup.

Figure 26 is a composite of the back foil response for ten surface discharges on the -1 Herculite II specimen. This figure provides a good indication of the flash-to-flash variations. Visual observation of the oscilloscope trace showed that some traces reached the full three division vertical displacement of 3000 volts, or a peak current in the 16 ohm load of approximately 188 amperes. This current lasts for only a few microseconds and is representative of very severe windshield charging.

Suppression of the class of transient shown in Figure 26 can be achieved by the use of a spark gap arrester. Arresters of this type have the characteristic of a near infinite open circuit impedance. When the voltage across the gap reaches the firing level, the impedance drops to a very low value and the voltage drop across the gap is very

small. Gaps alone are not a satisfactory arrester when there is a steady state voltage across the gap, such as supplied by the 400-cycle heating source for a windshield. For this case, when the gap fires the resulting low impedance will not only suppress the transient, it will present a very low impedance to the circuit supplying the heating voltage. The result is a heavy current drain from the heater supply circuit. This power supply current may last much longer than the original transient that initiated the firing of the gap, and may bring about the destruction of the gap. Therefore, most spark gaps that are used on circuits with steady state dc or ac voltage usually contain a resistor or an impedance element in series with the gap to prevent secondary destruction of the gap.



V = 1,000 V/DIV      H = 1  $\mu$ SEC/DIV

Figure 26. Multi-flash back foil response in 16-ohm load on -1 Herculite II specimen.

A spark gap assembly, typical of one actually used in the protection of windshield electrical systems, is shown in the diagram of Figure 27. This figure also shows a typical electrical filter element that might be used in conjunction with the spark gap. The spark gap assembly consists of the actual spark gap, with a low frequency arc over rating of 600 volts, in series with a 1-ohm, 3-watt resistor. The resistor also serves as a fuse in case the gap develops a continuous short circuit.

This fusing capability is desirable to protect the heater control circuits and to assure the continuation of the anti-icing function after failure of the gap. The remainder of Figure 27 shows the test setup used for additional transient suppression evaluations reported elsewhere in this section.

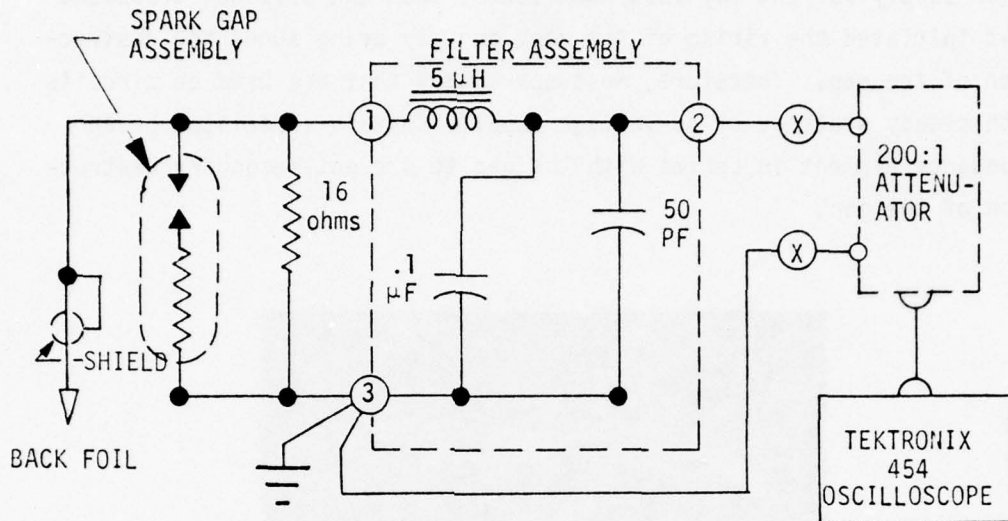
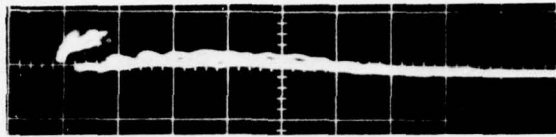


Figure 27. Composite of transient suppression test circuitry.

Figure 28 is an oscilloscope photograph of the suppressed transients of several surface flashes on the -1 Herculite II panel. The test circuit is that of Figure 27 with the filter out of the circuit. Note that the spark gap flashed in from 0.4 microseconds to about 1.8 microseconds in this 2-microsecond-per-division display. The firing voltage was at about the 600 volt low frequency rating of the gap.

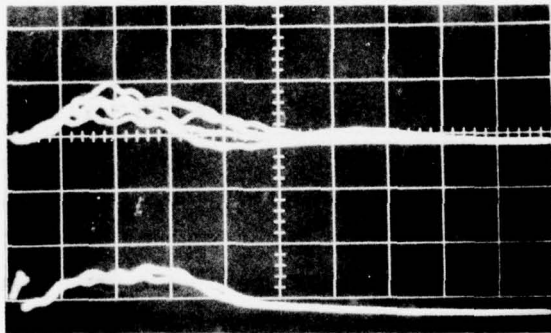
Figure 29 is an oscilloscope photograph of the response for the test setup shown in Figure 27. Figure 29 is a double exposure. The lower traces are several surface flashes on the -1 Herculite II specimen suppressed by the spark gap assembly only. This is the same gap assembly

and same circuit as used for the data of Figure 28, yet the responses are different. (The horizontal and vertical sensitivities are the same in both photos - 1000 V/DIV vertical and 2 microseconds per division horizontal.) The differences can only be explained by the fact that each response was caused by a different surface flash.



V = 1000 V/DIV    H = 2  $\mu$  SEC/DIV

Figure 28. Spark gap suppressed transients.



V = 1000 V/DIV    H = 2  $\mu$  SEC/DIV

UPPER TRACE: SPARK GAP PLUS FILTER

LOWER TRACE: SPARK GAP ONLY

Figure 29. Response traces for circuit of Figure 27.

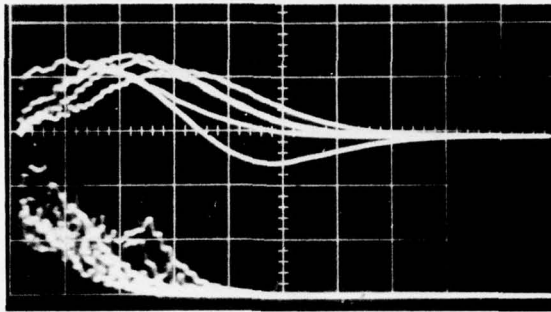
The upper traces on the photograph of Figure 29 are for the entire circuit of Figure 27, including the filter. It is apparent that the effects of the by-pass capacitors in the filter predominated and that the initial charging current in the capacitors did not cause sufficient voltage drop to develop across the inductance to permit the gap to fire. Also, note the tendency for the filter to ring during one of the flashes. This oscillatory ringing was evident in other tests using the same circuit but different serial numbered parts. Figure 29 shows that even with suppression, transients on the order of 1000 volts or more can occur across the 16-ohm load when severe surface flashing takes place.

Inspection of Figure 27 will reveal that the filter is terminated in a high impedance load. The filter response, so far, had been measured with this load. Low impedance termination is quite probable with certain controller configurations. Therefore, the circuit of Figure 27 was modified to study this effect by connecting a 16 ohm load across points x - x of the circuit. The effect on a typical response, such as the upper traces of Figure 29 shows a more rapid damping of the oscillatory waveform, but no significant impact on the peak amplitude of the response.

Figure 30 is similar to Figure 29 except the surface flashing is taking place on the -501 soda lime test specimen. For Figure 30 the vertical sensitivity is 200 volts per division. The lower traces (spark gap assembly only) show that the transient voltage never reached a level high enough to fire the gap. One of the upper traces clearly shows the effects of ringing in the filter.

The -511 Chemcor specimen was placed under the charge spray head and response signals were recorded. Figure 31 shows the electrical responses for eight surface flashes with only a spark gap arrester assembly across the 16-ohm load. (The circuit of Figure 27, - without the filter.) The specific gap assembly used for the tests depicted in Figure 31 had a firing level of around 1100 volts. The clamping action is demonstrated by the two flash traces which had the highest peak voltage. This figure

is recorded at 200 volts per vertical division. Peak voltages without suppression were very similar to the traces shown in Figure 31, thus indicating that the firing voltage of this specific gap was too high to be very effective in this specific setup.



V = 200 V/DIV    H = 2  $\mu$  SEC/DIV

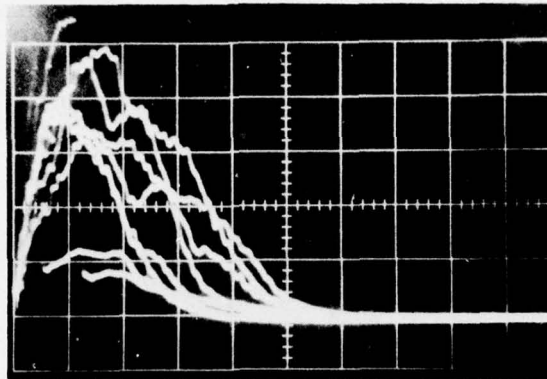
UPPER TRACE: SPARK GAP PLUS FILTER  
LOWER TRACE: SPARK GAP ONLY

Figure 30. Suppressed responses, -501 soda lime specimen.

#### Other Transient Suppression Methods

Metal oxide varistors and capacitors were investigated as simple means of suppressing the electrical transients caused by surface discharges.

The metal oxide varistor (MOV) is a highly non-linear, two-terminal device wherein the current varies exponentially with the applied voltage. A MOV is chosen with characteristics such that at the normal circuit voltage, such as the applied windshield heater voltage, the current through the MOV is very low. The highly non-linear voltage-resistance characteristics then cause the MOV to present a relatively low shunt resistance when subjected to a high transient voltage.



V = 200 V/DIV    H = 2  $\mu$  SEC/DIV

Figure 31. Suppressed responses, -511 Chemcor specimen.

The MOV does, however, present a finite shunt resistance at any voltage and consequently a high current, high voltage source will still present a significant voltage across the two terminals of the MOV. As an example, a MOV rated for a nominal operating voltage of 480 volts RMS was inserted in the circuit of Figure 25 in parallel with the 16-ohm resistor. Very little difference was noted in transient traces.

The evaluation was repeated with a second MOV of the same rating. The results were the same. Transients of 1800 to 2000 volts remained on the line. Calculations based on the manufacturer's data predicted a suppressed transient peak of approximately 1500 volts. A similar evaluation of a 39-volt nominal MOV lead to a prediction of peak transients of approximately 130 volts and actual measured peaks of approximately 250 volts.

These results should not be interpreted automatically as indicating inadequacy in the MOV. The parts available for evaluation were limited and not optimum for the application. The results do, once again,

emphasize the point that the method of suppression should be carefully matched to the requirements and characteristics of the total electrical circuit.

The MOV is a fairly recent development and its failure modes and probability of failure are not as well known as for other suppression components. A conservative application would probably require some type of short circuit failure protection, such as the series fuse-resistor used with the spark gap. This fusing device would tend to further increase the amplitude of the suppressed transient.

Capacitors as transient suppression devices were also briefly investigated. Since the reactance of a capacitor varies inversely with frequency, a high capacitance capacitor with low internal series resistance should present a low impedance to the high rate-of-rise transients. Theoretically, the value of the capacitor could be chosen high enough to suppress the transients to any desired value. However, practical limitations are quickly reached in the allowable physical size of high voltage capacitors that can fit in the confined regions available in the immediate vicinity of the windshield, and in the allowable reactive steady state current the capacitor draws from the alternating current supply of the anti-icing circuit.

To be most effective, the transients (or at least the high frequency components of the transient) should be suppressed right at the bus terminals of the anti-icing coating on the windshield. While space is at a premium in this location, a more remote location for the suppressor would require careful electrical shielding and/or rerouting of wiring - both costly in terms of money and weight.

Experiments were conducted wherein high voltage capacitors were placed in shunt with the 16 ohm resistor of Figure 25. The transient level across the resistor without any shunt capacitor was slightly above 2000 V peak on this -1 Herculite II specimen. A 0.93 microfarad

capacitor reduced the transient to approximately 700 volts; a 0.1 MFD capacitor reduced the transient to about 1500 volts; and a 0.01 MFD capacitor held the transient to about 2000 volts (essentially ineffective).

The suppressed values are not directly comparable because the original surface flash transients are not equal. However, to be effective the reactance of the capacitor must be substantially lower than the impedance (or resistance) of the resistive anti-icing circuit across which the capacitor is placed. The value thus found may then be sufficiently large that the reactive current drawn by the capacitor from the anti-icing circuit may be unacceptably high. Therefore, capacitors alone, for low impedance circuits do not appear as a very practicable approach for suppressing surface discharge transients. Capacitor suppression could be more effective on high impedance circuits, but those circuits have limitations as previously discussed.

#### Surface Discharge Current

The brilliant surface discharges obtained on all of the specimens suggested the presence of considerable discharge energy and high current in the "trunk" of the oak tree discharge. Further evidence of high current was found in bubbling and burning at the junction of a piece of aluminum foil which carried this current to ground. The burned junction was at the interface between two pieces of foil that were connected by the conductive adhesive which was affixed to this 3M brand conductive tape.

The ground lead from the peripheral edge foil (See Figure 22) was opened and a high current, 30 milliohm shunt was placed in series with the lead. The measurement circuit is shown in Figure 32. The electrical response is shown in the oscilloscope photograph of Figure 33 and indicates a peak current of approximately 4 kiloamperes. These data were taken on the -515 acrylic test panel. Other similar tests on the -515 acrylic specimen and on the -507 Chemcor specimen produced currents of 11

kiloamperes and 6 kiloamperes respectively.

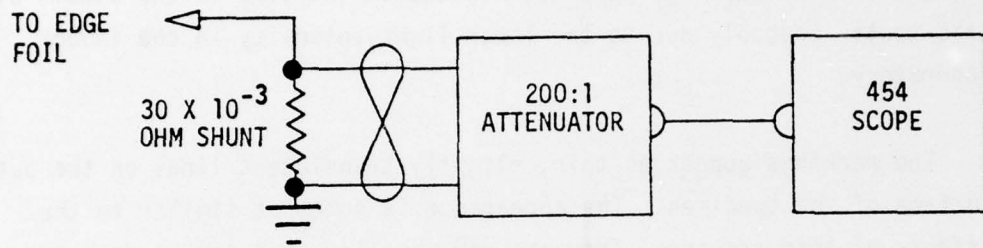
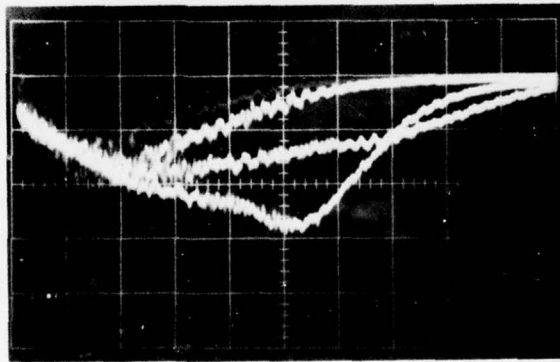


Figure 32. Circuit for measuring surface flash current.



V = 20 V/DIV    H = 1  $\mu$  SEC/DIV

Figure 33. Surface current response in a  $30 \times 10^{-3}$ -ohm shunt.

## Surface Markings

A peculiar type of surface marking was discovered on the -1 Herculite II specimen and on the -501 soda lime specimen. These markings were first noticed when the specimens were placed on the swept stroke lightning test fixture in the bright sunlight. Since lightning tests had not been conducted on any of the specimens prior to noticing the markings, the markings were attributed to effects of the static electric surface discharges. These markings were not noticed at the time of the static electric tests, probably due to the lower light intensity in the indoor laboratory.

The markings appear as thin, slightly translucent lines on the outer surface of the specimen. The appearance is somewhat similar to the effects of acid etching. They are very shallow, but can be detected by drawing one's fingernail across the lines.

None of these surface markings has the "oak tree" pattern photographed during the surface discharges. Some had an "octopus" type of pattern where several crooked lines (not necessarily eight) radiated outward from a central point. This central point drew suspicion as being a possible puncture point through the glass to the foil conductor on the opposite side. However, there were no signs of foil burns at these locations, and the precipitation static test data gave no indication of puncture. Further tests were made at these points using a pointed electrode placed right on the glass surface. A 15 kilovolt dc potential between the point electrode and back foil failed to show any steady state current flow. An initial charging "kick" of about one microampere was noticed, but this quickly dropped to zero after the capacitance of the circuit was charged. No recurring charging or signs of puncture were noted.

Figure 34 is a photograph of an "octopus" surface track on the -501 soda lime specimen. Large numbers of the surface tracks can be detected

on the surface of the -1 Herculite II specimen when the light and viewing angle are correct. Electrical tests did not indicate puncture of the glass surface.

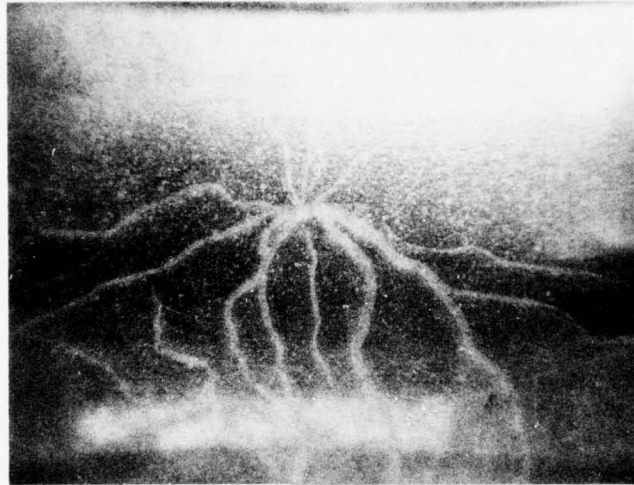


Figure 34. Surface tracking on -501 soda lime specimen.

None of these lines has been detected on the -515 acrylic specimen or on the -511 Chemcor specimen, yet each of these specimens was subjected to a large number of surface discharges during the testing.

The full significance of these surface markings has yet to be determined. It must be remembered that these test specimens were each subjected to many more surface discharges than would be expected during the service life of an actual aircraft windshield. Also, they are not too visible, and if present on a windshield, they might not present a significant distraction to the flight crew.

## Swept-Stroke Lightning Tests

### Test Site Description

The swept-stroke lightning tests were conducted at the Miami, Florida location of the Lightning and Transients Research Institute (LTRI) by Douglas and LTRI personnel. The facility is located on land and outside. Figures 35 and 36 are photographs of the test facility. Figure 35 shows the test specimen support structure mounted in front of the wind tunnel air outlet mouth. The test specimen, mounted to its wood pallet, is clamped to the test support structure by the 2 X 2 inch wood poles and "C" clamps. The high voltage insulators at the four corners of the support structure hold the overhead metal structure and lightning rod to which the lightning signal is delivered from the generators. The lightning rod is the "U" shaped pipe that hangs over the central region and close to the surface of the test specimen. The small building in the background contains the controls and oscilloscopes.

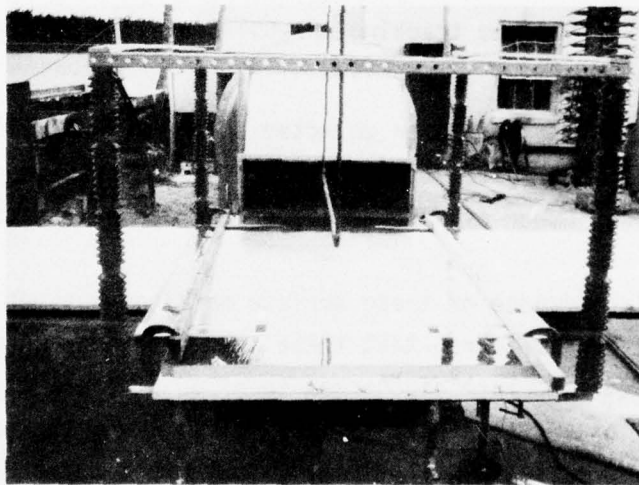


Figure 35. LTRI swept stroke lightning test setup view toward air exit of wind tunnel.

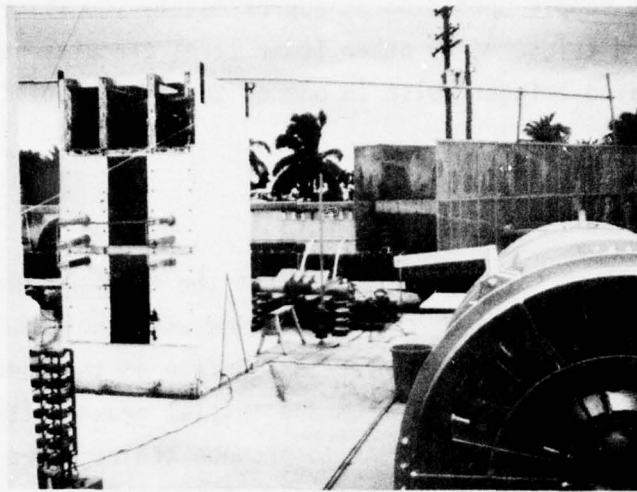


Figure 36. LTRI facility showing restrike generator, etc.

Figure 36 shows another view of the test facility. This picture was taken from the air intake end of the wind tunnel and shows one of the dual in-line air turbines. The tall box-like structure on the left is the high voltage restrike generator. The high voltage trigger supply for the restrike generator is at the left forward edge of the picture. Portions of the capacitor bank of the swept stroke generator are seen in the background.

The swept stroke generator consists in part of a bank of capacitors totaling 558 microfarads. The bank is rated at 25 kilovolts, but is normally charged to 20 kilovolts. Output from this capacitor bank is fed through a manually operated paddle switch through a 50 ohm water resistor to the lightning rod over the test specimen.

The restrike generator is of the Marx type and has an effective capacitance of 0.08 microfarads and a maximum voltage of 800,000 volts.

This generator is normally charged to between 500 and 600 kilovolts at the time of discharge. The restrike generator is triggered by a second Marx type supply operating at approximately 100 kilovolts. This supply is in turn triggered by other lower level circuits which originate from a delayed trigger pulse in one of the instrumentation oscilloscopes.

#### Swept Stroke Generation

The object of the testing was to subject the test specimen to a high current simulated lightning restrike at a time when the simulated initial strike ionized channel was swept over the surface of the specimen. If the impedance of the arc channel from the initial ground attach point at the time of restrike were sufficient to produce the required voltage drop when the high restrike current flowed, this voltage may have found some other more attractive (lower impedance) path than back along the ionized path to the original attach point. Several alternative paths were possible:

- (a) The path could have been through the test specimen (dielectric puncture) to the grounded conductor on the under side which represented an anti-icing coating.
- (b) The path could attach to any grounded anti-static coating that may have been on the exposed surface of the specimen.
- (c) The path could have swept across the surface of the specimen to the grounded peripheral metal which represented the metal airframe.
- (d) The arc could have swept downstream above the specimen surface to reattach to the grounded downstream metal border.

The sequence of test firing was as follows:

- (a) The swept stroke and restrike generators were charged to their desired capacity and held in a charged condition for controlled discharges at the desired times.
- (b) The wind tunnel was next brought up to speed using one or two turbines, as desired. One turbine provided approximately 140 mile per hour velocity across the test specimen, while two turbines produced a velocity of approximately 220 miles per hour. (Two turbines were used for all of the shots of Table IX.)
- (c) At the proper time the paddle switch was dropped, allowing current from the swept stroke supply to flow to the lightning rod over the test specimen. The current then flowed through a small (#30 AWG) copper fuse wire, previously strung between the upstream end of the lightning rod and the ground return, immediately upstream from the test specimen, vaporizing it and establishing an arc. The high velocity airstream then forced this arc downstream across the surface of the test specimen. One end of the arc channel slid along the overhead lightning rod while the other end hung onto the original ground point or skipped to other grounded surfaces along the downstream path.
- (d) The restrike generator was discharged at some predetermined point when the arc of (c) was being blown across the surface of the test specimen. The restrike delivered a high current to the arc path which was previously ionized by the swept stroke generator. The exact time of restrike was determined by a programmed delay in an oscilloscope, which received its starting signal from the current surge ambient signal caused by the initial current flow through the fuse wire.

Most of the time the restrike current either traveled back down the original swept stroke path to the initial ground attach point at the mouth of the wind tunnel, or it took alternative path (d) to reattach to the downstream metal border, missing the specimen completely. These paths are also the most probable alternatives to be expected in a real in-flight aircraft swept stroke encounter where the initial attach point is to the airframe just in front of the windshield.

Numerous shots at various restrike times were required on most specimens before the restrike current could be made to flow on the surface of the specimen. This was accomplished by carefully re-adjusting the time of restrike for each of the swept stroke shots.

#### Instrumentation

Photography - Each lightning shot was recorded on both still and high speed motion pictures. Still shots were taken with a tripod-mounted Polaroid camera placed to the left of the specimen, when viewed downstream. Each still photo consists of a double exposure. First a field shot was taken to show the test specimen and its surroundings. Next, the lens was fitted with a light filter and adjusted for a time exposure during the swept-stroke event. The shutter was opened by remote control just as the wind tunnel reached operating speed, as determined by its characteristic sound. The shutter was closed as soon as the discharge was heard. Some trouble was experienced with this camera and not all lightning shots were photographed with the still camera.

Motion pictures were also taken of each shot using a high speed Fastax camera. One 125-foot length of film was used for each shot. This was approximately 1700 frames per second. The camera was started just prior to activating the high current generator discharge.

Oscillography - Two oscilloscopes were used. A Tektronix 556 dual beam oscilloscope was always used with only a single horizontal sweep

generator, as the second horizontal sweep generator was not operating. The second oscilloscope was a single beam Tektronix 533A. This oscilloscope was used as the delay source for the restrike generator trigger system. Therefore, this oscilloscope always started its sweep when triggered by the initial swept stroke generator. Each oscilloscope was fitted with a Polaroid camera. Tektronix Type M plug-in units were used in all channels.

Current Transducers - Two current transformers (current probes) and a high current, low resistance shunt were employed to enable measurement of the electrical responses. Only two transducers were used at any one time. The parameters of these devices are as follows:

Current Transformer #1	Pearson Model 1880 0.005 volts output per ampere turn input (200 A/V transfor- mation ratio)
Current Transformer #2	Pearson Model 770-1 100 A/V transformation ratio
Current Shunt	Custom made by LTRI 0.0006 ohms

The transducer output was connected to the oscilloscope via coaxial cable. The cable was routed in steel conduit to reduce extraneous signal pickup. Whenever the current transformers were used, special care was used to isolate the case of the transformers from local grounds to help control spurious signal entry via ground loops. The resistance value of the shunt was not reliably known. Therefore, the shunt was used as a signal sampling point, but current through the shunt was calculated from the waveform and circuit parameters rather than from the resistance of the shunt.

All measurements of the back foil current were made with the back foil grounded.

## Facility Calibration

The basic LTRI swept stroke lightning facility had been in existence for a number of years as a shipboard installation on their research vessel. The laboratory is no longer on board the ship and this was the first major use of the swept stroke facility since its reassembly on land.

Prior to starting the planned swept stroke testing, the -515 acrylic test panel was mounted as shown in Figure 35. The surface of the panel was divided into five equal sections by placing one inch wide aluminum tape at equal intervals and at right angles to the wind flow. These tape segments were grounded. The purpose was to protect the test panel from dielectric breakdown and to provide multiple attach point possibilities as the discharge channel was swept over the surface.

The swept stroke generator was first discharged into a high current capacity shorted circuit placed between the overhead lightning rod and the ground plate at the mouth of the wind tunnel. Next, the high current short was replaced with a length of the #30 fuse wire and the swept stroke capacitor bank discharged. No airflow was used for both of these shots. Figure 37 shows the oscilloscope trace of the current in the short circuit (upper trace) and the current in the back foil of the acrylic sample; the specific photo is for the case where the fuse wire formed the shorting path. The trace is the same as it was for the high current capacity short, except that a slight "blip" seen in the upper trace after about 2 milliseconds appeared when the fuse wire vaporized. After vaporizing the wire, the current was carried in the arc channel at essentially the same amplitude as it was when the high capacity short carried the current. The current transformers were used as the transducers for these measurements.

Figure 38 shows the swept stroke and back foil responses when only the front turbine of the wind tunnel was in operation. The vertical and horizontal calibrations are the same as for Figure 37. Note the slightly

uneven current flow due to the variable length swept arc, and the significantly foreshortened length of time the arc was sustained before blowing open. The apparent shift in polarity of the upper trace after 30 milliseconds is characteristic of all measurements on the wind driven swept stroke current and is believed to be a peculiarity of this oscilloscope.

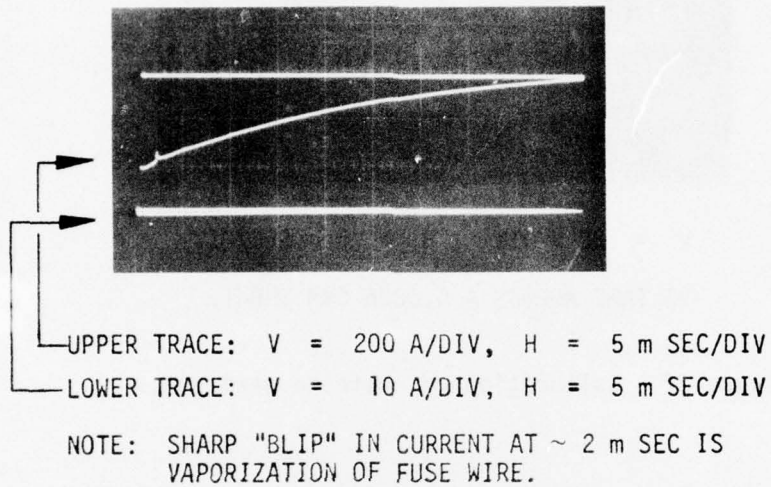


Figure 37. Calibration of swept stroke generator - no wind.

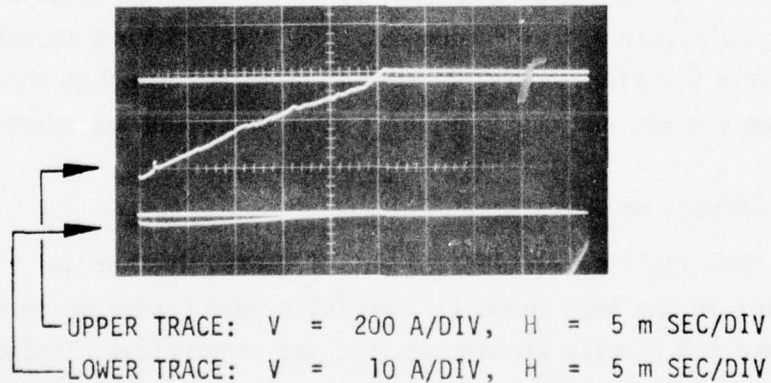
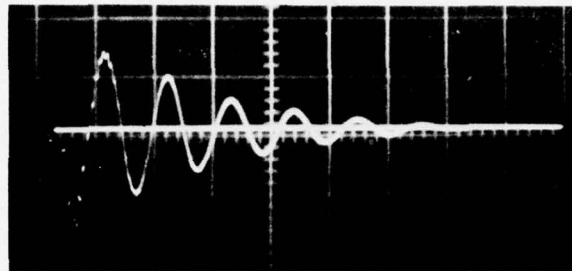


Figure 38. Calibration of swept stroke generator - with wind.

Figure 38, lower trace, also shows some induced signal in the back foil circuit. This is believed to be due to coupling from the overhead arc to the back foil.



V = 20 V/DIV    H = 5  $\mu$  SEC/DIV

VOLTAGE ACROSS A 0.0006 OHM SHUNT.

Figure 39. Calibration of restrike generator.

The restrike generator output was recorded by discharging the generator in an arc to the ground plate located under the leading edge of the lightning rod. No wind was flowing for this shot. The ground plate was in series with the shunt. Figure 39 is a photograph of this oscilloscope trace and shows a peak calculated current of 47 kiloamperes which was reached in approximately 1.3 microseconds. The total circuit inductance was approximately 9.3 microhenrys, circuit capacitance was 0.08 microfarads, the voltage was 550 KV, and the time for a full cycle was 5.4 microseconds.

#### Environmental Effects on Operations

Since the test facility was located out of doors, weather was an important factor in the test conduct. The tests were conducted in early January 1976 and the Florida weather was not too cooperative. Intermittent light rains would deposit some water on the test specimens before they could be covered. This required drying time before the tests could

continue. Deposits of water and dew on the high voltage system also required time to dry out in the sun.

#### Specimen Mounting Considerations

All of the specimens were mounted as shown in Figure 5; however, the wood frames were of two basic sizes to accommodate the two specimen sizes. The specimens were mounted in front of the wind tunnel mouth so that the air would sweep over the long dimension of the specimen.

Since the length of the swept stroke was an important factor in these tests, the length of all the specimens was equalized by stretching the effective length of the Chemcor specimens to be equal to the length of the other specimens. This was accomplished by mounting a nine inch wide non-conducting plywood board between the Chemcor specimen holders and the metal plate to which the swept stroke initiating fuse wire was attached. (See Figure 48.) This, in effect, caused the swept stroke to pass over the same length of dielectric, whether the specimen was the shorter Chemcor or the longer glass or acrylic. This artificial lengthening was justified because all of the significant restrike activity was expected to (and did) take place at or near the downstream end of the specimen.

The narrower width of the Chemcor specimens also required that they be mounted so that the overhead lightning rod was approximately 6 inches to one side of the glass centerline. This was necessary in order to permit the specimens to be properly secured against the forces of the high velocity wind. This off-center mounting produced some interesting results (discussed later), but this mounting is not believed to have altered the effectiveness of the tests.

#### Changes to Specimen Configuration

During the static electric tests the electro-mechanical geometry around the periphery of the specimens was found to be very important to the ability to produce surface discharges. Therefore, all test specimens

were modified to the edge foil configuration of Figure 22.

During the early phase of lightning testing, burn marks were noticed along the insulating gap between the back foil and edge foil. The main cause of this was traced to voltage drops in the grounding circuit of the specific test setup. To alleviate the problem, the edge foil was removed from under the specimen edge and cut back to leave about a one inch border, except at the downstream edge in the area of the swept stroke. These changes were not believed to affect the tendency of the lightning to touch the specimen surface and they do increase the reliability of the readings of back foil signal response. Alternate mounting methods could have eliminated these problems, but their high cost and lack of flexibility were unjustified for the objectives of these tests.

#### Changes to Original Test Planning

The original test planning contemplated a rerun of the surface resistivity and volume conductivity measurements just prior to each swept stroke lightning test. This was modified to a measurement of the surface resistivity on the anti-static coated parts along a path under the swept stroke region, and measurements of the volume conductivity in the regions of any suspected swept stroke damage. These changes were believed to provide more useful data and were necessary to make up for lost time due to the rainy weather.

#### Testing Overview

Fifty test shots were used to gather the swept stroke data for these tests. Each shot followed the test firing sequence previously discussed. The normal run-of-the-mill problems associated with any experimental laboratory measurement work were encountered, together with the added complications created by the weather induced moisture effects on the high voltage circuits.

Not all of the shots resulted in good data, nor are all the good shots discussed in this report. Table IX does, however, summarize all 50 shots with respect to the effects of the restrike current. Significantly, none of the shots fractured the specimens, nor did any shot result in dielectric puncture of a specimen. Some of the shots did result in attachment of the restrike ionized path to the specimen surface, which resulted in significant surface etching to the glass specimen surfaces, and a rather insignificant and slight discoloration of the flash path on the acrylic specimen.

The electrical signal induced in the simulated anti-icing coating on the back side of the specimens (back foil) was measured for many of the shots. Much of these data were invalidated by partial or complete arcing of the restrike flash to the back foil by a path around the edge of the specimen. At other times, the metal border around the specimen discharged under the specimen edge to the grounded back foil, as previously noted under "Changes to Specimen Configuration." While these unwanted arc paths to the back foil invalidated many of the back foil signal measurements, the experience with this flash path provided further excellent guidance regarding the design precautions necessary to the design of an actual aircraft windshield.

All of the shots of Table IX were run with a wind velocity of 220 miles per hour. The restrike time was the delay in firing the restrike generator from the time of current application to the swept stroke fuse wire (Step C in the firing sequence). Since the fuse wire took approximately 2 milliseconds to vaporize, the swept stroke moved at a velocity of 220 miles per hour or 3.9 inches per millisecond from the time of fuse wire vaporization or  $3.9(T - 2)$ , where  $T$  is the restrike delay. For example, a 17 millisecond delay would sweep the original stroke  $(17 - 2)(3.9) \cong 58$  inches downstream from the fuse wire location. This is only an approximation because the ionized air of the flash was not totally coupled to the whole volume of air leaving the wind tunnel.

AD-A037 196

DOUGLAS AIRCRAFT CO LONG BEACH CALIF  
EFFECTS OF LABORATORY SIMULATED PRECIPITATION STATIC ELECTRICITY--ETC(U)  
JUL 76 R C TWOMEY  
MDC-J6952

F/G 1/3

F33615-75-C-3105

NL

UNCLASSIFIED

AFFDL-TR-76-75

2 OF 2  
AD  
A037196



END

DATE  
FILMED  
4-77

TABLE IX. SUMMARY OF THE LIGHTNING SWEEP STROKE TESTS

SHOT	SPECIMEN	RESTRIKE TIME m SEC.	RESTRIKE RESULTS	COMMENTS
1	-515 Acrylic (0.125")	Not Applicable		Swept stroke only across surface segmented with aluminum strips.
2	-515 Acrylic	15	Attached to 3rd strip from leading edge.	
3	-515 Acrylic	15	Camera failed.	
4	-515 Acrylic	20	Went to downstream border.	No surface segments from now on.
5	-515 Acrylic	18	Attachment to downstream end.	No attachment to specimen surface.
6	-515 Acrylic	16	No restrike trigger.	Generator did not trigger.
7	-515 Acrylic	16	Attachment to leading edge.	No attachment to specimen surface.
8	-515 Acrylic	16	Premature trigger.	
9	-515 Acrylic	16	Attachment to leading edge.	No attachment to specimen surface.
10	-515 Acrylic	17	Attachment to leading edge.	No attachment to specimen surface (Testing on -515 continued at Shot 48).
11	-505 Soda Lime, Anti-Static (0.187" Thick)	17	Forked attachment to downstream end.	No attachment to specimen surface.

TABLE IX. SUMMARY OF THE LIGHTNING SWEEP STROKE TESTS (Continued)

SHOT	SPECIMEN	RESTRIKE TIME m SEC.	RESTRIKE RESULTS	COMMENTS
12	-505 Soda Lime, Anti-Static	16	Attachment to leading edge.	No attachment to specimen surface.
13	-505 Soda Lime, Anti-Static	17	Attachment to glass.	Etch mark on glass near downstream end. No puncture in glass.
14	-505 Soda Lime, Anti-Static	17	Attachment to glass.	See Figures 43 & 44 - no puncture.
15	-501 Soda Lime, (0.187" Thick)	-	No restrike trigger.	
16	-501 Soda Lime	-	Premature trigger.	
17	-501 Soda Lime	17	Attachment to glass.	See Figures 41 & 42 - no puncture.
18	-501 Soda Lime	17	Attachment to glass.	Specimen moved 6" to side, no puncture.
19	-501 Soda Lime	16	Attachment to leading end.	
20	-503 Herculite II - Anti-Static	16	Attachment to leading end.	9 KA peak coupling in back foil anti-static coating ungrounded.
21	-503 Herculite II - Anti-Static	17	Attachment to glass.	Anti-static grounded, See Figure 46.
22	-1 Herculite II - (0.110" Thick)	16	Attachment to glass.	See Figure 45 (includes Shot 23).

TABLE IX. SUMMARY OF THE LIGHTNING SWEEP STROKE TESTS (Continued)

SHOT	SPECIMEN	RESTRIKE TIME m SEC.	RESTRIKE RESULTS	COMMENTS
23	-1 Herculite II	16	Attachment to glass.	See Figure 45 - no puncture.
24	-1 Herculite II	17	Attachment to glass.	See Figure 45 - no puncture.
25	-507 Chemcor (0.085" Thick)	16	3 attachments to glass.	Surface tracking to end and side.
26	-507 Chemcor	15	Attachment to glass.	See Figure 49 for cumulative tracking picture.
27	-507 Chemcor	15	Attachment to glass.	Sideways surface tracking - Figure 49.
28	-507 Chemcor	15	Attachment to glass.	Repeat of Shot 27 with instrumentation change.
29	-509 Chemcor - Anti-Static (0.085" Thick)		No restrike trigger.	
30	-509 Chemcor - Anti-Static	15	Attachment to leading end.	No attachment to specimen surface.
31	-509 Chemcor - Anti-Static		Premature trigger.	Rain caused problems.
32	-509 Chemcor - Anti-Static		Premature trigger.	Rain caused problems.
33	-509 Chemcor - Anti-Static	15	Attachment to leading end.	No attachment to specimen surface.

TABLE IX. SUMMARY OF THE LIGHTNING SWEEP STROKE TESTS (Continued)

SHOT	SPECIMEN	RESTRIKE TIME m SEC.	RESTRIKE RESULTS	COMMENTS
34	-509 Chemcor - Anti-Static	15	Attachment to leading end.	No attachment to specimen surface.
35	-509 Chemcor - Anti-Static	15	Attachment to leading end.	No attachment to specimen surface. Bad weather - stopped for the day wet equipment.
36	-509 Chemcor - Anti-Static	15	No trigger.	
37	-509 Chemcor - Anti-Static	12	Attachment to leading end.	No attachment to specimen.
38	-509 Chemcor - Anti-Static	13	Attachment to leading end.	No attachment to specimen.
39	-509 Chemcor - Anti-Static	14	Attachment to leading end.	No attachment to specimen.
40	-509 Chemcor - Anti-Static	15	Attachment to leading end.	No attachment to specimen.
41	-509 Chemcor - Anti-Static	16	Attachment to glass.	Glass etching on downstream end.
42	-509 Chemcor - Anti-Static	16	Attachment to glass.	Anti-static ground removed - attachment to side.
43	-511 Chemcor (0.105" Thick)	16	Attachment to leading end.	Back foil completely removed for all -511 shots.

TABLE IX. SUMMARY OF THE LIGHTNING SWEEP STROKE TESTS (Continued)

SHOT	SPECIMEN	RESTRIKE TIME m SEC.	RESTRIKE RESULTS	COMMENTS
44	-511 Chemcor	17	Attachment to leading end.	No attachment to glass.
45	-511 Chemcor	18	Attachment to leading end.	No attachment to glass.
46	-511 Chemcor	19	Attachment to downstream end.	No attachment to glass.
47	-515 Acrylic	-	No restrike.	Specimen located 6" off centerline for this series of -515 tests.
48	-515 Acrylic	17	Attachment to leading edge.	
49	-515 Acrylic	18	Attachment to acrylic surface.	No surface etching - slight discoloration. Attachment approximately 2" in from downstream end.
50	-515 Acrylic	17	Attachment to leading edge.	No attachment to specimen.

The following subsections of this report discuss the swept stroke tests for each of the specimen types.

#### Tests on -515 Acrylic Specimen

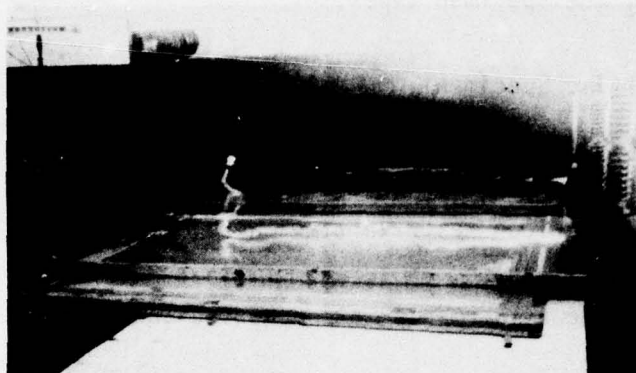
The surface mounted aluminum strips used during the facility calibration were removed from the acrylic test specimen and numerous swept stroke shots were fired. Various restrike times were used to provide a maximum opportunity for the flash to puncture or flash across the surface of the material. No surface attachments were achieved and the specimen was removed.

After the remainder of the specimens had been tested, the -515 acrylic specimen was returned to the test stand for additional testing. Figure 38 shows a photograph of a restrike timed for 17 milliseconds after the start of the swept stroke and the associated electrical wave forms. No surface attachment occurred as can be noted by the reflection of the ionized path on the surface of the specimen. Close coupling of the restrike path to the back foil did produce a back foil current of approximately 3 kiloamperes, and reached a peak in about 1.5 microseconds. The phase displacement between the restrike current and back foil current was believed due to the capacitance coupling and circuit reactance. The peak restrike current was calculated to be 39 KA.

The restrike timing was set for 18 milliseconds and another test conducted. This time the restrike flash attached to the surface of the acrylic about two inches from the downstream edge. Careful inspection revealed only the slightest indication that anything had happened to the specimen surface. There was no burning or melting, only a slightly noticeable discoloration.

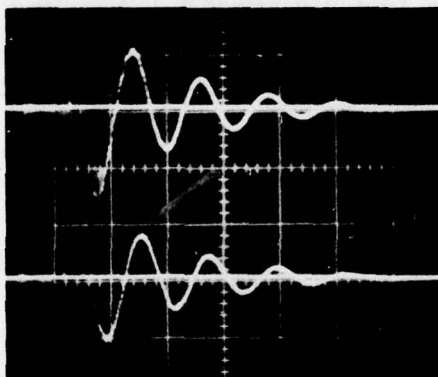
#### Tests on -501 Soda Lime Glass Specimen

Five shots were fired at various restrike times. At 17 milliseconds restrike delay, the flash touched down on the downstream end of the



A. RESTRIKE ILLUMINATION OF SWEEPED STROKE.

(NO CONTACT TO ACRYLIC SURFACE.)



B. UPPER - WAVE FORM OF RESTRIKE CURRENT - 50 V/DIV ACROSS SHUNT.  
LOWER - WAVE FORM OF BACK FOIL CURRENT - 2 KA/DIV IN CURRENT PROBE.

$t = 5 \mu \text{ SEC/DIV}$

Figure 40. -515 acrylic test specimen with restrike at 17 milliseconds.

specimen. A double attachment to the specimen surface took place and etched the surface of the glass. Figure 41 shows the photograph of the flash, while Figure 42 shows a photograph of the surface etching markings produced.

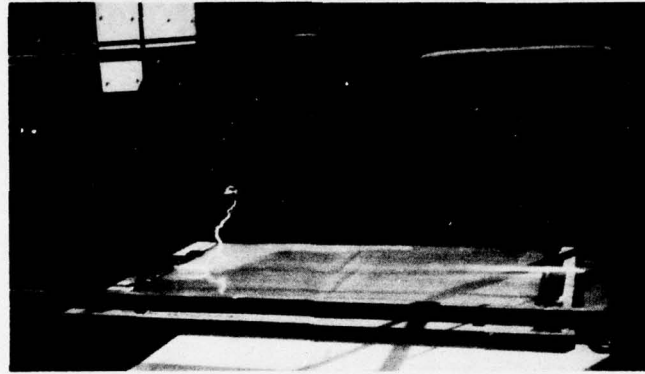


Figure 41. Restrike attachment to -501 soda lime glass specimen.

The markings appeared as an etch to the surface. There were no signs of melting. A powdery residue clung to the surface in the affected area. Each grain of the residue resembled a sliver of glass about 1/32-inch long and much smaller in diameter. The depth of etching was not great, but it appeared to be much more than the etching believed caused by the static electric discharges noted earlier in this report.

Tests with the high voltage probe of the volume conductivity meter showed no indication of puncture or other forms of damage not evident by visual inspection. Attempts to photograph the etching details have, so far, failed to show as much as can be seen by the naked eye.

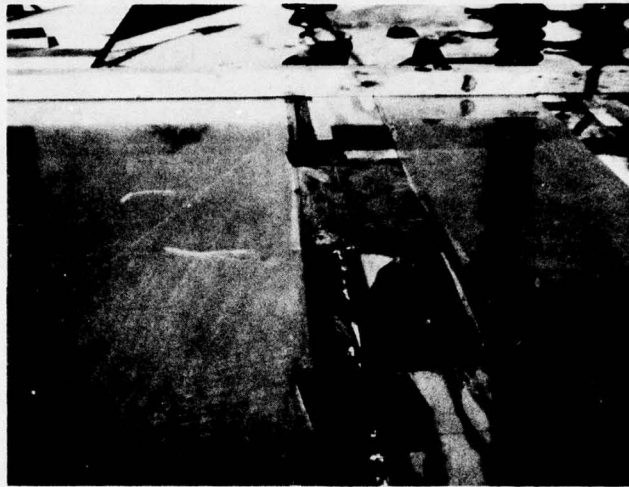


Figure 42. Restrike markings on -501 soda lime glass specimen.

#### Tests on -505 Soda Lime Glass Specimen

This specimen has an anti-static coating on the surface exposed to the swept stroke. The surface resistivity under the swept stroke path was measured at about three inch intervals from the upstream to the downstream end.

Only three shots were fired before surface attachment was achieved. Figure 43 shows a photograph of one of the shots that caused surface marking. The restriking delay was 17 milliseconds. The peculiar hook shaped marking is shown in more detail by the photograph of Figure 42. A second straight marking is also evident. This was caused by an earlier shot.

The surface damage was essentially of the same type noted on the uncoated soda lime specimen. The anti-static coating was completely

removed in the etched area, and for a fraction of an inch beyond the borders of the glass etching. The outer fringes of the damage area were discolored.

Electrical tests indicated no signs of puncture in the etched area, and none was evident to the naked eye.

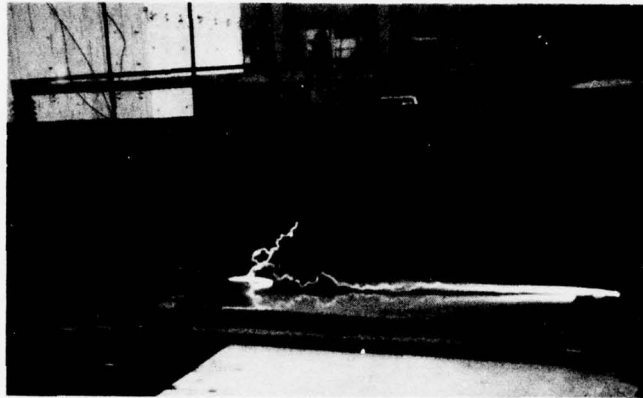


Figure 43. Restrike attachment to -505 soda lime glass specimen.

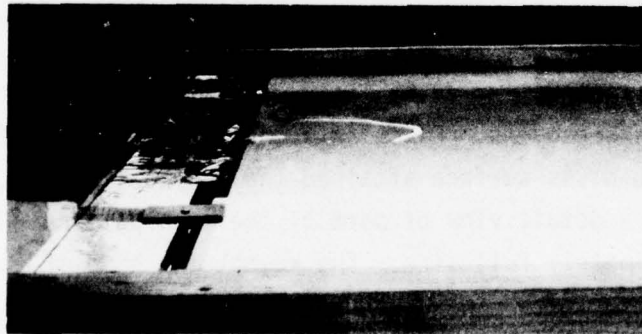


Figure 44. Restrike markings on -505 soda lime glass specimen.

#### Tests on -1 Herculite Glass Specimen

Three out of the three shots to this specimen resulted in restrike flash attachment to the surface of the glass. Extensive surface markings at the trailing edge of the specimen resulted from these three shots. Figure 45 shows the surface markings. The etched lines were very much like those run on the previous specimens. No electrical puncture or mechanical fracture of the glass was detected.

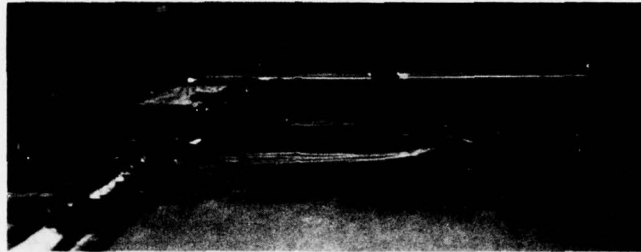


Figure 45. Restrike markings on -1 Herculite glass specimen.

#### Tests on -503 Herculite II Glass Specimen

The electrical resistance of the anti-static coating on the exposed face of this specimen was measured along the expected swept stroke path. The resistance readings were consistent with the previous reading taken in the same general area.

The results of this series of tests were similar to those recorded for the previous specimens. Flash attachment to the surface was achieved and the glass surface attained the now familiar etched effect. Figure 46 shows a detail view of part of the etch pattern. The photograph is approximately full size. The downstream edge of the glass specimen is on the left. The darkened portion of the damaged anti-static coating is shown around the etched glass area. Most of the specular appearance is due to reflection from the aluminum back foil and

is not due to surface etching of the glass. The anti-static coating was totally removed in the burned area. The resistive coating on the remainder of the specimen was not affected by the flash attachment.

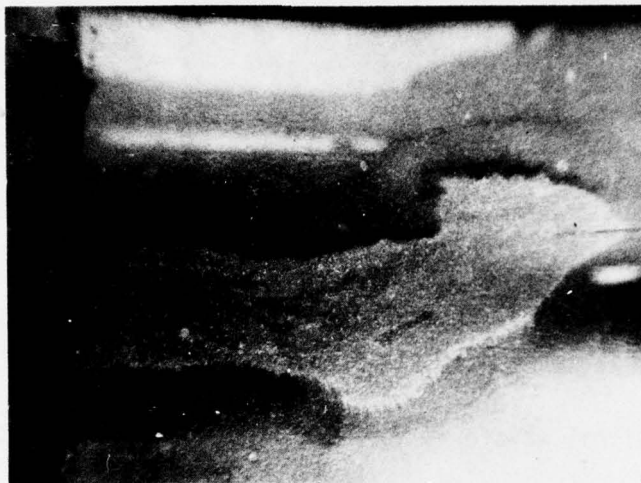
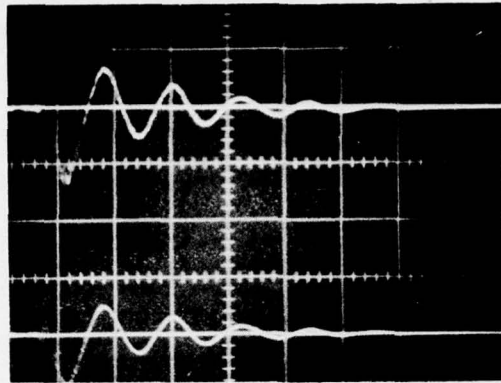


Figure 46. Restrike markings on -503 Herculite II glass specimen.

The -503 specimen mounting was carefully prepared to provide the least probability of the swept stroke attachment arcing to the back foil. Figure 47 shows the restrike current waveform (upper) and the waveform of the signal coupled to the back foil. The coupled signal was 9 kiloamperes peak, while the restrike current was 35 kiloamperes peak. The high level of the back foil coupled signal, as contrasted to the lower level coupled signal in the -515 acrylic specimen, was probably due to the direct attachment of the restrike flash to the Herculite II surface. The in-phase signal for the traces of Figure 47 as contrasted to the phase shifted signal of Figure 40B, might indicate volume conductivity rather than the suspected capacitance coupling of Figure 40B. However, not enough data are available on the nature of the signal path to be certain of this theory.



HORIZONTAL: 5  $\mu$  V/DIV  
 UPPER: RESTRIKE WAVEFORM 20 V/DIV ACROSS SHUNT  
 LOWER: BACK FOIL SIGNAL 10 K AMP/DIV

Figure 47. Signal waveforms for -503 Herculite II glass specimen.

#### Tests on -509 Chemcor Glass Specimen

The anti-static coating on this specimen was also measured all along the expected swept stroke path. These readings were also quite similar to the values previously measured in the same general region of the glass surface.

As noted under "Specimen Mounting Considerations," the specimen was arranged so that one long edge of the specimen was about one foot outboard from the swept stroke path. This mounting offered an electrical ground path to the side of the swept stroke as well as grounded paths at the beginning and end of the sweep. Figure 48 is a photograph of a restrike that had surface flashes to the edge of the test panel. These etched their mark in a multi-fingered path to the side. In addition, the restrike flash split in the air above the panel and the downstream fork attached to the test panel and followed the surface marks made by a previous stroke.

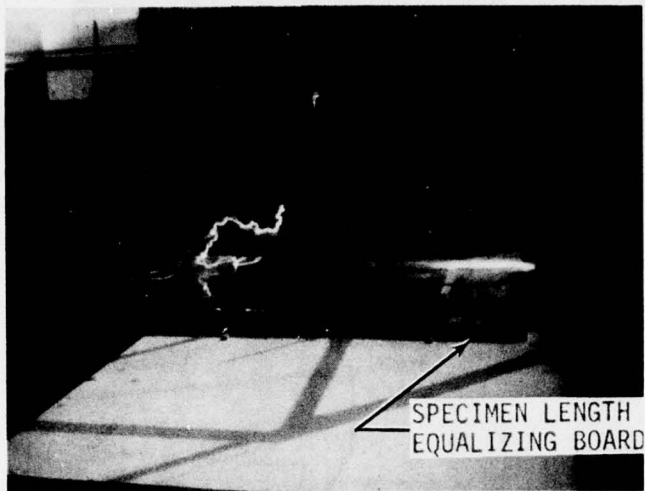


Figure 48. Restrike to -509 Chemcor glass specimen.

The surface markings have the same characteristics as those of previous markings on other panels of different material. The surface etching removed the anti-static coating in the immediate area of the surface attachment. A dark border, characteristic of the damaged anti-static coating, encircled the area. There was no evidence of electrical puncture or mechanical fracture.

#### Tests on -507 Chemcor Glass Specimen

This specimen was also mounted off center so that the swept stroke was about one foot in from a long edge. Several swept strokes with restrikes produced the surface markings shown in the photograph of Figure 49. This specimen did not have an anti-static coating. Some of the surface flashes went to the side and some went to the downstream end. The surface markings had the same characteristics as noted on previous panels. There was no surface electrical puncture or mechanical fracture of the glass.

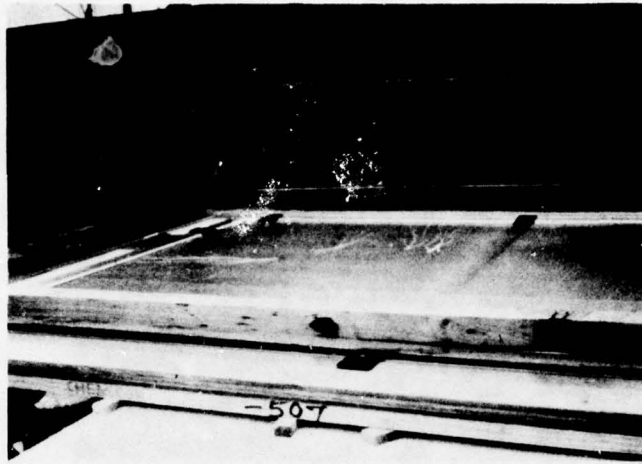


Figure 49. Restrike markings on -507 Chemcor glass specimen.

#### Special Test on -511 Chemcor Glass Specimen

The -511 Chemcor specimen and its anti-static coated equivalent, -513, were intended to be back ups for the 0.085-inch-thick -507 and -509 specimens if the latter specimens were fractured during any of the tests. The -511 and -513 specimens were 0.105-inch thick. Since the -507 and -509 specimens survived the static electric and swept stroke tests, it was decided that additional useful information might be obtained if a totally clear specimen were tested in the swept stroke environment. To accomplish this, the aluminum foil that simulated the anti-icing coating was removed from the back of the -511 specimen.

Numerous swept stroke tests with different times of restrike application were conducted on the -511 glass. No surface attachment could be achieved. From this it was concluded that the clear glass does not have an affinity for the ionized swept stroke that is exhibited on dielectric specimens with a grounded, good conductor on the opposite side.

## SECTION IV CONCLUSIONS

The preceding sections cover the highlights of the program to evaluate the effects on large area windshield systems when subjected to static electric surface charging and swept stroke lightning. Certain significant conclusions can be drawn from this work which can aid in influencing the design of a windshield outer ply and the design of windshield anti-icing systems.

One overall conclusion that can be drawn from this work is that the potentially adverse effects of external electrical environments can be adequately prevented or their probabilities significantly reduced when available technology and materials are properly used. However, a fully interrelated and coordinated design approach is required. (A summary and recommendations are in Section V.)

The following are the most significant conclusions:

1. The multi-electrode charge spray technique can be used successfully to simulate triboelectric (precipitation static) charging of aircraft windshields. Because this technique achieves a charge deposit in a manner different from that of an aircraft in flight, the differences must be understood and accounted for. The work reported herein has explored many of these differences and the conclusions are believed to be valid. However, it is acknowledged that more exploration would be desirable.
2. The present methods of measuring surface resistivity do not appear to be very consistent. Standard methods and equipment are needed, such as the work of the ASTM. The proposed ASTM probe configuration (Figure 3) needs to be more precisely defined with respect to form and materials if repeatability of configuration and test

results are to be obtained. Simplification of the design and consequent cost reduction appear possible.

3. The surface resistivity and volume conductivity of the windshield outer ply material directly affect the tendency for a windshield to acquire a precipitation static charge sufficiently high to result in surface arcing. For a given thickness and geometry, high loss material, such as soda lime glass, will have less tendency to surface arc than lower loss materials, such as acrylic. During these tests, charging conditions were reached which were sufficient to produce surface discharges on all specimens.
4. Anti-static coatings applied to glass windshield outer surfaces of the specimens used reduced the visible light transmission by as much as 7.4 percent. Application of the coatings on the test specimens by present manufacturing techniques did not produce a very uniform resistance coating. This should be taken into consideration where high resistance and high light transmission are desired.
5. Anti-static coatings can be inadvertently removed or unacceptably discolored by certain chemicals.
6. Anti-static coatings, when properly grounded, can be totally effective in preventing surface discharges and the electromagnetic interference sometimes associated with these discharges.
7. Static electric discharges on windshield surfaces can induce high voltages and/or high currents in anti-icing heating elements and their associated control

circuitry. Depending upon circuit components, transient voltages in an ungrounded system may exceed 40,000 volts peak-to-peak with sub-microsecond rise time, while transient currents and voltages in a grounded system may be on the order of 200 amperes and 3,000 volts with approximately 4 microseconds rise time.

8. The current in the surface flash may reach a value of approximately 10,000 amperes, with time to peak of approximately 5 microseconds. Windshield outer circumference metal members must be designed to withstand this level of electrical transient.
9. The tendency for static electric charges to build to the flash over point is greatly affected by the edge geometry of the windshield. Electro-mechanical designs can be selected which will substantially reduce the tendency to surface arc. This control alone may be inadequate to prevent surface arcing in the central regions of large windshields during periods of severe charging.
10. Electrical transients caused by static electric surface discharges can be suppressed by available techniques and hardware. The degree of suppression required is determined by the total windshield electrical system design and the susceptibility of other coupled circuits.
11. During the swept stroke lightning tests, transient currents of 3,000 amperes rising to a peak in about 2.5 microseconds were induced in a simulated low impedance windshield heater system even though the lightning flash did not attach to the surface of the windshield. When attachment occurred, the transient current reached approximately 9,000 amperes, with a time to peak of

1.5 microseconds.

12. The effects of the dielectric characteristics of the outer ply material on the tendency for swept stroke attachment were not clear. All specimens with conductive rear coatings sustained swept stroke surface attachment, although the tendency was least pronounced on the acrylic material, which had the lowest dielectric loss. Swept stroke attachment could not be attained in the absence of a conductive back coating.
13. Windshields having the greatest dimensions in the swept stroke windstream will have the greatest tendency for restrike attachment.
14. Prior exposure to heavy static electric surface discharges did not appear to affect the tendency toward lightning restrike attachment.
15. Anti-static coatings do not appear to alter the effects of swept stroke lightning attachment to the windshield surface. However, when lightning does attach, the anti-static coating is destroyed in the localized area of the attachment.
16. Severe and multiple static electric discharges and lightning discharges did not fracture the acrylic or glass test specimens. Electrical puncture was not detected either. Mild surface track etching believed due to static discharges was discovered on the soda lime and Herculite II uncoated specimens; none was found on the acrylic or Chemcor uncoated specimens. This tracking is not expected to seriously affect the aircrew's vision.

Simulated swept stroke lightning surface tracking caused very noticeable surface etching on all glass specimens, but the effect was hardly discernible on the acrylic specimen.

17. There have been no known service reports of the surface etching as produced during these tests. Also, surface discharges of the severity produced in these tests are not known to have been reported, although reports of smaller oak tree surface discharges have been numerous. Several factors may account for the lack of in-service reports of the etching and severe discharges:
  - a. The test conditions might be too severe or unrealistic.
  - b. The conditions may be very realistic, but the probability of in-flight occurrence may be very low.
  - c. There is very little flight experience with very large area windshields.

SECTION V  
SUMMARY AND RECOMMENDATIONS

Overall Design Approach

The design and development of an aircraft windshield is a highly complex undertaking. Since most of the problems to be solved are non-electrical, care must be taken so that the electrical problems are not overlooked or assigned an inappropriate priority. No other recommendation is as important as the following:

- ° Identify and interrelate all requirements early in the design program.

Many of the design options which relate to electrostatic charge and lightning are controlled or highly influenced by other, non-electrical design considerations. Even the most obvious electrical requirements dealing with anti-icing are interactive with the electrostatic and lightning environment.

Control of Electrostatic Charging

The amount of electrostatic charge that can be acquired by a windshield is a direct function of the frontal area of the windshield. Therefore, all other factors being equal:

- ° The intensity of electrostatic charging is related to the size of the windshield; large windshields can accumulate large charges.

The amplitude of the electrostatic voltage build up on a windshield, for a given triboelectric charging rate, is directly related to the ability to retain the charge on the windshield. Factors, such as the surface resistivity and bulk electrical conductivity of the outer ply windshield material and the electrical edge geometry of the outer

surface are important to the ability to drain the charge from the windshield surface before electrical breakdown potentials are reached.

If the electrical losses on and in the windshield can dissipate the charge fast enough, flashover levels will not be achieved and most, if not all, of the effects associated with static electricity can be eliminated. The observations described in Section III of this report showed that charge retention on a windshield specimen surface did differ for the various materials tested. The soda lime glass had the greatest volume conductivity and held an electrostatic charge for the shortest time. At the other extreme, the acrylic plastic had the least volume conductivity and held an electrostatic charge for the greatest length of time. Stated another way, for a given rate of charging, a windshield with an outer ply of soda lime glass would have the least tendency to have surface flashing, followed in order by Herculite II and Chemcor. A windshield with an acrylic outer ply would have the greatest tendency to surface flash, for the types of material studied.

However, from a practical standpoint, all of the materials can achieve flashover potentials; the better insulating materials merely achieve the flashover potential in less time. A far more effective method of preventing flashover is to deliberately prevent the build up of surface charge. From a purely electrical standpoint, the following statement can be made:

- ° Anti-static coatings are fully effective in preventing surface electrical discharges due to triboelectric charging and are recommended for use.

However, this statement must be qualified. At the present time, permanent anti-static coatings are available for only glass materials. These stannous oxide coatings require high temperatures for their successful application. Even for glass substrates, stannous oxide

anti-static coatings have some disadvantages:

- Uniformity of coating density is difficult to obtain when a high resistivity coating is desired.
- A high resistivity coating (approximately one megohm per square) is desirable to reduce light transmission losses, yet provide adequate charge drain. However, lack of manufacturing controls may result in a lower resistivity coating and a resulting light transmission loss of 5 or 6 percent over that of an uncoated sample.
- Some chemicals can discolor and/or remove the stannous oxide coating.
- The presence of the anti-static coating prevents post-manufacturing operations on the glass surface. Some manufacturers "fine-tune" the optical performance by localized polishing or grinding on the outer surface. This would remove some of the anti-static coating.

On the positive side, an anti-static coating will eliminate static electric discharges and the resulting high voltages or high currents that these discharges can induce into the anti-icing film. These transients may be a contributor to the degradation of the anti-icing films. However, a special program would be required to definitize this phenomena. Transient suppression techniques can eliminate or control the effects of the transients in circuitry which interfaces with the anti-icing film but they cannot eliminate the transient in the film.

Sufficient data are not yet available to clearly establish that the service life of a stannous oxide anti-static coating is consistent with the service life of the remainder of the windshield system. This information is needed because the complex factory techniques required for the application of stannous oxide do not permit this coating to be considered as a repairable item.

If anti-static coatings are used the resistivity should be controlled by a specification that establishes the maximum resistivity at a value of approximately two megohms per square and a minimum resistance controlled by the maximum light transmission degradation that can be tolerated. The light transmission degradation to be allocated to an anti-static coating must be determined from a detailed trade study of the entire windshield design. Values of 2 to 3 percent degradation appear achievable and realistic (Reference 5).

The uniformity of anti-static coating is most important at the periphery of the sheet where the charge will be transferred to the metal structure of the aircraft. Voids in coverage should not be permitted at or near the periphery, although voids of six to eight inches in diameter in the central region of the windshield offer little probability of causing localized surface arcing in a practical installation.

Specifications for anti-static coatings should require the complete removal of any conductive material from the edge of the outer ply material to which the anti-static coating is applied. Overspray of the anti-static coating to the back side must also be eliminated or made compatible with any anti-icing coating which may be applied to this side. Adequate tests are a necessity to assure meeting these requirements.

Suggested design requirement specification words to assure adequate electrical isolation of the anti-static and anti-icing conductive coatings are as follows:

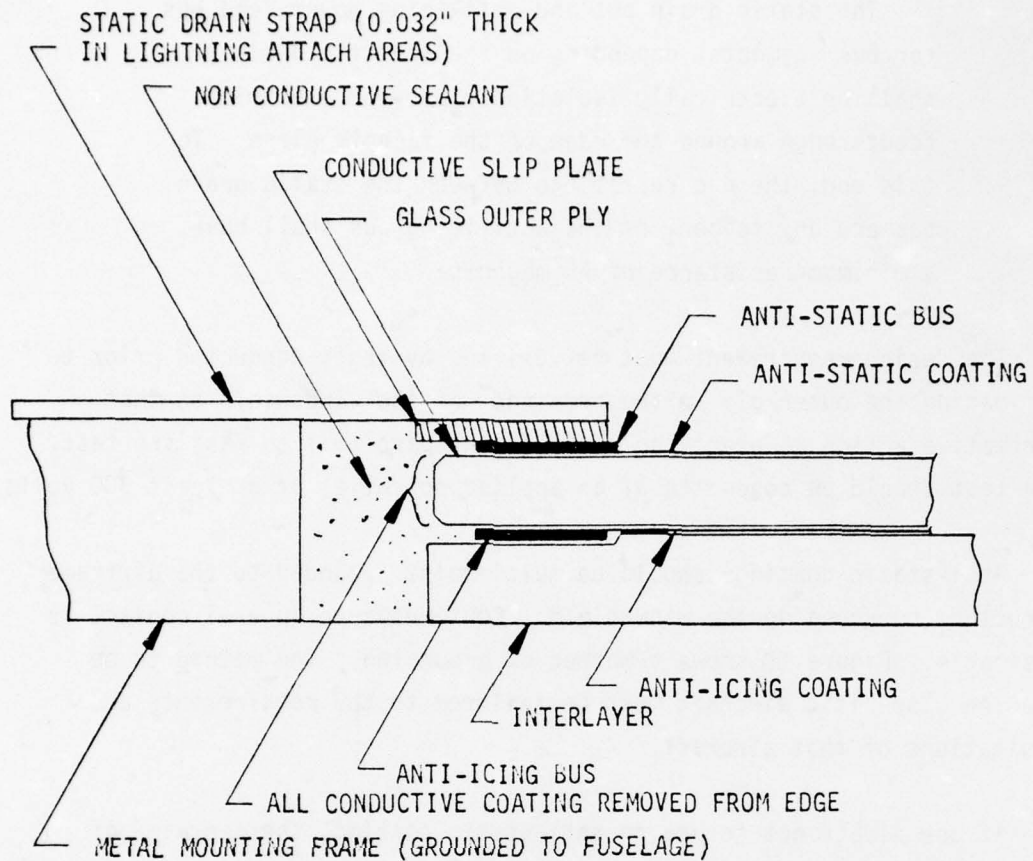
The static drain bus and anti-icing power feed bus (or bus segments, depending on the specific design) shall be electrically isolated to prevent electrical feedthrough around the edge of the faceply glass. To this end, the d c resistance between the static drain bus and any segment of the anti-icing bus shall have a minimum resistance of 75 megohms.

The design requirement must be verified by tests conducted prior to laminating the outer ply to the remainder of the windshield so that corrective action is practicable should the part fail to pass the test. The test should be conducted at an applied potential of at least 500 volts.

Anti-static coatings should be multi-point grounded to the airframe structure surrounding the windshield. Continuous peripheral contact is desirable. Figure 50 shows a method of grounding. The method to be used on a specific aircraft must be tailored to the requirements and limitations of that aircraft.

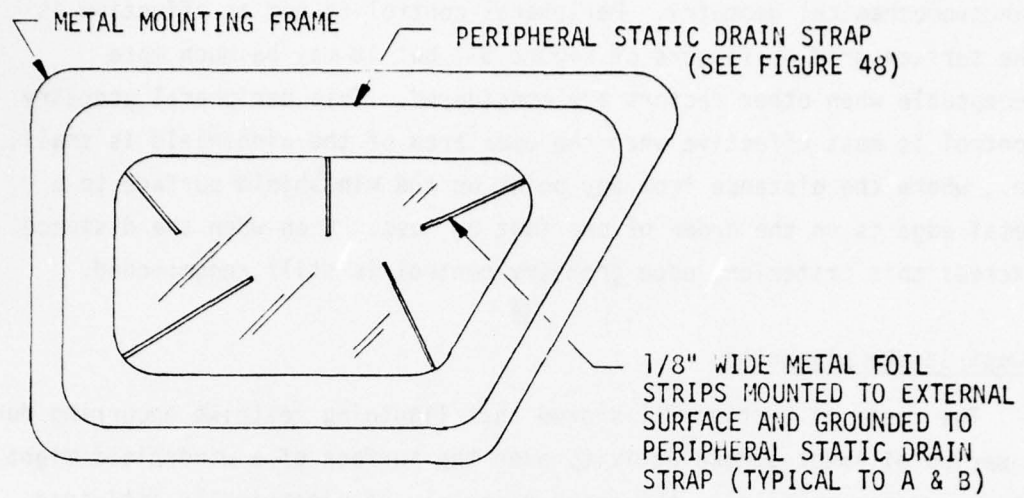
If one elects not to use an anti-static coating, the geometry of the windshield outer ply should be designed to reduce the charge build up on the outer ply. An electrically effective method is to reduce large areas to small areas by the application of narrow (approximately 1/8 inch wide) conductors to the outer windshield surface, as shown in Figure 51. While quite effective from the standpoint of electrostatic charging, this method may be rejected for other reasons, such as visual blockage due to the conductors and higher probability of damage to the conductors by lightning.

A more practicable method of surface charge control is to treat the outer surface periphery the same as recommended for the grounding of an anti-static coating. (See Figure 50.) Placing conductors on the surface periphery has been shown in the tests of Section III to be effective in reducing the tendency toward surface arcing and to reduce the area

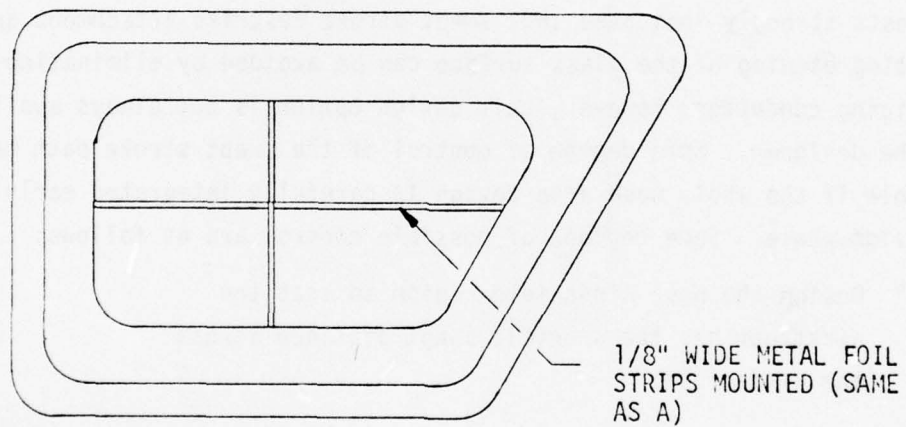


- NOTES:
1. THE ANTI-STATIC BUS IS AN INTEGRAL PART OF THE GLASS OUTER PLY.
  2. THE ANTI-STATIC BUS, CONDUCTIVE SLIP PLATE, AND STATIC DRAIN STRAP ARE LOCATED AROUND THE ENTIRE PERIPHERY OF THE WINDSHIELD.
  3. THIS SURFACE EDGE TREATMENT IS RECOMMENDED WHETHER OR NOT AN ANTI-STATIC COATING IS USED ON THE GLASS SURFACE.

Figure 50. Outer surface edge grounding method.



A. FINGER METHOD



B. GRID METHOD

Figure 51. Methods for reducing electrostatic charging area.

of arcing when the charging rate exceeds the control level of this electromechanical geometry. Peripheral control is not as effective as the surface grid or fingers of Figure 51, but it may be much more acceptable when other factors are considered. This peripheral geometry control is most effective when the open area of the windshield is small, ie., where the distance from any point on the windshield surface to a metal edge is on the order of one foot or less. Even when the distance exceeds this criterion, edge geometry control is still recommended.

#### Swept Stroke Lightning

The tests of Section III showed that lightning restrike occurring during a period of swept stroke activity over the surface of a windshield might cause surface etching to the outer glass ply of electrically anti-iced windshields. These tests also showed that the swept stroke with restrike to the surface can induce a large electrical transient into the anti-icing circuitry.

The tests strongly indicated that swept stroke restrike attachment and the resulting etching of the glass surface can be avoided by eliminating the anti-icing conductor; however, this design option is not always available to the designer. Some degree of control of the swept stroke path may be available if the whole nose area design is carefully integrated early in the design phase. Some regions of possible control are as follows:

- ° Design the nose windshield region so that the airstream has the shortest swept distance across the windshield.
- ° Design the nose region in front of the windshield to provide lightning attach points that reduce the tendency of the swept stroke to cross the windshield surface.

Control of the lightning attach points may be more feasible than one might first imagine. Most modern aircraft employ nose mounted radar antennas which are housed within radomes. These radomes usually require lightning protection, and an effective method of protection employs lightning diverter strips. These strips control the lightning attach point to the radome and divert or conduct this stroke to the metal frame of the fuselage. The radome lightning protection design may have the latitude to terminate or direct the lightning to the fuselage skin at a point where subsequent swept stroke action may miss the windshield or cause the swept stroke to pass over a narrow portion of the windshield, thus reducing the probability of restrike attachment to the windshield. Once again, this design possibility requires thorough and early interdisciplinary design coordination and a detailed understanding of the entire lightning event.

When the swept stroke lightning paths are identified, those that begin or end on the periphery of a windshield require adequate electrical conductivity to transfer the charge without unacceptable pitting of the metal. To accomplish this, the conductive outer border of the windshield, as shown in Figure 50, should employ metal of approximately 0.032-inch thickness or heavier in the regions of lightning attachment.

#### Control of Electrical Transients

When an anti-static coating is not used on the outer surface of larger windshields, triboelectric charging and subsequent surface flashing will introduce electrical transients into the anti-icing electrical coating. Swept stroke lightning activity will also introduce electrical transients into the anti-icing electrical coating regardless of whether or not there is an anti-static coating on the outer surface of the

windshield. The data of Section III give an indication of the amplitudes and durations of these transients. The probability of having lightning activity is much less than the probability of triboelectric charging.

What one should do about these transients must be determined by a system study of the specific aircraft. Among the data needed are the following:

1. Transient susceptibility of the anti-icing controller heater feed circuits and temperature sensing circuits.
2. Probable wire routing paths from windshield to controller so that induced coupling to other circuits can be evaluated.
3. Available space at the inside periphery of windshield to provide information on permissible size of transient control elements such as spark gaps and filters.
4. Weight, space, and test data to evaluate the feasibility and extent of wire shielding.
5. Grounded circuit/floating circuit trade study data as it relates to the status of the windshield heater elements.

If the specific system study shows the need for transient suppression, the suppression hardware must be selected to be compatible with the anti-icing control circuit. Transient clamps, such as spark gaps, must be selected with flashover voltage ratings above those generated by the maximum voltage supplied by the anti-icing control circuitry. The clamped impedance presented to the controller must not appear as a circuit fault, otherwise false shut down or damage might result to the controller. Conversely, the transient clamp must be capable of sustaining

the transient energy as well as the energy developed by any follow current supplied by the controller.

Transient control components must be selected to be compatible with the overall reliability requirements for the windshield system.

#### Radar Cross Section Control

Some military aircraft have a requirement that the echo signal presented to an interrogating radar be held to a minimum level and have as few identifiable characteristics as possible. Large, non-conducting window areas may permit the penetration of radar signals to the interior area where the electrical geometry within the aircraft may reflect strong and identifiable signals.

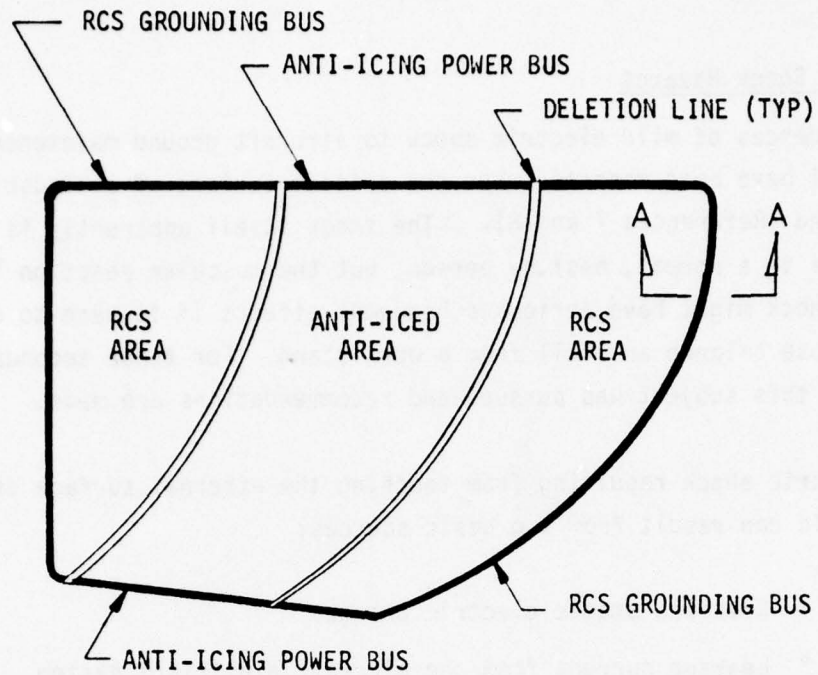
These reflections may be substantially reduced if the windshield area is treated to reflect the electromagnetic radiation before it penetrates to the inside of the aircraft. Reflection at many radar frequencies can be achieved if the windshield is covered with a conductive coating having a surface resistivity of as much as 30 ohms per square; however, a lower value of 10 ohms per square would be more effective and is recommended (Reference 6). These coatings are usually applied to the rear surface of the outer windshield ply.

When the windshield is anti-iced electrically by the use of a heating film, the conductivity of this film is usually low enough to be an effective radar reflector. However, for electrical reasons, the anti-icing coating may not cover the total area of the windshield. Under these circumstances, a dummy unheated coating may be added to the remaining area of the windshield to provide the total coverage needed for good radar cross sections (RCS) control. On some aircraft not requiring RCS, unheated areas may also be coated to provide more uniform optical light transmission.

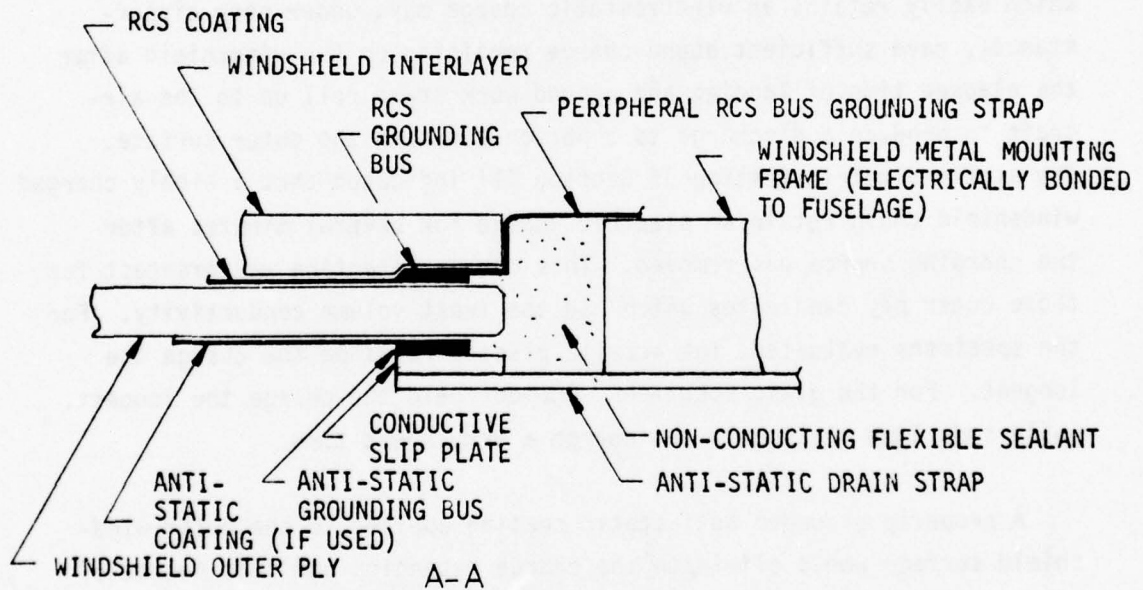
When external anti-static coatings are not employed, the RCS coatings and unheated but conductive coated areas of the windshield should be adequately grounded to prevent high voltage flashover or burning of the coating. The data of Section III showed that ungrounded back coatings or coatings grounded via high impedance paths can develop very high voltage. This voltage build up can be prevented by grounding the coating to the metal periphery of the windshield. Multiple ground paths are desirable to reduce the current density (and tendency to burn) in the ground path and especially in the conductive film adjacent to the ground point. In practice, this is best achieved by an integral grounding bus around the external perimeter of the unheated conductive film. The bus itself can be single point grounded to the airframe structure if control of static electric charge is all that is to be achieved. However, multi-point, low impedance grounding of this bus would enable this unheated coating to be more effective as a Faraday shield against external electromagnetic energy having wavelengths longer than those of the microwave signals usually associated with radar. Figure 52 illustrates the recommended ground bus and grounding.

#### Electromagnetic Pulse (EMP) Effects in Windshield Design

The interaction of the windshield with an electromagnetic pulse (EMP) environment was not within the scope of the original task. It was added at a later date. Therefore, this subject is covered in Appendix B of this report.



A. VIEW SHOWING CONDUCTIVE COATINGS ON REAR SIDE OF WINDSHIELD OUTER FACE PLY.



B. VIEW A-A SHOWING WINDSHIELD OUTER PLY WITH PORTIONS OF WINDSHIELD FRAME (EXPANDED SCALE).

Figure 52. Method for grounding RCS coating.

### Electric Shock Hazards

Incidences of mild electric shock to aircraft ground maintenance personnel have been reported when the outside surface of a windshield is touched (References 7 and 8). The shock itself apparently is not dangerous to a normal, healthy person, but the muscular reaction to even a mild shock might have serious subsequent effects if it were to cause one to lose balance and fall from a work stand. For these secondary reasons, this subject was pursued and recommendations are made.

Electric shock resulting from touching the external surface of a windshield can result from two basic sources:

- ° Retained static electric charge.
- ° Leakage current from the aircraft electrical system.

Aircraft which employ windshields having an outer surface material which easily retains an electrostatic charge may, under some circumstances, have sufficient bound charge remaining on the windshield after the elapsed time of landing and ground work stand roll up to the aircraft to produce a discharge to a person touching the outer surface. The static electric testing of Section III indicated that a highly charged windshield could retain an electric charge for several minutes after the charging source was removed. This charge retention was greatest for those outer ply candidates which had the least volume conductivity. For the specimens evaluated, the acrylic plastic retained the charge the longest. For the glass specimens, Chemcor held the charge the longest, while soda lime glass held the charge a very short time.

A properly grounded anti-static coating applied to the outer windshield surface would eliminate the charge retention and this source of electric shock. Unfortunately, permanent anti-static coatings are not available for plastics and plastics will, in general, retain the highest charge for the greatest time.

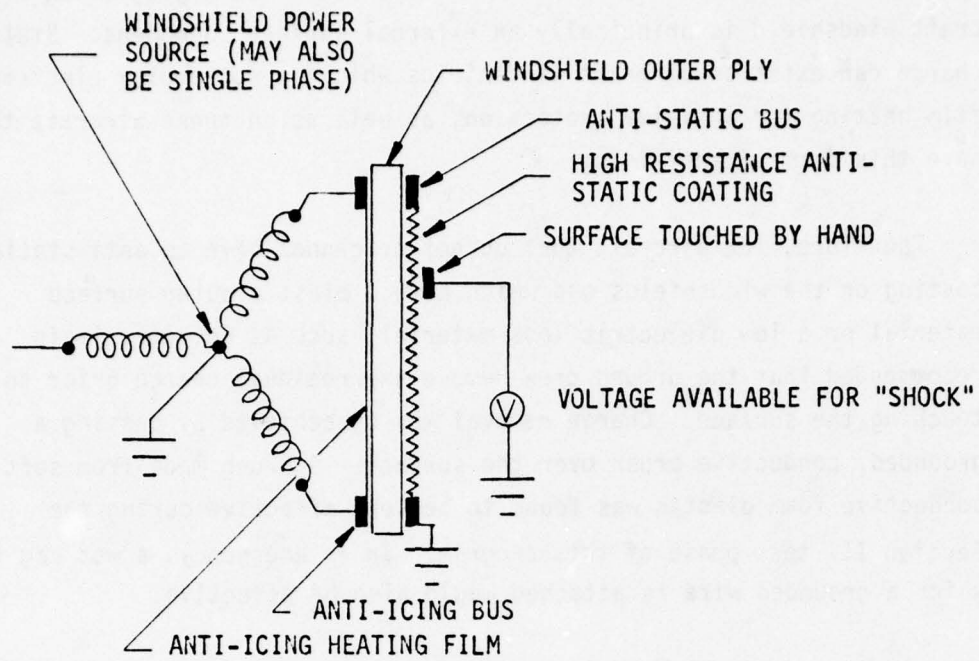
It is important to again reiterate that static charging of an aircraft windshield is principally an external surface phenomena. Static charge can exist on aircraft windshields which do not employ electrical film heating for anti-ice protection, as well as on those aircraft that have this form of anti-icing.

Therefore, for aircraft that do not or cannot have an anti-static coating on the windshields and which have a plastic outer surface material or a low dielectric loss material, such as Chemcor, it is recommended that the ground crew remove any residual charge prior to touching the surface. Charge removal may be achieved by passing a grounded, conductive brush over the surface. A brush made from soft conductive foam plastic was found to be very effective during the Section III test phase of this program. In an emergency, a wet rag to which a grounded wire is attached would also be effective.

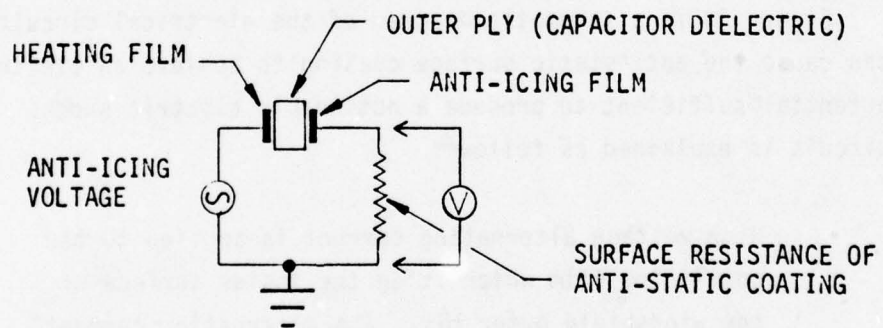
The preceding paragraphs note that a grounded anti-static coating will eliminate shock hazard due to electrostatic charge retention. Unfortunately, this same anti-static coating may be a source of electric shock from another source.

Figure 53 is a schematic diagram of the electrical circuit which can cause the anti-static surface coating to achieve an electrical potential sufficient to produce a noticeable electric shock. The circuit is explained as follows:

High voltage alternating current is applied to the anti-icing film which is on the inside surface of the windshield outer ply. The alternating current source is referenced to the conducting aircraft fuselage. The anti-static coating on the outside surface of the windshield outer ply forms the second electrode of a capacitor for which the outer ply is the dielectric. Alternating current



A. SCHEMATIC OF CAPACITOR FORMED BY OUTER PLY AND CONDUCTIVE FILM.



B. SIMPLIFIED SCHEMATIC

Figure 53. Schematic diagram of potential electric shock circuit.

will flow, via the reactance of this capacitor, from the aircraft electrical power source to the anti-static coating and through the resistance of this coating to the aircraft structure. Because the anti-static coating has a high resistance from any given area to the fuselage, the reactive current through the capacitor can cause a potential difference between a spot on the external surface of the windshield and the fuselage or grounded work stand. Thus, an electric shock might be felt if a person were to place one hand on the windshield and one hand on a bare metal portion of the fuselage (or on a grounded work stand when the aircraft is also grounded).

The most obvious cure for this possible shock hazard is to turn off the windshield anti-icing system during the period when someone might come in contact with the windshield. This approach is not always as direct and effective as it sounds. If the windshield employs phase-to-phase power and the power controller opens only one leg of the circuit, there is still a phase to ground (neutral) path that could cause the windshield "capacitor" to be charged even though no anti-icing current is flowing. For this case, both legs of the phase-to-phase power circuit must be opened to eliminate the electrical path through the windshield.

For anti-icing circuits employing phase-to-neutral power, opening the one phase lead, either via the controller or by the circuit breaker, will disconnect the shock hazard source.

Some aircraft operators are experimenting with operating procedures which have power applied to the windshield at all times - even on the ground - in order to reduce thermal shock in the windshield. For this

condition, the maintenance crew would have to establish special procedures which would allow the temporary removal of all windshield power.

A grounded discharge brush or grounded wet rag is not effective for removal of alternating current originated shock hazards.

Alternate, but not always practicable, methods of eliminating the alternating current source of shock voltage would be to power the anti-icing system from direct current, or to retain the ac power but lower the surface resistivity of the anti-static coating to a value that does not provide a shock producing voltage differential between areas on the windshield and the fuselage. Peripheral grounding of the anti-static coating will produce the effect of lowering the surface-to-fuselage resistance for much of the area as compared with a single point static ground. Peripheral grounding is also recommended for other reasons, as discussed elsewhere in this report.

#### Design Verification Tests

The recommendations of this report should enable a design team to formulate a design which has a high probability of success in achieving satisfactory operation when used in an adverse external electrical environment. However, it is strongly recommended that the windshield and the associated anti-icing control system be evaluated in the presence of the expected electrical transient environment. Environment simulation would be necessary to hold the cost within reason.

Other tests should verify the continuity and resistivity of anti-static coatings, if they are used. The electrical isolation between the outer surface discharge path and the anti-icing conductors should be verified by high voltage resistance tests.

#### Areas Recommended for Further Study

The depth of study permitted by the present contract did not permit some areas to be covered as thoroughly as might be desired. In other

instances, the work uncovered areas which were not initially identified for study, which nevertheless may have an important bearing on the design, manufacture, or use of windshield systems. These areas are discussed in the following paragraphs.

A. Anti-Static Coatings:

The use of anti-static coatings on the outer surface of windshields will provide very beneficial system effects by preventing the build up and discharge of static electricity. However, some very important questions regarding anti-static coatings remain unanswered or only partially answered. Because of the potential benefits of anti-static coatings, it is strongly recommended that these questionable areas be resolved as follows:

1. Determine factual data on the visible light transmission efficiency versus surface resistivity of candidate materials. (Manufacturers present claims and limited test data do not always correlate - Transmission appears lower than claimed.)
2. Conduct a thorough review of the manufacturing methods and procedures used to apply anti-static coatings. The objectives would be to better identify present capability and, if needed, to promote the development of economical methods of achieving better control over the application, testing and quality control of permanent anti-static coatings.
3. Determine the wear resistance characteristics of anti-static coatings when subjected to erosion from rain, hail, dust, windshield wipers, and window cleaning. Coating thickness and composition, as well as the substrate material, are expected to be contributing factors.

The wear resistance of candidate coatings and coating techniques must be compared with the life expectancy of the remainder of the windshield assembly.

4. Determine the short and long term susceptibility of anti-static coatings to damage from chemicals and fluids which may be used on or in the vicinity of an aircraft windshield.
5. Determine the state of development of permanent anti-static coatings for plastic surfaces. Promote the development of coatings, if adequate progress is not apparent, by defining the long and short range need for such coatings, and by identifying the technical requirements, user requirements, manufacturing interface requirements, and the quality assurance requirements.

B. Surface Resistivity Standards

Measurement of the surface resistivity of anti-static and anti-icing conductive coatings, as expressed in ohms per square, requires an accepted, standard method. No standard appears to exist at the present time. Subcommittee F7.08 of the American Society for Testing and Materials (ASTM) is preparing such a standard method. It is recommended that the work of this subcommittee be encouraged and supported by all who may have use for and information pertinent to this area so that a practicable and workable standard can be established. When the standard is established it is further recommended that the use of the standard be contractually required in procurement specifications.

C. Effect of Dielectric Characteristics and Dielectric Thickness on Swept Stroke Lightning Attachment

The testing conducted during this program indicated that the dielectric qualities and the local field conditions influenced the tendency for swept stroke lightning to attach to the outer ply material of the windshield. Some aircraft that do not employ an anti-icing coating close to the outer surface may use an RCS coating that is significantly farther away from the outer surface than the simulated anti-icing coating used in the test specimens.

It is recommended that additional investigation be devoted to the determination of the effects of the dielectric quality and of the proximity to the outer surface of a conductive coating on the probability of swept stroke lightning attachment. The study should also investigate the extent of possible damage to the windshield material, including the conductive coatings.

D. Effect of Windshield Discharges on the Buried Transparent Electrically Conductive Coatings.

Precipitation static discharges on the surface of a windshield that is not equipped with an effective anti-static coating can induce appreciable current in the anti-icing or RCS coatings on the buried inner surfaces of the windshield. Similar, but much higher currents are induced by swept stroke lightning, whether or not the lightning channel touches the windshield surface. EMP can also be a source of less concentrated current.

The test specimens used in the measurements described in this report employed aluminum foil to simulate the more costly transparent conductive coatings. Yet, damage to the aluminum foil was noted during the swept stroke lightning tests and may have been caused by the induced current. This damage was in the form

of heat bubbles formed between overlapping segments of the foil that was joined by conductive adhesive.

The current carrying capability of the aluminum foil, including the joints, was considerably higher than that of typically thin, transparent conductive film. Furthermore, it is almost certain that the induced current from a surface flash does not spread evenly over the conductive film surface as it is designed to do in an electrically heated application. The induced transient current will be, to a large extent, the reflected image of the path of the surface discharge. The result is a very high current density in this reflected path. It is strongly suspected that the high current density path may suffer deterioration when the surface discharge is caused by relatively low intensity P-static conditions. Destruction of the high current density path in the anti-icing film might result from the induced current of a swept stroke lightning discharge.

No conclusive evidence of this suspected phenomena has been found during this windshield study program, but it was very evident that the anti-static exterior coating was thoroughly removed from the surface in the path of the attached lightning stroke. A much smaller degree of damage to the anti-icing coating would be more than sufficient to seriously degrade or ruin the anti-icing performance of the heated film. The practical result would be a ruined windshield. It may be quite possible that the synergistic effects of induced transient current, moisture, normal heating current, and other factors may be the cause of many of the reported windshield conductive coating failures.

Laboratory techniques are available to adequately and economically simulate the surface discharges caused in nature by triboelectric charging (which results in P-static) and swept stroke

lightning. Therefore, it is strongly recommended that studies be conducted to investigate the effects of induced transients in the buried conductive films and to develop methods of preventing excessive currents.

#### E. Effects of Surface Discharge Markings

Surface marking on some of the glass samples occurred during the static electric discharge studies reported earlier in this report. One particular surface marking resembled an octopus pattern with the surface marking tentacles converging to a localized point. High voltage, high gradient probing did not reveal any indication of surface puncture, yet the octopus pattern has been the typical indication of dielectric puncture in other studies. If undetected puncture did occur it could deliver a very high energy, highly localized current to the anti-icing or RCS conductive coating on the other side, which might damage the coating.

A study is recommended to determine if there are self-healing properties in some of the candidate *outer ply* windshield materials which would permit an undetected high voltage puncture to take place. The information derived from the study would be valuable in the selection of outer ply material, especially for applications where anti-static coatings are not going to be used.

## REFERENCES

1. Sharp, P. J., "Static Electrification of Windscreens and Canopies," 1975 Conference on Lightning and Static Electricity, Culham Laboratories, England.
2. Oh, L., Huang, G. C., Goldman, R., et. al., "Natural and Induced Effects on Integrated Antennas and Circuits at Frequencies to  $10 \text{ GHz}$ ," Technical Report AFAL-TR-69-210, Commercial Airplane Group, The Boeing Company, (September 1969).
3. Brick, R. O. and Mowery, J., The Boeing Company, ASTM Subcommittee F7.08 Coordination Correspondence, (August 1975).
4. Tanner, R. L. and Nanevicz, J. E., "Precipitation Charging and Corona - Generated Interference in Aircraft," Technical Report 73, SRI Project 2494, Contract AF 19(604)-3458, Stanford Research Institute, Menlo Park, California, (April 1961).
5. Olson, J. B., Sierracin Corporation, Private Communications, (October 1975).
6. Olendorf, G. and Overholzer, J., Rockwell International, Private Communications, (September 1975).
7. Brick, R. O., The Boeing Company, Private Communications - Electrostatic Shock, (February 1976).
8. Timmons, T., Eastern Airlines, Private Communications - Windshield A.C. Shock Hazard Potential, (January 1976).

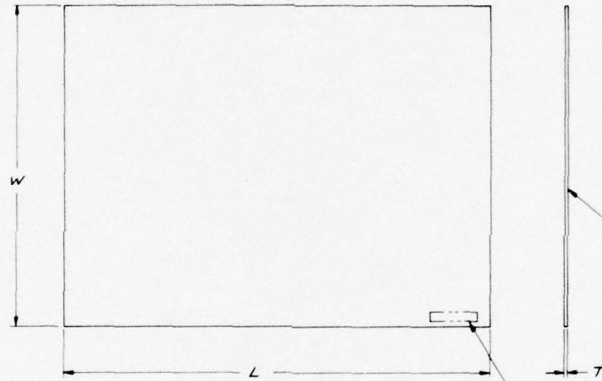
APPENDIX A

This appendix consists of drawing Z5942632 which describes the test specimens used in the static electric and swept stroke lightning tests.

GENERAL NOTES (CONT'D)

60 INSPECTION

- 61 OPTICAL INSPECTION PER MIL-G-25667, PARAGRAPH 38, IS NOT REQUIRED.
- 62 LUMINOUS TRANSMITTANCE TO BE MEASURED PER MIL-G-25667, PARAGRAPH 4.4.5 FOR ALL PANES (AFTER ANTI-STATIC COATING, IF SO COATED). A MINIMUM OF 10 MEASUREMENTS TO BE MADE AT POINTS AT LEAST 10 INCHES FROM EACH OTHER.
- 63 SURFACE RESISTIVITY OF THE ANTI-STATIC COATED PANES TO BE MEASURED AT A MINIMUM OF 10 POINTS AS IN PARAGRAPH 6.2.



APPLY ANTI-STATIC COATING TO ONE SURFACE OF -503, -505, -509 & -513 PER GENERAL NOTE 10

IDENTIFICATION - SEE GENERAL NOTE 40

	L	W	T
-1	6200	4800	110
-501	6200	4800	187
-503	6200	4800	110
-505	6200	4800	187
-507	5300	3700	085
-509	5300	3700	085
-511	5300	3700	105
-513	5300	3700	105
-515	4800	6200	125



Preceding page BLANK

APPENDIX B

This appendix contains the results of the study to consider the electromagnetic pulse (EMP) effects in windshield design.

APPENDIX B  
ELECTROMAGNETIC PULSE (EMP) EFFECTS IN WINDSHIELD DESIGN

Addition of the EMP Study

After the original precipitation static and swept stroke lightning work of the overall report was well underway it became evident that a third electrical environment, EMP (electromagnetic pulse), should be included to encompass all of the expected environments. The results of this EMP study are included in this appendix, since the basic report was essentially completed prior to the main effort of the EMP study.

Purpose of the EMP Study

Some military aircraft have the requirement that they be capable of effective operation during and after the high altitude detonation of atomic explosives. One of the byproducts of the detonation is an electromagnetic signal (to be discussed in more detail later) that might react in a negative way with a modern aircraft windshield subsystem. This interaction needs to be understood so that the aircraft design can be further optimized.

The subject of EMP is very complex and far-reaching. When hardening (immunizing) an aircraft against EMP is a requirement, the budget for this work usually far surpasses the budget for the windshield design. A team of highly trained EMP specialists is usually assigned to the job. Therefore, one of the objectives of the EMP windshield study is to acquaint windshield subsystem designers with the role the windshield may play in the overall EMP hardening scheme so that the windshield designers may more effectively work with the EMP specialists.

Background

What is EMP? A full explanation is far beyond the intent of this report. However, a simplified explanation may better enable

the windshield subsystem designer to appreciate how EMP may affect his area of speciality. A more detailed, yet unclassified explanation may be found in References 1 and 2. In a broad sense, an electromagnetic pulse is a burst of radio frequency energy which is radiated from its source and incidentally received by the aircraft on which the windshield is mounted. There are two of several sources of EMP which are of importance to this study. The first is natural lightning. The second results from the high altitude detonation of an atomic bomb.

Lightning EMP results from the electromagnetic radiation from a lightning stroke, especially those strokes which do not include the aircraft as a part of the stroke path. The radiation has a broad frequency bandwidth, with most of the energy concentrated in the very low frequency (long wavelength) portion of the radio frequency spectrum. Because the airplane is an inefficient receptor of this very low frequency radiation, lightning will be the least intense, but most frequent of the two main sources of EMP.

Nuclear detonations can also produce EMP. The radiated spectrum and energy content are highly dependent on the bomb characteristics and on the location of the blast. Detonations above the majority of the earth's atmosphere, known as high altitude bursts, are usually the most important because the effects of a single high altitude burst can cover thousands of square miles of the earth's surface with very high intensity EMP radiation. Furthermore, the spectral content of the radiated energy is very broadband and contains high energy where the aircraft is an efficient receiver of this energy.

The specific mechanism of EMP generation is not too germane to this discussion, but the mechanism of reception is important in determining the energy available at an aircraft windshield. The short duration electromagnetic pulse encounters the aircraft in a manner (for a simplified description) similar to a clapper striking a bell. The EMP wavefront strikes the airframe and moves on at the speed of light. The encounter

with the airframe sets up electrical oscillations much like the clapper sets up mechanical oscillations in the bell. The electrical oscillations in the fuselage cause large currents to surge back and forth along the airframe as damped oscillatory waves which decay in a few microseconds. Several resonant modes are usually occurring at about the same time, depending on the specific portions of the airframe that have been excited into resonance.

The basic frequency of the fuselage oscillations is dependent on the path length. The larger the aircraft, the longer the resonant paths available and the lower the frequency of oscillation. When two aircraft are mechanically (and electrically) joined in an in-flight refueling operation their combined geometry is excited by the EMP and the principal structural electrical oscillations are of a lower frequency. Because the energy distribution in the usual EMP is greater in the lower frequency portion of the radiated EMP spectrum, the longest of the various resonant paths will create the largest amplitude of oscillation.

The structure of the aircraft is actually acting as a radio frequency antenna. The extremes of the aircraft, such as the nose and tail, will assume the role of the ends of a one-half wavelength antenna, and like this type of antenna they will be points of voltage maximum, while the current will be maximum at the electrical center, somewhere near the center of the fuselage. Since most aircraft have a "fat" cross section compared to a thin wire, the EMP induced current does not distribute in sinusoidal fashion as with a thin wire. Rather, the current amplitude may be rather large at the windshield region even though the current must be zero at the most forward location of the metallic nose portion of the airframe. (Long, plastic, nose-mounted radomes don't contribute to the electrical length of the airplane unless they contain electrical conductors.)

Electric fields around the fuselage will be maximum when that portion of the aircraft is at a voltage maximum. Likewise, magnetic fields will

be maximum where the aircraft skin is conducting the maximum current. The windshield designer need not fully understand the EMP field conditions surrounding the windshield, but he should appreciate that the windshield is subjected to some very strong electromagnetic fields that can interact with electrical conductors placed in and on the windshield. Likewise, large EMP induced currents can flow in the structure surrounding the windshield, especially in the vertical posts that separate segments of the total windshield installation.

It must also be recognized that the shape and extent of the structure in front of the windshield will highly influence the electromagnetic field conditions at the windshield. The relationship of the fields to the windshield will be explained shortly; however, it should be noted that an airframe configuration which places the windshield at or very close to the forwardmost portion of the airframe will be less subject to the influence of localized magnetic fields, and electric fields will predominate for the major portion of the EMP excitation. This configuration is exemplified by some transport aircraft types.

When the windshield is placed farther back on the fuselage, larger EMP-induced fuselage currents will be encountered in the structure surrounding the windshield. For this case the magnetic fields can be quite large. This configuration is typical of some of the needle-nose supersonic aircraft.

Turning attention now to the windshield, the transparent material used in the usual windshield is a non-electrical conductor. For all practical purposes the basic windshield material is transparent to the EMP fields that most strongly excite the airframe. Therefore, a windshield which contains no anti-icing or anti-fogging electrical coatings will act like a large hole in the airplane. This hole will allow a very significant "leakage" of the external EMP-created electromagnetic fields into the cockpit area. The EMP engineer must counter this leakage with special wire routing, shielding and special design of the electronic

circuits. This might result in much additional weight and cost. The windshield engineer and the EMP engineer can do little to stop this leakage for the simple, electrically uncoated windshield.

Many modern windshields have electrical conductors coated across their surface. As discussed in previous sections of this report, these coatings may serve various purposes, such as anti-icing, defogging, or radar cross section control. If just one of these coatings were a perfect electrical conductor and the coating were peripherally connected to the surrounding airframe, the coating would exclude the entry of all EMP signals through the windshield and into the cockpit area.

Unfortunately, the state-of-the-electrical-art has not produced a perfect, or even a very good conductive coating that is highly transparent. By the time the coating has become acceptably transparent the surface resistivity of the coating is around 8 ohms per square or more. This is a very high value of resistance compared to even a thin foil of aluminum.

#### Shielding Characteristics of Transparent Metal Coatings

The preceding background material now leads to the question of what contribution the conductive coating might make to the control of the EMP signal entry via the windshield. Transparent conductive coatings have been used as electromagnetic shields for at least several decades. Some of the sales literature has listed the shielding effectiveness of these coatings in excess of 100 decibels. If this were the full story, these coatings would be capable of totally solving the problem of EMP signal entry through the windshield.

An extensive literature search was undertaken to determine the prior research in the field of electromagnetic shielding properties of transparent conductive films. It was expected that many useful references could be found because the subject is not at all new. Hundreds of potential references were tracked down, but surprisingly, very few addressed

the specific subject and still fewer were directly applicable to the windshield application. Some of the more useful references are tabulated in the referenced listings.

The amount of shielding which is potentially available from a conductive coating is dependent on the electromagnetic field conditions at the windshield. Although plane wave conditions could exist at the start of the encounter between the aircraft windshield area and the oncoming EMP wavefront, the greatest excitation amplitude results from the induced aircraft structure resonances, as described in the preceding section. Therefore, the shielding test data most applicable to the windshield will be for the near field condition. Electric field shielding effectiveness data by Lasitter (Reference 3) are shown in Figures 1a and 1b. These data show that electric field shielding effectiveness in the critical 1 to 10 megahertz region can be in excess of 60 dB for a conductive coating of 10 ohms per square, a representative value for the conductivity of anti-icing coatings. Measurements by the same author indicate a magnetic field shielding effectiveness of approximately 10 to 20 dB for the same frequency range and surface resistivity. The lower value applies to the lower frequency end of the range, whereas the electric field shielding is highest at the lower frequencies. These data are an example of the eternal shielding problem: electric field shielding is easily attained while magnetic field shielding is much more difficult to achieve.

While much more detail on attenuation is presented in the references, for practical considerations one must conclude that for windshield locations that have significant EMP induced current flowing in the surrounding structure, and accompanying high magnetic fields, the conductive coating will not contribute significant shielding. If the windshield is far forward on the airframe, such that very small currents flow in the surrounding structure, the electric field will prevail and some useful shielding may be achieved - if the coating is properly grounded to the airframe structure.

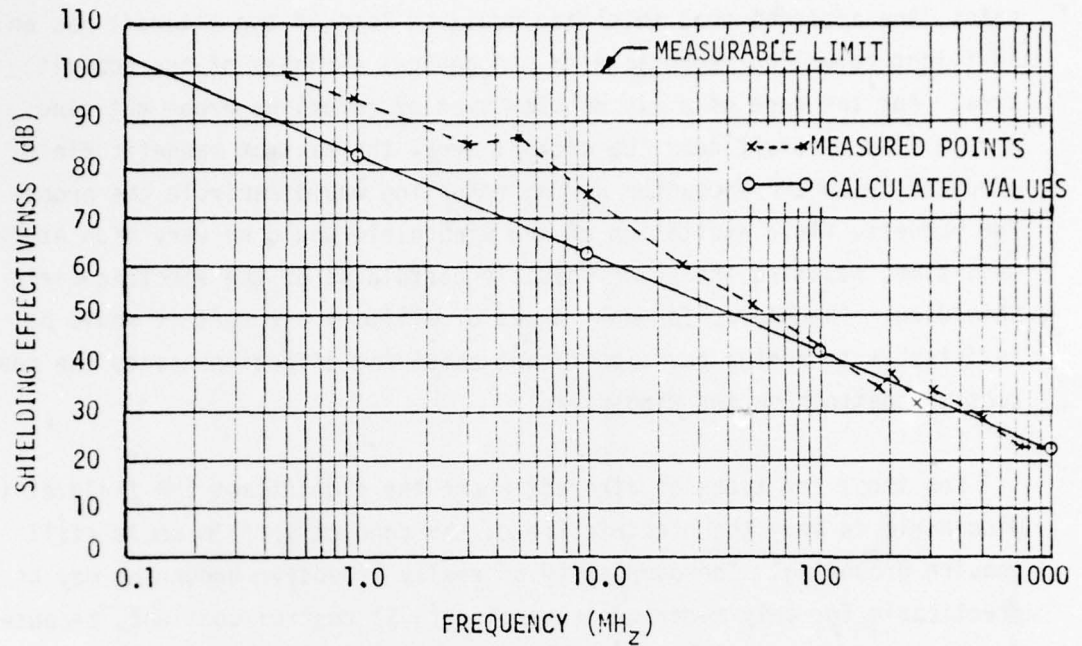


Figure 1a. Values of shielding effectiveness of 10-ohm/square conductive coating on glass.

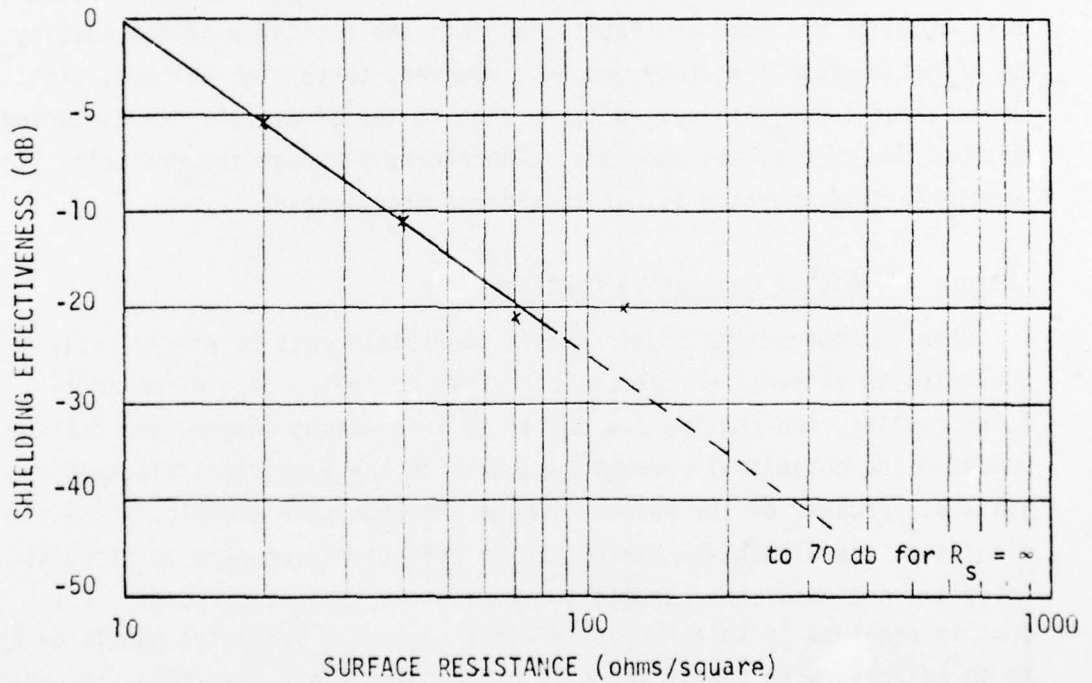


Figure 1b. Reduction of shielding effectiveness versus surface resistivity. Reference resistivity is 10-ohms/square.

Even if the windshield were located where the electric field predominates, the apparent good shielding could be lost if the aircraft has an in-flight refueling receptacle in the general vicinity of the cockpit area. For the case of a flying boom type of refueling probe entering a receiving aircraft near the cockpit area, the maximum magnetic field produced by an EMP encounter during refueling would encircle the probe. The magnetic field excitation of the windshield would be very high at this time, negating the prior possible usefulness of the electric field shielding. Therefore, for many types of military aircraft it would be inadvisable to assign any significant shielding effectiveness to the conductive coatings on the windshield.

For those few types of aircraft where the significant EMP field at the windshield is only the electric field, the conductive film would still require grounding. The complexity of really effective grounding may be practicable for only radar cross section (RCS) control coatings, because heated coatings cannot be directly grounded around their periphery and still be connected to the electric power. Special low impedance capacitors might be designed and fabricated into the periphery of the coating to effect a radio frequency ground. However, these high voltage, high capacitance techniques are quite foreign to the windshield manufacturing methods now used by the industry. Therefore, although theoretically possible, this approach is not considered practicable.

#### Antenna Effects of Conductive Coatings

When the conducting coatings on a windshield must be electrically connected to external electrical circuits, as in the case of an anti-icing coating, the coating can act as an inadvertent antenna and deliver unwanted and potentially damaging signals to the electrical/electronics systems. Because of the nature of high frequency EMP signals, these signals on the windshield wiring can be effectively coupled to circuits which are not even connected to the windshield support circuits. All that is required is that the other wires be in the same wire bundle or be in an adjacent wire bundle for part of the wire run. Therefore, the antenna effect can be important and may require special design attention.

The antenna effect was not found described in the prior literature but it is, nevertheless, a significant source of EMP signal entry. A typical anti-icing conductive coating would be accompanied by at least one temperature sensor located in the clearview area of the windshield. This combination provides two "antennas" which can electrically couple to the EMP fields at the windshield to deliver unwanted EMP signals via the wires which connect the windshield to the temperature controller. The heated coating covers the larger area and is the greater source of the EMP signal.

Both the heated coating and the temperature sensors can act as dipole antennas and as loop antennas. The dipole mode is excited when an electric field is present, and a loop mode is excited when a magnetic field is present. The specific size and configuration of the conductive coating, the associated bus bars, and exposed wiring will determine the effectiveness of this antenna configuration for a given field condition. The same criteria apply to the sensors and associated wiring which are exposed to the EMP field.

#### Control of EMP Entry Via the Windshield

The EMP signal amplitude induced on windshield conductive coatings and temperature sensors may be controlled to some extent by judicious design of the conductor layout. For example, the effective length of the dipole formed by the sensor element and the length of the exposed wiring might be reduced by choosing a sensor of minimum area and locating it so that the exposed wiring is as short as possible. The effective loop area of the sensor may be minimized by first selecting a compact sensing element and then connecting it with short, closely spaced wires. Also, a high impedance sensor will tend to reduce the loop current.

The above possibilities for reducing the induced EMP signal must be considered in the full light of other, and possibly conflicting, requirements. Trade studies are clearly called for.

When the windshield electrical layout is optimized, the remaining EMP signals on the external wiring may still far exceed an acceptable level. Two general solution approaches are available. The first is to confine the undesired signal by twisting the wiring and by providing radio frequency shielding over the wires. This approach, if properly applied, will keep the EMP signal on the wires from contaminating other wires; it will not contribute much to the attenuation of the EMP signal delivered to the temperature controller.

The second solution is to eliminate the EMP signal or attenuate it to an acceptable level by electrical filters and/or transient suppressors. When this is accomplished right at the windshield, wire shielding may not be required. If the choice is, instead, to twist and shield the wires it is most likely that some filtering or transient suppression will still be necessary where the wires enter the temperature controller.

The techniques for EMP transient control are similar to, and may be common to, the control of swept stroke lightning induced transients, or precipitation static transients, when anti-static coatings are not used. Therefore, all forms of electrical transients should be identified and controlled by one unified approach.

The three forms of transients - p-static, swept stroke lightning and EMP - do not have identical electrical characteristics. However, their differences may be accommodated in one overall transient control approach. The specific, individual transient characteristics will differ for different types and sizes of aircraft, and for different types and sizes of windshields. Therefore, no single design will be optimum for all aircraft. Generally, however, the lightning induced transient may have the greatest amplitude, and the EMP transient may have the fastest rise-time.

There are many good, electrical reasons why transients should be eliminated right at the windshield electrical terminals. The most

important is that the transient will not be available to contaminate other circuits. Confining high level transients within the windshield wiring is difficult with the normal quality of electrical shielding employed in most aircraft construction. Highly effective shielding is more expensive and weighs considerably more than conventional wire shielding. On the other hand, space for transient control hardware is usually difficult to find immediately adjacent to the windshield electrical terminals. Again, in-depth trade studies, conducted early enough to be of use, are a necessity.

Trade studies should consider the possibility of controlling the transients in steps, whereby the transient level is limited to a substantially lower value at the windshield terminals by some small-size device. Further amplitude reduction or frequency control, if required, could then be applied at another location where more space is available. This approach might permit the use of lighter weight, lower cost wire shielding in the run between the first level suppressor at the windshield and the second level filter at the remote location.

Zener diodes, varistors, and spark gaps are candidate first level suppressors. When the transient appears on circuits which are normally at high voltage, such as heater circuits, the complexities introduced by bipolar line voltage, bipolar transients and high voltage may render the zener diode approach uneconomical in cost and size. When high transient currents must be substantially suppressed in the first step of control, varistors may not provide the necessary transient clamping action. The slow reaction time of some spark gaps may limit their useful clamping action to the slower rise time transients and not provide the desired multi-source transient protection.

Some newer designs of spark gaps have the desired fast reaction time, small size and adequate peak current and energy dissipation characteristics. Their use should be considered for this application.

## An Alternate Shielding Approach

The previous sections have dealt with the EMP interaction with more or less conventional windshield designs. There is another approach which is worthy of serious consideration. This might be classified as the "brute force" approach, wherein a metal screen is stretched across the windshield and peripherally grounded to the airframe. The metal-to-open area ratio must be kept high enough to permit proper vision, yet not too open as to impair the shielding effectiveness.

The metal screen can be placed on the inside surface of the windshield, or it might be laminated within the windshield. To be most effective the metal elements of the screen must maintain good mutual electrical contact. This is difficult to achieve when conventional wire weaving techniques are employed since the individual wire strands make contact only by touching each other; there is no solid electrical bond. This problem is accentuated when fine wire and large openings are used. Alternate approaches have been investigated which achieve satisfactory electrical contact. One of the most promising is metal etching which starts with a solid foil and removes metal to provide the visual openings.

The electromagnetic shielding effectiveness of a properly grounded, homogeneous screen can be considerably better than the shielding provided by a highly transparent conductive film. Optically, the screen will degrade the light transmission. The psychological effects of seeing the screen can be diminished by selecting a screen color that blends unobtrusively into the windshield and background.

If screen EMP shielding is used in conjunction with a film heated anti-iced windshield design, thermal requirements would probably lead to placing the screen behind the heated outer windshield ply. Therefore, the heating film and its associated temperature sensors would be outside of the shielded area provided by the screen, and the antenna effect of the anti-icing coatings and temperature sensors would still remain to some extent. The close proximity of the anti-icing coating and temperature sensors to the grounded metal screen would reduce the EMP signal pickup in the anti-icing coating and sensors. However, the extent of this reduction would have to be thoroughly

investigated before one could conclude that signal coupling had been reduced to a negligible level.

#### Application of EMP Control to Other Transparent Apertures

Many aircraft, especially military aircraft, have optical or infrared transparencies through which the transmission or by which the conduction of EMP is not desired. A common area of EMP entry could be the remaining windows in the cockpit area. Some or all of these windows may be equipped with defogging systems which employ electrically heated conductive coatings on the inner or near-inner surface of the window. The electrical wiring to these defogging coatings is a source of EMP signal entry that must be investigated. If the EMP signal entry via this path is unacceptable, protective measures similar to those discussed for the windshield may be applicable.

Some military aircraft have radar cross-section control conductive coatings on many of their transparencies. While no external wires are normally connected to these coatings, the coatings should be multi-point grounded to the airframe structure to prevent charge buildup and internal arcing. The grounding should employ short, direct, low impedance paths. Peripheral grounding is recommended.

Some military aircraft also employ devices to prevent flash blindness to the crew. These devices may be metal shields. These shields should be equipped with adequate low impedance grounding directly to the structure to prevent shock or internal sparking in the crew area.

#### Conclusions

Optical transparencies which employ electrically heated conductive films and associated electrical temperature sensors can be the source of unwanted EMP signal pickup. For most applications the conductive coating is not an effective electromagnetic shield, but it can be an inadvertent antenna which couples to the EMP electromagnetic field. If corrective action is not taken this antenna effect can conduct high current or high voltage transients to the heater control equipment. The transients may

also be induced into other unrelated circuits by coupling within the wire bundles. The conducted or coupled transient signals may be of such an amplitude as to cause improper operation or damage to the electrical/electronic equipment. Temperature sensors or other electrical conductors exposed in the clearview portion of the window may also receive and deliver unacceptable signals to their connected or coupled circuits. Design techniques are available which can control the transients and prevent improper operation or damage to electronic circuits.

### Recommendations

The prime recommendation relating to EMP is the same recommendation made in the main body of the report:

- Identify and interrelate all requirements early in the design program.

Windshield designers must coordinate with the EMP specialists during the formulative stages of design so that no surprises will surface later in the program and so that an effective, economical, and maintainable design will evolve.

- Coordinate and integrate the transient suppression requirements of P-static, swept stroke lightning and EMP. A common design can usually be achieved.
- If EMP protection is not a contract requirement at the beginning of a program, but the future use of the aircraft may bring about a protection requirement, a small design trade study may yield large dividends. If control of other environmentally produced transients is necessary, protection for EMP might be possible for little or no additional cost, weight and complexity.
- Suppress the transients at the windshield whenever possible. This will require an early commitment of space at the windshield.
- Coordinate the transient control circuitry and components with the design of the connected electronics. This is essential to

assure operating compatibility and may enable some components to serve multiple purposes.

Conduct system development tests to assure the effectiveness of the transient protection and compatibility of all components.

## REFERENCES FOR APPENDIX B

1. "EMP Threat and Protective Measures", Department of Defense/Office of Civil Defense, Publication TR-61, August 1970.
2. "DNA EMP Awareness Course Notes", Defense Nuclear Agency Publication 2772T, August 1971.
3. Lasitter, H. A., "Low-Frequency Shielding of Conductive Glass", IEEE Transactions on Electromagnetic Compatibility, EMC-6, No. 3, July 1964.

Additional general references not specifically identified in the text are listed below.

4. Liao, S. Y., "Light Transmittance and RF Shielding Effectiveness of a Gold Film on a Glass Substrate", IEE Transactions on Electromagnetic Compatibility, Vol. EMC 17, No. 4, November 1975.
5. Hawthorne, E. I., "Electromagnetic Shielding With Transparent Coated Glass", Proceedings of IRE, Vol. 42, March 1954.